DYNAMIC ANALYSIS OF SKELETAL FRAMES SUBJECTED TO GROUND MOTIONS

(A theoretical and experimental study)

by

SUDHAKAR MURTHI

A Thesis Submitted for the Degree of

Master of Science.

Department of Civil Engineering,

University of Glasgow.

January, 1988.

ProQuest LLC.
789 East Eisenhower Parkway
P.O. Box 1346
Ann Arbor, MI 48106 – 1346

TO MY PARENTS

ACKNOWLEDGEMENTS

The work described herein was carried out in the Department of Civil Engineering at the Univerity of Glasgow, under the general guidance of Professor A. Coull.

The author would like to express his appreciation to Professor A. Coull and Dr. D. R. Green for the provision of facilities in the department.

The author is greatly indebted to Mr. R.W Watson for his valuable supervision, encouragements and advice during the course of this study.

My grateful thanks are also due to:

Mr. A.Burnett and all the staff of the departmental workshop for the assistance offered during the experimental study.

My friends M. Bouazza, Z. Merouani, R.Saadi, M. Souici, J.Moussa and F.Abidi for their useful discussions and comments.

I especially thank my friend Y.K To for his extensive help in all aspects of my study.

I wish to express my gratitude to Mr. A.Gray for his active involvement in the design and construction of the shaking table.

Thanks are also due to Messrs. R.McCaskie, I.Todd and A.Yuill for the help offered while testing the models.

The assistance recieved from Mr.G.Irving and various other members of staff is gratefully acknowledged and appreciated.

Thanks also to Messrs. M.Bendehgane,S.Djelleb,R.Manaa and M.Benroudane for the encouragement offered.

Finally, my special thanks are reserved for my family for their boundless patience and continual encouragement throughout the years.

TABLE OF CONTENTS

ACKNOWLEDGEMENTS i

SUMMARY vi

CHAPTER 1

INTRODUCTION

1.1 *INTRODUCTION* 1

1.2 *REVIEW OF PREVIOUS RESEARCH WORK* 1

1.2.1 *Materials suitable for modelling* 3

1.2.2 *Accurate modelling and fabrication of structures* 9

1.2.3 *Case studies* 13

1.3 *OBJECTIVES AND SCOPE* 20

1.4 *CONCLUSIONS* 20

CHAPTER 2

DYNAMIC ANALYSIS OF TWO DIMENSIONAL FRAMES 25

2.1 *INTRODUCTION* 25

2.2 *DYNAMIC ANALYSIS OF SINGLE DEGREE OF FREEDOM SYSTEM* 26

2.2.1 *Undamped system* 27

2.2.2 *Damped system* 27

2.2.3 *Response to general seismic loading* 29

2.2.4 *Numerical evaluation of the Duhanel integral* 30

2.2.5 *Response to force at mass level* 32

2.2.6 *Nonlinear model* 32

2.2.6.1 *Numerical evaluation of the equation of motion* 33

2.2.6.2 *Linear acceleration method* 34

2.2.7 *Nonlinear structural behaviour* 36

2.2.7.1 *Algorithm for step by step integration procedure* 38

2.3 *DYNAMIC ANALYSIS OF MULTISTOREY SHEAR BUILDINGS* 39

2.3.1 *Free vibration of a shear building* 39

2.3.1.1 Orthogonality property of the modes 42

2.3.2 Forced vibration of a shear building 43

2.3.2.1 Determination of the damping matrix 43

2.3.2.2 Direct integration of the equation of motion 45

2.3.2.2.1 The Wilson-θ Method 46

2.3.3 Algorithm for the direct integration technique 47

2.3.3.1 Linear analysis 48

2.3.3.2 Nonlinear analysis 49

2.4 NUMERICAL EXAMPLES USING THE COMPUTER PROGRAMS 49

2.4.1 Structural details and results 50

2.5 CONCLUSIONS 50

CHAPTER 3

DYNAMIC ANALYSIS OF THREE DIMENSIONAL FRAMES 62

3.1 INTRODUCTION 62

3.2 ELEMENT STIFFNESS AND MASS MATRIX 62

3.3 COORDINATE TRANSFORMATION 64

3.3.1 Transformation matrix 65

3.3.1.1 Rotation of element about member 'x' axis 69

3.4 ELEMENT STIFFNESS MATRIX IN THE GLOBAL AXES SYSTEM 71

3.5 ELEMENT MASS MARTIX IN THE GLOBAL AXES SYSTEM 74

3.6 FREE VIBRATION ANALYSIS 76

3.6.1 Dynamic Condensation 77

3.7 FORCED VIBRATION ANALYSIS 79

3.8 DESCRIPTION OF THE COMPUTER PROGRAMS 79

3.9 NUMERICAL EXAMPLE 81

3.9.1 Discussion of results 82

3.10 CONCLUSIONS 84

CHAPTER 4

DYNAMIC MODELLING THEORY 98

4.1 *INTRODUCTION* 98

4.2 *BASIC MODELLING THEORY* 99

4.2.1 *Geometric Properties* 100

4.2.2 *Material Properties* 101

4.2.3 *Initial Conditions* 101

4.2.4 *External Influences* 102

4.3 *DIMENSIONAL ANALYSIS* 102

4.4 *SIMILITUDE RELATIONSHIPS AND TYPES OF MODELS* 104

4.5 *PHYSICAL MODELS FOR SHAKING TABLE STUDIES* 106

4.5.1 *True Replica Model* 106

4.5.2 *Adequate Models* 109

4.5.2.1 *Models with Artifical Mass Simulation* 109

4.5.2.2 *Model tests without Simulation of Gravity Forces* 113

4.5.3 *Distorted Models* 114

4.6 *CONCLUSIONS* 116

CHAPTER 5

EXPERIMENTAL STUDY 120

5.1 *INTRODUCTION* 120

5.2 *DESIGN AND CONSTRUCTION OF THE SHAKING TABLE* 120

5.2.1 *Modification of existing supporting framework* 120

5.2.2 *Design of the shaking table* 121

5.2.3 *Design of the table supporting mechanisms* 122

5.2.4 *Performance of the shaking table* 123

5.3 *THE EXPERIMENTAL PROCEDURE* 123

5.3.1 *Experimental apparatus* 124

5.4 *EXPERIMENTAL STUDY OF MODEL 'A'* 126

5.4.1 *Description of model 'A' and instrumentation used* 126

5.4.2 Determination of damping ratio 127

5.4.3 Determination of natural frequency of model 127

5.4.4 Response to harmonic motion 128

5.4.5 Response to ramdom vibration 129

5.4.6 Discussion of results 130

5.5 EXPERIMENTAL STUDY OF MODEL 'B' 131

5.5.1 Description of model 'B' and instrumentation used 131

5.5.2 Determination of damping ratio 132

5.5.3 Determination of the natural frequencies 133

5.5.4 Response to random excitation 133

5.5.5 Discussion of results 134

5.6 CONCLUSIONS 135

CHAPTER 6

CONCLUSIONS AND RECOMMENDATIONS 157

REFERENCES 160

Appendix 1 - Jacobi's Method 163

Appendix 2 - Accelerogram of Adak earthquake 168

SUMMARY

In this study it was intended to study both the mathematical and experimental behaviour of skeletal frames and to examine the feasibility of using small scale models to predict the behaviour of prototype structures.

Mathematical analysis of both two and three dimensional structures was carried out. Computer programs were written using the relevant mathematical models and response of typical structures subjected to ground motions. For two dimensional frames both linear and nonlinear behaviour of structures was studied.For three dimensional structures to reduce the size of the eigenvalue problem, a technique known as Dynamic Condensation was incorporated.

To carry out the experimental study on small scale models, a small unidirectional shaking table was designed and constructed in the departmental workshop. Two small scale models were tested using this table. The natural frequencies for these models were obtained experimentally and their response to both harmonic and random vibrations was studied. Comparisons were made between the experimental values recorded and theoretical values obtained by using the computer programs.

The correspondence between experimental and analytical results was reasonably good for both the models. Experimental losses and distortions produced during fabrication procedures lead to experimental values being smaller than the corresponding theoretically computed values. It was not possible to induce nonlinear behaviour in either of the models due to the limited capabilities of the experimental equipment used.

From this study it can be concluded that the use of small scale models can be successfully used to predict the dynamic behaviour of simple prototype structures. It is however essential to accurately design and construct these models to represent the characteristics of the prototype being studied.

CHAPTER 1 INTRODUCTION

1.1 INTRODUCTION

The rapid advances that have been made in the methods for analysis of the dynamic response of structures since the advent of powerful computers are obvious. However, these achievements tend to obscure the fact that the analytical procedures, no matter how powerful, cannot lead to reliable estimates of the dynamic behaviour of a real structure unless the mathematical model truly represents the physical properties of the actual system. In general, the proof that a given analysis procedure is producing reliable results can only be obtained by comparison of the analytical predictions with the behaviour of a real structure subjected to dynamic loads i.e by correlation of analysis with experiment.

In most cases it is not feasible to perform dynamic tests on full scale structures. In the field of earthquake engineering, where a structure is subjected to random excitations at the base of the structure, it is essential to design the structures to enable them to dissipate the applied energy without sustaining major damage to the main load bearing structural elements. Other factors which have to be taken into consideration in the designing of earthquake resistant structures include the establishment of an adequate representation of the most severe earthquake motions that may possibly occur at the site. The response must be calculated taking account of interaction between the soil and the foundation and the participation of non structural elements.

The dynamic analysis theory of two and three dimensional skeletal frames is presented in chapters two and three. Computer programs were developed to give the response of framed structures subjected to ground accelerations and results produced for typical structures analysed are included. Studying the

response of small scale models subjected to simulated base motions in the laboratory is a useful technique for understanding the behaviour of structural members undergoing rapid reversals in loading. The models should accurately represent the characterestics of the prototype structure. In practical structures it is essential that the inelastic behaviour of the structure be mobilised to make the design economical. Such considerations impose severe restrictions on the possible choice of materials for model testing. Section 1.2.1 deals with the choice of model materials in greater depth. The initial part of Chapter 4 is concerned with the relevent material properties which have to be taken into account when choosing a model material to simulate the properties of the prototype material.

The dynamics of any structure is governed by an equilibrium balance of the time dependent forces acting on the structure. These forces are the inertia forces that are a function of the local mass and acceleration, the spring forces which are a function of the stiffness of the structure in the particular direction in which motion is occuring and the damping forces which are related to the material properties. The similtude requirements that govern the dynamic relationships between the model and prototype structure depends on the geometric and material properties and on the type of loading. The latter part of Chapter 4 contains the modelling laws which are suitable for the studying the response of models subjected to simulated seismic forces.

The use of shaking tables is a well established technique for the simulation of base excitation for model structures in the laboratory. The capability and performance characteristics of these tables vary depending largely on the equipment used to drive them. To enable the dynamic response of small scale models to be monitored, when subjected to ground motions, a unidirectional shaking table was built in the department workshop. Details of the design of the shaking table, its performance characteristics and data aquisition equipment used are presented in Chapter 5. A description of the models constructed,

experiments performed and comparisons of the experimental and theoretical results are also presented in this chapter . The final chapter (Chapter 6) deals with the conclusions drawn from this research work and recommendations for future enhancements which may possibly be carried out.

1.2 REVIEW OF PREVIOUS RESEARCH WORK

Research work carried out in the field of small scale modelling of structures subjected to dynamic loading can broadly be divided into three main sections

1) Materials suitable for modelling
2) Accurate modelling and fabrication
3) Case studies

A succint review of the work done in these fields is presented herein

1.2.1 Materials suitable for modelling

A model material should ideally demonstrate similarity of all material properties i.e the thermal and mechanical properties should be identical to those of the prototype material after the application of scaling laws. In practical modelling problems similarity is only required for those material properties which significantly affect the response of quantities of interest in the study. Within this section the suitability of modelling materials such as plastic,microconcrete and steel are reviewed.

In 1964 an investigation was made by Peerce and Davies[31] into materials suitable for modelling. Their study into the use of plastics as a modelling material is examined here. When using plastics as a modelling material, the different factors which were taken into consideration included the stress strain relationship between the prototype material and the model material, the

correspondence of Poisson's ratio of the two materials and ductility of the two materials.

For linear models of reinforced concrete structures subjected to static loading it was found that plastic models could adequately reflect the deflection characteristics of the original structure, since they exhibit a linear stress strain relationship and have a low modulus of elasticity. The mechanical properties of plastics were noted to have been affected by the rates at which stresses and strains were applied. It was shown that when the strain rate was increased from 10^{-5} / sec. to 10^{-2} / sec., the tensile strength of a perspex specimen tested at 20 °C increased by 50% and the modulus of elasticity increased by 25%. This variation in properties is obviously not a problem for statically loaded models in which loads are applied slowly but can lead to serious inaccuracies in the interpretation of test results for dynamically loaded models.

Roll[33] studied the suitability of different materials for structural models. He performed static load tests on specimens made from both thermosetting (e.g epoxies,polymers etc.) and thermoplastic (e.g acrylics,P.V.C etc.) plastics. The responses using both these types was found to be satisfactory for static loading. Thermosetting plastics were found to display greater ductility and suggestions were made regarding the possibility of using it as a suitable model material for dynamically loaded models. However, the induced strain rate effects due to dynamic loading were an important factor to be considered in the interpretation of test results obtained. A suggestion to scale the results affected by the increase in yield strength was made.

In 1970, Carpenter et. al.[8] investigated different materials which were being used as model materials for concrete structures. They too examined the suitability of plastics for elastic models of concrete structures. Thermoplastics, which have a modulus of elasticity of approximately 350 MPa and a Poisson's ratio of approximately 0.35, were found to be particularly suitable as the low modulus of elasticity resulted in producing measurable strains and deformations

on the application of relatively small loads. However, the fact that the Poisson's ratio does not compare well with that of concrete (0.15– 0.20) led to a conclusion that care must be taken in the interpretation of results where the Poisson's ratio may affect the results. Thermosetting plastics were found to be modelling shell models as curved surfaces with any desired thickness could be cast.

Two properties of plastics were noted to cause most problems in model tests; first the time dependent behaviour and second, the low thermal conductivity. The time dependent behaviour primarily affects the test procedure, while the low thermal conductivity affects fabrication when heat is used and instrumentation when electrical resistance strain gauges are used. The time dependent behaviour is apparent as creep, or continued deformation with time, when the material is subjected to a constant stress. To overcome this problem the variation of the modulus of elasticity with time has to be determined after which the material can be treated as linearly elastic and therefore is suitable for purposes of elastic modelling.

Due to the fact that creep is an important factor in the interpretation of results using plastic models, the authors arrived at the conclusion that such models would be unsuitable for dynamic loading due to the time dependent nature of the loading, and also the materials inability to give a true representation of the behaviour of concrete structure, in terms of displacements and deformations produced by such loading.

Several researchers have investigated the modelling of small scale reinforced concrete structures in the inelastic range. The difficulties when analysing reinforced concrete structures, lie essentially in the nature of the material. Reinforced concrete, being a three component material consisting of a framework of aggregates, the cement matrix and steel bars as reinforcement, is essentially a non– isotropic and non– homogeneous material. Therefore, for modelling of concrete structures subjected to inelastic deformation, it is not

possible to use anything but "concrete like" materials such as cement mortar, gypsum mortar or microconcrete. While the static behaviour of microconcrete models has been studied extensively, the research conducted into the dynamic behaviour of such models is limited.

In 1977 Chowdhury and White[10] studied the reliability of 1/10 scale reinforced concrete models for predicting frame behaviour under severe reversing lateral loads. The prototype study into the seismic resistance of reinforced concrete beam column joint was carried out by Hanson and Conner[18] in 1967. The authors found that successful small scale modelling of the behaviour of reinforced concrete structures loaded to failure depended primarily upon the properties of the model materials. Though geometric and load similitude requirements are easy to achieve, the attainment of proper model materials was found to be difficult task.

It was found impractical to attempt to reproduce all the prototype material properties such as the failure criteria of concrete, tensile properties of the reinforcement, the effects of repeated and reversing loads on material strengths and stiffnesses and the bond between the steel and concrete. The authors chose to model the following properties

a) Uniaxial compressive strength of concrete

b) Split cylinder tensile strength of concrete

c) Yield strength of steel

d) Post yield characteristics of steel

e) Ultimate bond strength

The model concrete using similar materials and mixes as the prototype was found to have similar stress strain curves as that of the prototype concretes. The tensile strength of the model concrete was found to be higher than normal prototype values but not significant to produce problems in scaling. Considerable effort was involved in modelling the reinforcing steel. Commercially available deformed wires of 2.87 and 4.04 mm. diameter were

used. To simulate the bond characteristics of the prototype reinforcement, the wires had four lines of rectangular patterns embossed into the surface at 6 mm. spacing. Because of the cold working involved in the embossing process, the wires did not have a well defined yield point and various heat treatment procedures were adopted to achieve a suitable yield point. These involved, full annealing at about 870 ^{0}C, with slow cooling through the critical range which produced very low yield points, normalising by heating the steel to approximately 965 ^{0}C and then cooling in air which resulted in higher yield strength and lower ductility than full annealing, and process annealing at 480– 650 ^{0}C which achieved proper model steel yield points. Heat treatment of model steel should be done under closely controlled conditions using a single furnace with temperature control of ±3 ^{0}C.

For all models tested the yield strength of the steel was found to be 6% lower than that of the prototype and the applied loads had to be scaled accordingly. In some models the concrete strengths were found to vary considerably with the design value and this fact was taken into account in the interpretation of the results.

Overall the results obtained indicated a reasonable agreement between the model and prototype studies for all models and only one model showed close conformity of results. This study highlights the complications involved in the manufacture of small scale reinforced concrete models subjected to nonlinear deformations and the large degree of variation in the properties of different specimens made using the same model materials.

Another aspect of importance in the use of microconcrete in dynamically loaded models is the effect of strain rate on the compressive strength of concrete. Sabnis et al[34] examined this effect by studying the results of tests done on 44 specimens. A series of 50 X 100 mm. cylinders of microconcrete with a mix of water– cement– sand ratio of 0.9:1:4.5 was tested at increasing strain rates in uniaxial compression. The 44 specimens were tested at four

rates of strain ranging from 10^{-5} to 10^{-2}/sec. Fig. 1−1 shows the comparison of the effect of strain rates on the compressive strength of microconcrete and ordinary concrete, and clearly shows the sensitivity of microconcrete to strain rate effects. The results of a similar study on the effect of strain rates on model reinforcement is shown in Fig. 1−2. However, since the increase in yield stress at higher strain rates is very similar to that of the prototype reinforcement, its effect is neglected in microconcrete models with reinforcement. The authors concluded that the effect of strain rate is particularly significant in models encountering continual reversal of stresse, and hence should be taken account of when analysing the results.

Despite the extensive use of steel in structural design the number of model studies performed on steel structures is very small compared to the number of tests conducted on reinforced concrete structures. This is mainly because steel being a homogeneous material, its properties in the linear and nonlinear range are well understood, and several full scale tests on the behaviour of steel connections have been performed thus providing a well defined picture of the behaviour of steel structures in general.

Krawinkler et al[20] made a thorough study of suitable model materials for steel structures. They examined the use of plastics as a model material, but ruled out their use because of the low elastic modulii and the high Poisson's ratio which they possess compared to steel. One of the conclusions made was that because of the specific nature of the stress strain diagram of structural steel, non ferrous materials were unsuitable as modelling materials.

Among the ferrous materials the most obvious choice, structural steel itself, was examined for its suitability as a model material. The identical shapes of the stress strain diagrams of the model and prototype materials, and the ability to closely simulate prototype connections make structural steel, within certain limitations, the best suited material for models of steel structures. The effect of higher strain rates caused by dynamic loading, which leads to an increase in

strength in the model material is a factor of considerable importance. When this effect is quantitatively known for the selected length and time scale it is relatively simple to account for by modifying the gravity loads and dynamic input.

In 1966 Nagaraja et al[26] performed a study on strain rate effects on the yield strength of structural steel. The emperical formula derived using the yield stress obtained at a strain rate $\dot{\epsilon} = 2 \times 10^{-4}$ / sec. as the normalising value is

$$\sigma_y/(\sigma_y)_{2X10-4} = 0.923 + 0.703\ \dot{\epsilon}^{0.26} \qquad (1.1)$$

The effect of strain rates is discussed in greater detail in Chapter 4.

Krawinkler et al also examined the suitability of copper alloys such as brass and phosphor bronze. Even though certain material properties such as stress strain curves and Poisson's ratio compare well to those of structural steel, but other features such as weldability and cyclic behaviour (hysteresis loops) etc. render their use very limited.

From this study by Krawinkler et al. it can be deduced that structural steel is the most suitable modelling material for steel structures. Its ease of availability, simplicity of fabrication, material properties compatibility between the model and prototype, and low price display the advantages in using it as a modelling material.

1.2.2 Accurate modelling and fabrication of structures

In any evaluation of structural models, the importance of accurate modelling and fabrication must be given prominent attention. The factors affecting model accuracy include model material properties, scaling laws, fabrication accuracy, loading techniques, measurement methods and interpretation of results. The aspect of model material properties and scaling laws are dealt with in greater depth in Chapter 4. Since this study is primarily concerned with the behaviour of frames subjected to dynamic loading, the

fabrication techniques for plastics, which are suitable only for statically loaded models, will not be examined.

Breen[6] performed a general study into fabrication of reinforced concrete models. For reinforced concrete models, the fabrication techniques used follow the fabrication procedures used in the prototypes. The major element in fabrication of such models is the development of a reduced scale concrete or microconcrete which will reproduce the important mechanical characteristics of the prototype.

For the manufacture of microconcrete the materials used are the same as for the prototype concrete. The maximum size of the model aggregate is normally established from the minimum member thickness in the model. To decrease laboratory time requirements the use of Rapid hardening Portland cement is recommended. The author suggests the use of perspex or plexiglass as the most suitable formwork material for model concrete since

1) Its transparency facilitates placement, visual inspection of the reinforcement and subsequently of the microconcrete.

2) No releasing agent is required as the concrete does not adhere to it.

3) It does not absorb water from the mixture and joints can be adequately sealed.

Placement of microconcrete generally requires good vibration for proper compaction. Small members may be cast on a vibrating table or if the dimension of the section permits, a poker vibrator operating at reduced power may be used. For the curing of concrete, it has been suggested that the formwork be left in place as a moisture barrier by spraying the exposed surfaces with a membrane curing compound and then covering it with curing blankets.

For reinforcement in the models round steel wires or rods, deformed wires

or deformed bars may be used. Reinforcement cages are usually prepared by tying small wire or by spot welding. While using spot welding, proper precaution should be taken to avoid excess heat input at the joint. This is particularly important for welded cages with closely spaced wires.

Litle and Foster [22] undertook a project to fabricate small scale steel models. They studied the fabrication of small scale I sections by milling bars. In these models both welded and bolted joints were used. The use of bolting was found to be limited mainly because the drilling of the sections substantially reduced the effective area of the member and the bolts used had to be very small to achieve geometric similitude. Since the use of such small bolts were impractical normal size bolts were considered, but this was only suitable for relatively larger sections. Welding was widely used but the operation required great skill and, to minimise distortions caused by concentrated heating, intermittent welds were used wherever possible. The main drawback in the modelling of steel structures is the amount of machining required to produce small scale sections. Since this process may induce initial stresses partially due to heat generated by the machining procedures, it is essential to have a cooling fluid which must be used.

Sabnis et al.[34] have examined the different aspects of modelling, a brief description of the various techniques and instrumentation required is presented next. In dynamic tests of small scale structures, the aims are to examine the free vibration of the model initially and secondly to study the behaviour of the model when subjected to forced vibration. Free vibration measurements can be accomplished, in some cases by pulling on the structure, then releasing quickly and measuring the free motions of the structure. Most laboratory vibration tests to study free vibrations are achieved by forcing the structure to vibrate in one of its natural modes. This is normally accomplished by the use of mechanical

or electromagnetic oscillators or by placing the model on a shaking table. To study the forced vibration the models are fixed on a shaking table and subjected to the required type of base motion.

The data which is normally required from dynamic modelling studies is a measure of the displacements and accelerations at different positions in the structure. For the measurement of displacements linear variable differential transformers (LVDT's), which are mounted on a rigid frame, which is unaffacted by the input motions, are positioned against appropriate positions of the structure. The output produced a LVDT is a change in current induced by the movement of the model against a spring loaded shaft. This current can be related to the displacement of the model at the specific position.

Accelerometers are used to measure the acceleration at any particular position in the model. The accelerometers are attached to the model itself and any variable movement in the direction of their major axis induces changes in current, which are conditioned and continously recorded.

Accurate and reliable test results and their interpretation are absolutely essential to a successful model technique. A high degree of accuracy is completely dependent upon a detailed knowledge of the material properties. In order to guard against the loss of accuracy the equipment used for monitoring the experimental data should be calibrated. When interpreting an experimental result, it is advisable to compare it with some available theory. In case of difference between the two sets of results, provided that the theory is well established, an attempt should be made to check for any possibility of error in the measurement of the test results or in the modelling technique. If no error can be found in the experimental technique, the mathematical model must be carefully examined to see how it can be improved to account for the differences produced. It must however be emphasised that several experiments must be carried out to confirm the trend before altering the mathematical model.

The above discussion emphasises the need for accuracy in modelling to achieve valid comparisons between analytical and experimental studies.

1.2.3 Case studies

The use of shaking tables to obtain the seismic response of models has been widespread in the last few years particularly in Japan and the United States of America. Several researchers have used shaking tables for testing structural components such as piles used in nuclear power stations, beam column connections etc. The University of California, Berkely embarked upon a comprehensive model testing program in the 1970's using the extensive range of testing facilities which they possess.

Clough and Tang[13] studied the response of a three storey building frame (Fig. 1−3) which was considered to be the prototype. The structure was subjected to a series of different base inputs from the shaking table. Phase I of the study was related to the examination of the behaviour of structural joints which were underdesigned deliberately so that yielding would take place there. In the second phase these zones were strengthened by the addition of plates thereby forcing yielding to occur at the ends of the beams and columns. The structure was subjected to six types of ground motion, each applied at progressively increasing intensities. The N−S component of the 1940 El−Centro earthquake was used as the input ground motion. The two input accelerations which were chosen to enable the various parameters in the elastic and inelastic ranges had peak intensities of 0.24 and 0.57g respectively (i.e about 74 percent and 175 percent of the actual earthquake intensity).

The main objective of this test program was to obtain experimental data on the actual earthquake performance of a steel frame structure so that the effectiveness of available analytical procedures could be tested. The test structure consisted of two parallel single bay, three storey moment resisting

frames which were seperated by a distance of 1.83m (6 ft.). The structural elements used in the structure were standard rolled sections with a yield strength of 316.5 N/mm^2. The structure was braced in the direction perpendicular to the base motion, in order to achieve vibrations predominantly in one direction. In order to provide a period of vibration in the range appropriate to actual steel buildings, and also to apply a gravity load to the beams, blocks of concrete weighing about 3600 kg. (8000 lb) per floor were attached to the structure. Because the beams were to play an important role in characterising the behaviour of a typical moment resistant frame, it was important that their stiffness properties should not be affected by attaching the concrete blocks to them. Specially designed load transferring devices were mounted on top of each beam to serve this purpose.

The natural frequencies of the structure moving in the excitation axis direction using analytical procedures were found to be 2.5, 8.9 and 17.9 Hz. The lateral bracing system was made stiff enough so that the frequencies of the transverse and torsional modes were higher than the second natural frequency and hence no significant response was expected in these other modes.

The instrumentation used in these tests was quite elaborate. Although in principle it would have been necessary to measure the behaviour of only one of the identical parallel frames, sufficient instrumentation on the second frame was included to verify the similarity obtained in the response. The instrumentation included strain gauges, LVDT's, potentiometers and accelerometers. Strain gauges were used to measure the strains in parts of the structure which were assumed to remain elastic even for the most severe response conceivable for the structure, from which the internal member forces at any desired section could be determined from these gauge readings.

Floor accelerations and displacements were measured using the transducers (LVDT's) and potentiomemters. Both these measurements were taken in the

direction of table motion for all three floors. The absolute accelerations and displacements were measured using three accelerometers and four potentiometers. All the measurements were taken at the level of the beam centre lines. The accelerometers were located at the middle of the cross beams connecting the two frames, and their signals represented the absolute accelerations of the masses assumed to be lumped at these levels.

The first mathematical model developed for these studies called Model 'A' is shown in Fig. 1−4(a). In this model panel zone shear deformations were included, but the joint zones were considered rigid in flexure and axial loading, thus the flexible length of the members extended only to the joint faces. The mass of the concrete blocks and the steel frame was lumped at the joint centres, and a mass propotional damping matrix which provided 0.5% critical damping was assumed. The fundamental frequency computed for this model, 2.44 Hz., agreed quite well with the free vibration of 2.40 Hz. However, the predicted structural response when the structure was subjected to the first base input was not at all similar to the observed motion as may be seen from the comparitive plots of the third storey displacements. (Fig. 1−5). The reason given by the authors for this serious discrepancy was that the apparent frequency of the observed response was only 2.24 Hz., and the fundamental frequency of the structure had a controlling influence on the response.

A modified mathematical model called Model 'B' (Fig. 1−4(b)) which had a natural frequency of 2.24 Hz. was developed. In this model, the columns were assumed to be flexible within the panel zones (i.e centre to centre of the joints) but the system otherwise was the same as model 'A'. Using this model excellent agreement was achieved between the analytical and experimental results (Fig. 1−6(a)). Because Model 'B' gave rather good correlation with the experimental results in the elastic range, it was used also as the basis for the inelastic analysis response to the second base motion input. The results shown

in Fig. 1−6(b) show that the agreement between the experimental and theoretical analyses is not very good. The possible reason for this difference could be due to residual stresses due to fabrication as well as dead load stresses which may have an important influence on the member yield moments, thus leading to uncertainities in the mathematical modelling. The authors did not propose to make any justification for using model 'B' even though the results obtained were good for the elastic case.

The conclusions made by the authors regarding this study were

1) The period of vibration of the mathematical model has a controlling influence on the predicted response; if it agrees well with the observed response period the analytical response is good.

2) The higher modes contribute little to the response of this structure, so the correlation was not sensitive to the accuracy of the model in the higher modes.

3) The inelastic mathematical model must be based on a good elastic model, and in addition must define accurately the member yield behaviour.

This study mainly highlights the value of shaking table test data in evaluating and making improvements in computer analyses procedures. Although mathematical models can predict the response of structures, the assumptions made when construing such models not always be valid and experimental studies can be used to check their validity.

Mills [23] examined the use of small scale models to study the nonlinear response of steel framed motions to seismic motions. The three storey which was previously tested by Clough and Tang[13] was used as the prototype. Tests were performed on a 1/6 scale model of the prototype where steel was used as the modelling material. The gravity loads on the structure were simulated using a technique known as Artificial mass simulation. Modelling by

AMS involves the addition of structurally uncoupled mass to augment the density of the model and permits selection of a model structural material without regard fro mass density scale. Fig. 1－7 shows the configuration of the small scale model.

In the prototype study the behaviour of the joint panel zone was critical to the inelastic behaviour of the structure, to achieve similarity, the detailing of the beam column connections was reproduced in the model. The I sections used in the model was produced by milling bars, using the same grade of steel as the prototype. All the primary structural elements were welded using the tungsten inert gas process with argon as the shielding gas. The welding at such a reduced scale required great skill and precautions were taken to minimise distortions caused concentrated welding. After fabrication the frame was heat treated at 595°C for one hour and then cooled in ambient temperature to remove the distortion produced by high initial stresses without altering the base material. As a result the model did not reproduce the initial stress state of the prototype. The welds used were inevitabily larger than those required to simulate a true scale reduction. The yield levels were found to be 10 to 20% higher for the model as a consequence of slightly higher yield stresses and the smaller joint panel zones produced by oversized welds.

The model was subjected to actual and artificial earthquake records to produce both elastic and inelastic structural response. The comparison of the prototype and model natural frequencies is shown in Fig.1－8. The correspondence between the base shears induced due to inelastic deformations can be seen in Fig. 1－9.

A summary of the test results showed that accurate simulation of the prototype was demonstrated by the similar dynamic properties of the model. Minor discrepancies in correlation were produced by inadequate modelling of the initial stress state and the oversised welds of the model. These welds contributed to an increase of approximately 10% in yield strength and a

propotional increase in inelastic stiffness.

The authors concluded that within limitations it was possible to accurately reproduce the nonlinear dynamic response of structures to earthquake motions by testing small scale models on earthquake simulators. Artificial mass simulation was found to be a suitable modelling technique provided that the mass could be effectively isolated from the structural load resisting material. The drawbacks concerned certain aspects of modelling, for instance it was not possible to reproduce the initial stress state of the prototype for this study, thus, phenomena that are related to the initial stress state such as buckling could not be studied. Also, distortions in the model's weld sizes would preclude the application of these techniques to studies of weld fracture.

Nakamura et al [27] performed an experimental study on single storey braced and unbraced steel model frames subjected to base motions on a shaking table. The object of the exercise was to investigate the hysteritic restoring force characteristics of the columns in an elastic plastic range and to understand the dynamic response behaviour up to failure.

Small scale models of single storey braced and unbraced steel frames composed of four columns, a rigid roof and floor plates were tested. The span length and bay width were 1m and 0.8m respectively. The clear height of the specimens were 40,80 or 120 mm. The total weight of the roof blocks were 548kg and 1946kg. in the case of unbraced and braced frames respectively. Fig. 1−10 shows the test set up for both types of frames.

Each of the models was tested on an electromagnetic type shaking table at Kyoto University in Japan. The instrumentation used to obtain the response consisted of one acceleromemter positioned at the floor level to record the motion of the shaking table and three other accelerometers were attached to the undersurface of the roof plate to measure the movements in the two horizontal and the vertical direction. Relative displacements between a floor

and a roof was measured by two LVDT's. The fundamental dynamic properties of the models were examined under sinusoidal wave excitations. A free vibration test was also performed by subjecting the models to a sudden shock using a mallet.

The natural frequencies were found to be 10.85 and 18.70 Hz. for the unbraced and braced frames respectively. The corresponding values using analytical methods were 12.2 and 20.9 Hz. The authors attributed the difference between the two due to the fact the elastic stiffness of the model was smaller than the calculated value. They felt that slight imperfections in the rigidness of supporting blocks for the columns in the unbraced frames and imperfections in straightness of bracing members in the braced frames contributed to a reduction in model stiffness.

The models were subjected to the ground acceleration input of the 1940 El Centro earthquake (N−S componemt). The input values were reduced by a factor of 2 for all but one model. Fig. 1−11 shows the analytical and experimental storey displacements for two of the models. Static horizontal loading tests were performed for similar models tracing the history of the storey drift which was measured in the shaking table, to investigate the effect of a high strain rate in dynamic loading on hysteritic restoring force characteristics. It was found that the horizontal load carrying capacities of the frames in the shaking table were about 10 − 25% higher than those of the frames in the static loading tests in the elastic range.

On the basis of the experimental and analytical results, the following conclusions were made by the authors

1) Dynamic elastic plastic behaviour of unbraced and braced frames were followed well by the experimental models.

2) Careful consideration should be paid to the effect of strain rate on the load carrying capacity in the formulation of hysteretic restoring force characteristics, which could be used to predict the

load carrying capacity and dynamic response behaviour of the models in dynamic tests.

This study clearly shows the increase in yield strength caused by the high strain rate. It accounts for the increase in load carrying capacity of the frame and effectively should be taken account of to make valid comparisons of analytical and experimental results.

1.3 OBJECTIVES AND SCOPE

The two main objectives of this study are to examine the dynamic behaviour of skeletal frames by using suitable mathematical models and to examine the feasibility of using small scale models to predict the response of the prototype structures. Computer programs which will incorporate the appropriate mathematical models will be used for the analytical study. For the experimental study small scale models will be tested on a small shaking table.

Due to the limited capabilities of the experimental equipment available, the models to be tested have to be made fairly small and light.

1.4 CONCLUSIONS

The main conclusions which may be drawn from the study of previous work done in modelling are :—

1) Among the different materials examined for their suitaility as dynamic modelling materials, the use of plastics could be ruled out completely. Microconcrete is suitable for modelling reinforced concrete structures in both the linear and nonlinear ranges but is a fairly difficult modelling material with which to construct complex models . Steel was found to the most suitable material for modelling steel structures. Its main advantage is the reproduction of all the prototype material properties. It however has the drawback that in the fabrication of small sections distortions could be introduced due to machining procedures.

2) Accurate modelling and fabrication are essential if valid comparisons are to be made between the experimental and analytical results. Attention should be paid to the measurement methods used and the interpretation of experimental results obtained.

3) From the study of the previous case studies the need for experimental studies to confirm analytical results is shown to be essential. Within certain limitations, small scale modelling, appears to be a valid technique , for studying and predicting the behaviour of prototype structures.

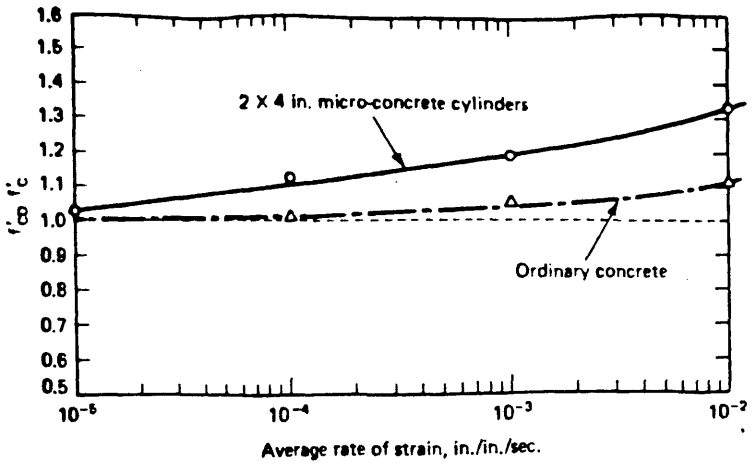

Fig 1-1 Effect of increased strain rate on the unconfined compressive strength

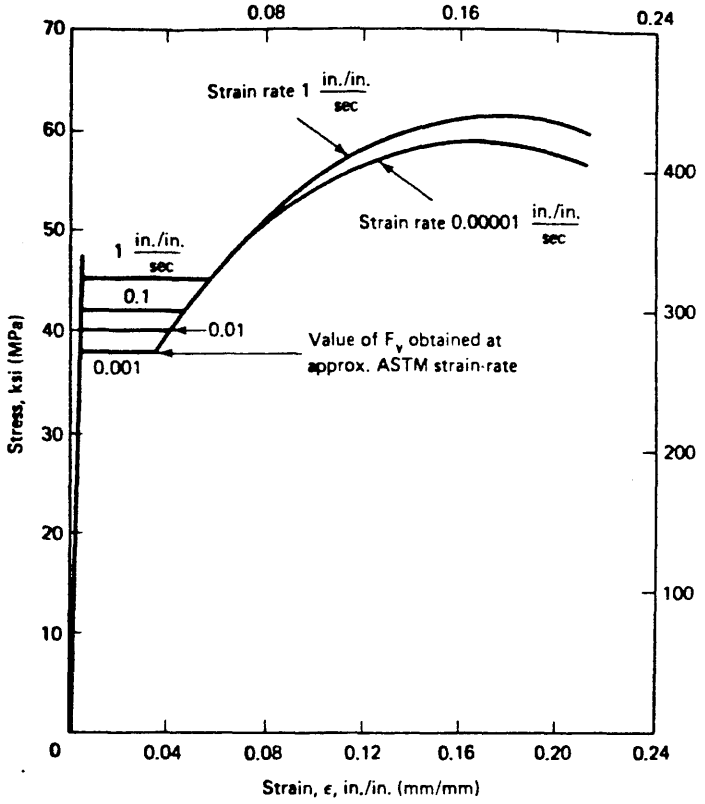

Fig. 1-2 Effect of strain rate on stress strain curve of steel

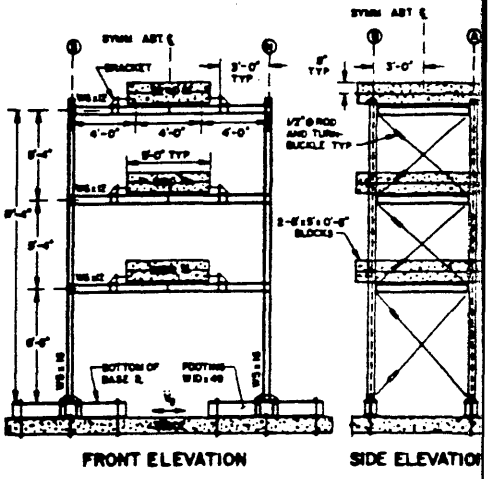

Fig. 1-3 Test structure

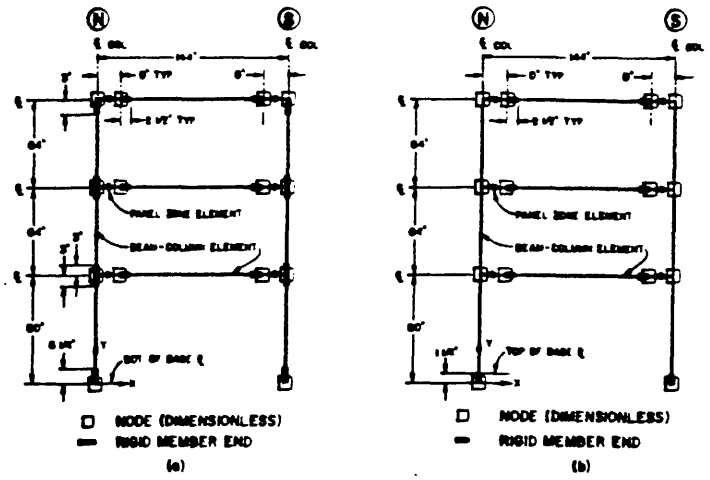

Fig. 1-4 Mathematical models

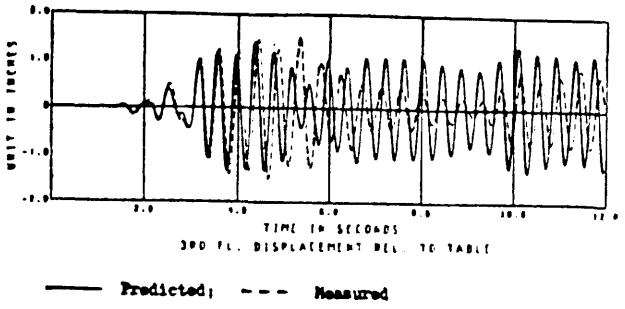

Fig. 1-5 Linear correlation using model 'A'

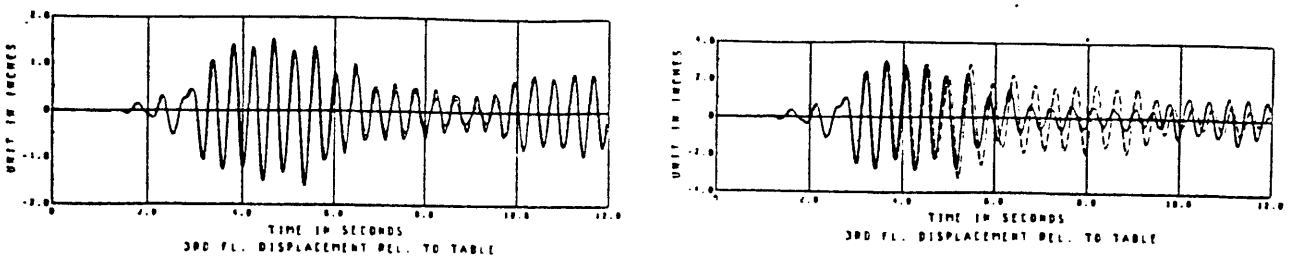

Fig. 1-6 Linear and nonlinear correlation using model 'B'

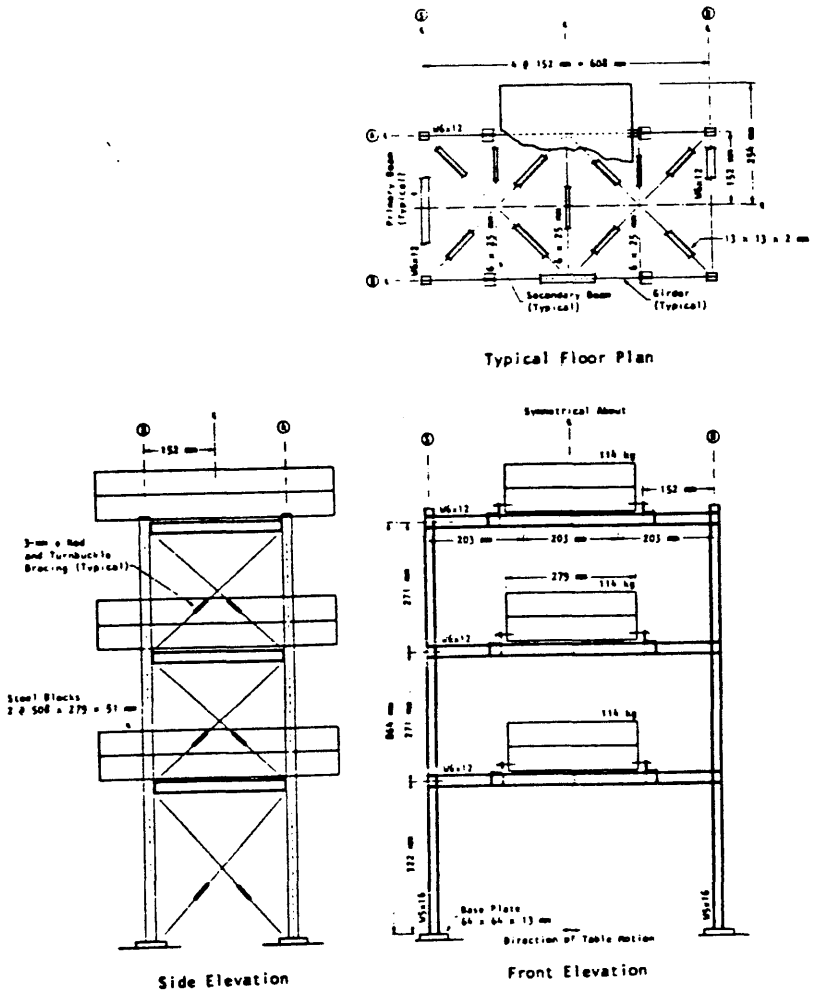

Fig. 1-7 Model structure

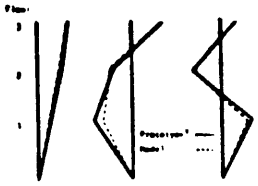

Property	Mode		
	1st	2nd	3rd
Frequency, Hz			
Prototype	2.3	7.8	15.2
Model	2.4	8.3	15.5
Damping, %			
Prototype	0.11	0.08	0.57
Model	0.28	0.16	0.29

Fig. 1-8 Comparison of prototype and model linear dynamic properties

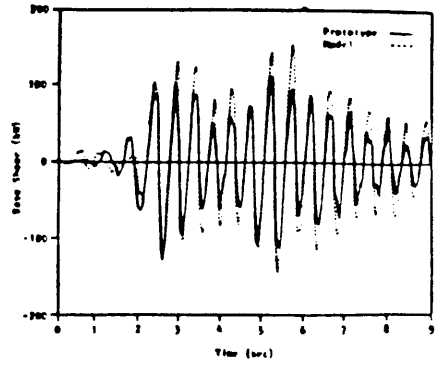

Fig. 1-9 Inelastic response to earthquake

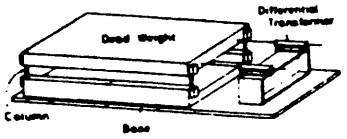

(a) Test Set-up of Pure Frames.

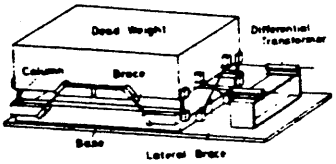

(b) Test Set-up of Braced Frames.

Fig. 1-10 Model set up

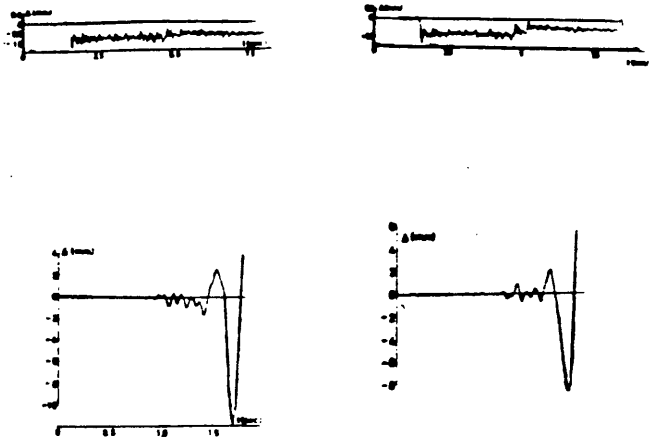

Fig. 1-11 Comparison of results

CHAPTER 2 DYNAMIC ANALYSIS OF TWO DIMENSIONAL FRAMES

2.1 INTRODUCTION

Structures whose behaviour is predominantly two dimensional can be accurately analysed using two dimensional mathematical models. In this chapter the dynamic behaviour of such structures with either single or multiple degrees of freedom is considered.

Structures such as water tanks, single storey shear frames etc., where the mass of the structure can be assumed to be lumped at one position may be idealised as single degree of freedom systems. In this chapter the dynamic behaviour of single degree of freedom systems is described intitally. The linear response of structures subjected to excitation at the base of the structure or at the position of the mass is explained next.

In cases where the structures have to be designed for excitations of large magnitudes such as strong motion earthquakes or the effects of nuclear explosion, it is not realistic to assume that the structure will remain linearly elastic and it is necessary to design the structure to withstand deformation beyond the elastic limit.

The nonlinear dynamic analysis of single degree of freedom systems is presented in the next section. The material is assumed to follow an elastoplastic behaviour in which the structure is assumed to remain elastic until it is subjected to a stress greater than the yield stress (in tension or compression) after which the displacement remains constant until the motion reverses its direction and the structure returns to elastic behaviour.

A numerical procedure is adopted to solve the resulting differential equation. The step by step linear acceleration method which is adopted, uses a simple algorithm and provides satisfactory results.

The dynamic analysis of multi degree of freedom systems is considered in

the second half of this chapter. The analysis presented is suitable for multistorey structures which can be assumed to behave as shear buildings. The assemblence of the equations of motion and the determination of the natural frequencies and mode shapes is described.

The procedure for the determination of the linear and nonlinear responses of multi degree of freedom structures subjected to ground accelerations is explained next. The step by step acceleration method used earlier for the determination of the response of single degree of freedom systems is modified to obtain the response of multi degree of freedom systems.

Finally numerical examples and graphs showing the results obtained from computer programs written for the analysis presented in the chapter is presented.

2.2 DYNAMIC ANALYSIS OF SINGLE DEGREE OF FREEDOM SYSTEMS

To enable the analysis of any structure to be performed, it has to be initially idealised into a simple mathematical model. Fig. 2−1 shows the mathematical model for a single degree of freedom system which has the following components :

1) A mass component m which represents the mass and inertial characteristics of the structure

2) A spring component k which represents the stiffness and elastic restoring characteristics of the structure.

3) A damping component c which represents the frictional and energy dissipating characteristics of the structure.

4) An excitation force $F(t)$ representing the external forces acting on the structure. $F(t)$ is a function of time.

The free body diagram shows the external force acting on the structure and the inertial, damping and spring forces.

2.2.1 Undamped system

The analysis of the simple single degree of freedom system neglecting frictional forces or damping is studied initially. Further the system is considered to be free from external actions or forces during its motion. Under these conditions, the motion of the system is governed only by the initial conditions, i.e the velocity and displacement at time $t = 0$.

A mathematical model is as shown in Fig. 2−2(a) , in this figure the mass m is restrained by a spring of stiffness k .From the free body diagram shown in Fig. 2−2(b) the internal and external forces acting on the structure can be seen. Applying D'alembert's principle the equation of motion is obtained as

$$m\ddot{x} + kx = 0 \qquad (2.1)$$

Equation (2.1) is a linear second order differential equation which has a general solution of the form

$$x = A \cos \omega t + B \sin \omega t \qquad (2.2)$$

Constants A and B can be determined from the initial conditions while ω is a quantity known as the circular natural frequency and is given as

$$\omega^2 = k/m \qquad (2.3)$$

When $x = x_0$ and $\dot{x} = \dot{x}_0$ at time $t = 0$ the constants A and B are

$$A = x_0 \quad B = \dot{x}_0/\omega \qquad (2.4)$$

The natural frequency f of the system expressed in hertz is related to the circular natural frequency ω as follows

$$f = \omega/2\pi \qquad (2.5)$$

2.2.2 Damped system

In considering damping forces in the dynamic analysis of structures, it is usually assumed that these forces are propotional to the magnitude of the velocity and opposite to the direction of motion. Considering the mathematical model and the free body diagram shown in Fig. 2−3 and applying

D'alembert's principle the equation of motion is given as

$$m\ddot{x} + c\dot{x} + kx = 0 \qquad (2.6)$$

or by dividing this equation by m we get

$$\ddot{x} + 2\xi\omega\dot{x} + \omega^2 x = 0 \qquad (2.7)$$

where $2\xi\omega = c/m$ and $\omega^2 = k/m$ (2.8)

The solution of eqn.(2.7) is,

$$x = A \exp(\lambda_1 t) + B \exp(\lambda_2 t) \qquad (2.9)$$

where $\lambda_1, \lambda_2 = \omega [-\xi \pm (\xi^2 - 1)^{\frac{1}{2}}]$ (2.10)

From eqn.(2.10) it can be seen that λ_1 and λ_2 vary depending on the value of ξ , hence the solution in eqn.(2.9) changes its form according to the value of ξ.

If $\xi^2 < 1$ then

$$x = \exp(-\xi\omega t) (A \cos \omega_D t + B \sin \omega_D t) \qquad (2.11)$$

or $x = C \exp(-\xi\omega t) \sin (\omega_D + \Theta)$ (2.12)

where $C = (A^2 + B^2)^{\frac{1}{2}}$, $\Theta = \tan^{-1} A/B$ and $\omega_D = (1-\xi^2)^{\frac{1}{2}}.\omega$

ω_D is called the *damped natural frequency.*

If $\xi^2 > 1$, the system does not oscillate because the effect of damping overcomes the oscillation.

When $\xi^2 = 1$ a limiting value of damping is achieved ,the system loses its vibratory characteristics and this is called *critical damping.* If c_{cr} denotes the damping coefficient at critical damping ,from eqn. (2.8)

$$c_{cr} = 2\omega m \qquad (2.13)$$

ξ can be defined in terms of c_{cr} as

$$\xi = c/c_{cr} \qquad (2.14)$$

ξ is the ratio of the coefficient of viscous damping to its value at critical damping and is called the *damping ratio.* Constants A,B,C and Θ in eqns.(2.11) and (2.12) are determined from the initial conditions. If $x = x_0 = 0$ and $\dot{x} = \dot{x}_0$ at time $t = 0$

$$x = \frac{\dot{x}_0}{\omega_D} \exp(-\xi\omega t) \sin \omega_D t \qquad (2.15)$$

The above equation is the general solution to the differential equation shown in eqn. (2.7)

2.2.3 Response to general seismic loading

The response of a single degree of freedom damped system subjected to arbitrary ground motion will now be considered. To compute the response, ground motion is assumed to correspond to the sum of a series of impulsive loads. An impulsive load is a load applied during a short duration of time. The corresponding impulse is defined as the product of the force and the time of its duration. The shaded area in Fig. 2−4 denotes the impulse of the force $F(\tau)$ during the time interval $d\tau$ and is equal to $F(\tau).d\tau$. The effective external force $F(t)$ caused by arbitrary ground motion is

$$F(t) = -m\ddot{x}_g \qquad (2.16)$$

The impulse acting on a body of mass m produces a change in velocity which can be determined from Newton's second law of motion namely

$$m\, dx = F(\tau)\ .d\tau \qquad (2.17)$$

This means that during a time interval of $d\tau$ the velocity of the mass (dx) changes by $F(\tau)\ d\tau/m$. These provide the initial conditions to the solution of eqn.(2.15) which are

$$x = 0 \text{ and } \dot{x} = F(\tau)\ d\tau/m \qquad \text{at } t = \tau$$

By substituting the initial velocity $\dot{x}_0 = [F(\tau)/m]\ d\tau = -\ddot{x}_g(\tau)d\tau$ at time $t = \tau$ and $t = t-\tau$ into eq.(2.15) we get

$$x(t) = -[\ddot{x}_g(\tau)\ d\tau/\omega_D]\ \exp\ [-\xi\omega(t\ -\ \tau)]\ \sin\ \omega_D(t-\tau) \qquad (2.18)$$

The above equation represents the vibration of a system when it is subjected to an impulsive load of $F(\tau) = -m\ddot{x}_g(\tau)$. If this impulse $F(t)$ is applied to the system continously , the response of the system is obtained by summing eqn.(2.18) with respect to time τ. Thus

$$x(t) = -\frac{1}{\omega_D}\int_0^t \ddot{x}_g(\tau)\ \exp\ [-\xi\omega(t-\tau)]\ \sin\ \omega_D(t-\tau)\ d\tau \qquad (2.19)$$

This equation is called the *Duhamel's integral.*

Since in most buildings $\xi << 1$, $(1-\xi^2) \approx 1$ and $\omega_D \approx \omega$, hence eqn. (2.19) can be approximated as

$$x(t) = \frac{1}{\omega} \int_0^t \ddot{x}_g(\tau) \exp\,[-\xi\omega(t-\tau)] \sin \omega(t-\tau)\, d\tau \qquad (2.20)$$

Alternatively this equation may also be written as

$$x(t) = \frac{1}{m\omega_D} \int_0^t F(\tau) \exp[-\xi\omega(t-\tau)] \sin \omega(t-\tau)\, d\tau \qquad (2.21)$$

2.2.4 Numerical evaluation of the Duhamel integral

In the case of seismic motion the applied loading function is known only from observations made and the response must be evaluated by using a numerical method. For this purpose the trigonometric identity $\sin \omega (t-\tau) = \sin \omega t \cos \omega\tau - \cos \omega t \sin \omega t$ is made use of in eq. (1.3.6) .Assuming zero initial conditions eq.(1.3.6) can be rewritten as

$$x(t) = \{A_D(t) \sin \omega_D t - B_D(t) \cos \omega_D t\} \frac{\exp\,[-\xi\omega t]}{m\,\omega_D} \qquad (2.22)$$

where $$A_D(t) = \int_0^t F(\tau)\, e^{-\xi\omega t} \cos \omega\tau\, d\tau \qquad (2.23)$$

and $$B_D(t) = \int_0^t F(\tau)\, e^{-\xi\omega t} \sin \omega\tau\, d\tau \qquad (2.24)$$

The calculation of Duhamel's integral requires the evaluation of $A(t)$ and $B(t)$ numerically, several numerical techniques including Simpson's rule and Trapezoidal rule may be used but to increase accuracy an exact method proposed by Paz[28], which includes only rounding off errors is used.

In using this exact method it is asumed that $F(\tau)$, the forcing function may be approximated by a segmentally linear function as shown in Fig. 2–5. To obtain a complete response history the integrals $A_D(t)$ and $B_D(t)$ are expressed in an incremental form as given below

$$A_D(t) = A_D(t_{i-1}) + \int_{t_{i-1}}^{t_i} F(\tau)\, e^{\xi\omega t} \cos \omega\tau\, d\tau \qquad (2.25)$$

$$B_D(t) = B_D(t_{i-1}) + \int_{t_{i-1}}^{t_i} F(\tau)\, e^{\xi\omega t} \sin \omega t \, d\tau \qquad (2.26)$$

As shown in Fig. 2−5, $F(\tau)$ may be expressed as

$$F(\tau) = F(t_{i-1}) + \frac{\Delta F_i}{\Delta t_i} (\tau - t_{i-1}) \qquad t_{i-1} \leq \tau \leq t_i \qquad (2.27)$$

where $\Delta F_i = F(t_i) - F(t_{i-1})$

and $\Delta t_i = t_i - t_{i-1}$

By substituting eqn.(2.27) in eqs.(2.25) and (2.26) the following integrals have to be evaluated,

$$I_1 = \int_{t_{i-1}}^{t_i} e^{\xi\omega\tau} \cos\omega_D\tau \, d\tau = \frac{e^{\xi\omega\tau}}{(\xi\omega)^2 + \omega_D^2} (\xi\omega\cos\omega_D\tau + \omega_D\sin\omega_D\tau) \Big|_{t_{i-1}}^{t_i} \qquad (2.28)$$

$$I_2 = \int_{t_{i-1}}^{t_i} e^{\xi\omega\tau} \sin\omega_D\tau \, d\tau = \frac{e^{\xi\omega\tau}}{(\xi\omega)^2 + \omega_D^2} (\xi\omega\sin\omega_D\tau - \omega_D\cos\omega_D\tau) \Big|_{t_{i-1}}^{t_i} \qquad (2.29)$$

$$I_3 = \int_{t_{i-1}}^{t_i} \tau e^{\xi\omega\tau} \sin\omega_D\tau \, d\tau = \left[\tau - \frac{\xi\omega}{(\xi\omega)^2 + \omega_D^2}\right] I_2' + \frac{\omega_D}{(\xi\omega)^2 + \omega_D^2} I_1' \Big|_{t_{i-1}}^{t_i} \qquad (2.30)$$

$$I_4 = \int_{t_{i-1}}^{t_i} \tau e^{\xi\omega\tau} \cos\omega_D\tau \, d\tau = \left[\tau - \frac{\xi\omega}{(\xi\omega)^2 + \omega_D^2}\right] I_1' - \frac{\omega_D}{(\xi\omega)^2 + \omega_D^2} I_2' \Big|_{t_{i-1}}^{t_i} \qquad (2.31)$$

where I'_1 and I'_2 are the integrals indicated in eqns.(2.28) and (2.29) before their evaluation at their limits.In terms of these integrals $A_D(t_i)$ and $B_D(t_i)$ may be calculated using

$$A_D(t_i) = A_D(t_{i-1}) + \left[F(t_{i-1}) - t_{i-1} \frac{\Delta F_i}{\Delta t_i} \right] I_1 + \frac{\Delta F_i}{\Delta t_i} I_4 \qquad (2.32)$$

$$B_D(t_i) = B_D(t_{i-1}) + \left[F(t_{i-1}) - t_{i-1} \frac{\Delta F_i}{\Delta t_i} \right] I_2 + \frac{\Delta F_i}{\Delta t_i} I_3 \qquad (2.33)$$

Finally by substituting the values obtained from eqns. (2.32) and (2.33) into eq.(1.4.1) the displacement at time t_i is given as

$$x(t_i) = \frac{e^{-\xi\omega t}}{m\ \omega_D}{}_i \{\ A_D(t_i)\ \sin\ \omega_D t_i\ -\ B_D(t_i)\ \cos\ \omega_D t_i\} \qquad (2.34)$$

2.2.5 Response to force at mass level

When the structure is excited by a force at the level of the mass, the procedure used to perform the dynamic analysis is the same as described for the seismic excitation. In the case of the seismic input, the effective force on the structure $F(t)$ $(= -m\ddot{x}_g)$, was due to the acceleration at the base of the structure, in this case however, $F(t)$ is an arbitrary loading function. To perform the analysis it is considered as an impulsive load applied during an infinitesimal time interval $d\tau$ as shown in Fig. 2−5. The response of the system is obtained by solving a Duhamel's integral. The procedure described in section (2.2.4) can be applied to solve the resulting duhamel's integral.

2.2.6 Nonlinear model

Considering Fig. 2−1, the equilibrium of the system at any time $t(i)$ can be obtained by equating the forces shown in the free body diagram and is expressed as.

$$F_I(t_i) + F_D(t_i) + F_S(t_i) = F(t_i) \qquad (2.35)$$

At a short time later

$$F_I(t_i+\Delta t) + F_D(t_i+\Delta t) + F_S(t_i+\Delta t) = F(t_i+\Delta t) \qquad (2.36)$$

Subtracting eqn. (2.35) from eqn. (2.36) results in

$$\Delta F_I + \Delta F_D + \Delta F_S = \Delta F \qquad (2.37)$$

Assuming the damping force to be a function of the velocity and the spring force to be a function of displacement and the inertial force propotional to the acceleration, each of the incremental forces in eqn. (2.37) can be expressed as

$$\Delta F_I = m\Delta\ddot{x} \qquad (2.38)$$

$$\Delta F_D = c_i\Delta\dot{x} \qquad (2.39)$$

$$\Delta F_S = k_i \Delta x \qquad (2.40)$$

where the incremental displacement Δx, the incremental velocity $\Delta \dot{x}$ and the incremental acceleration $\Delta \ddot{x}$ are

$$\Delta x = x(t_i+\Delta t) - x(t_i) \qquad (2.41)$$

$$\Delta \dot{x} = \dot{x}(t_i+\Delta t) - \dot{x}(t_i) \qquad (2.42)$$

$$\Delta \ddot{x} = \ddot{x}(t_i+\Delta t) - \ddot{x}(t_i) \qquad (2.43)$$

The coefficients k_i and c_i are defined as the current value of the derivatives of the spring and damping forces with respect to displacement and velocity respectively.

$$k_i = \left[\frac{dF_S}{dx} \right] \qquad (2.44)$$

and

$$c_i = \left[\frac{dF_D}{dx} \right] \qquad (2.45)$$

These two coefficients k_i and c_i are represented as the slopes of the curves shown in Fig. 2–6.

Substituting eqns. (2.38)–(2.40) into eqn. (2.37), a convenient form of the incremental differential equation is obtained

$$m\Delta \ddot{x}_i + c_i \Delta \dot{x}_i + k_i x = \Delta F \qquad (2.46)$$

In the above equation the coefficients c_i and k_i are evaluated at time t_i and are assumed to remain constant during a time step Δt.

2.2.6.1 Numerical evaluation of equation of motion.

The step by step integration method used is one of the most effective integration techniques and the algorithm is simple to understand and program. The response is evaluated at successive increments of time Δt which are usually taken to be the same. At the beginning of each time interval, the displacements and velocity are evaluated from which the stiffness and damping coefficients (k and c) can be found. The displacement and velocity values at the end of one time step are used as the initial values for the next one.

The stiffness and damping coefficients are assumed to remain constant during any particular time step, thus the nonlinear behaviour of the system is approximated by a sequence of successively changing linear systems. To integrate eqn. (2.46) the *linear acceleration method* is used, where as the name suggests the acceleration is assumed to vary linearly within any particular time step. For the implementation of this method the stiffness and damping coefficients may include any nonlinearity i.e these coefficients do not necessarily have to be specified only as functions of displacement and velocity.

2.2.6.2 Linear acceleration method

Consider Fig. 2–7 where the variation of acceleration in any particular time step is shown. The acceleration at any time t may be expressed as

$$\ddot{x}(t) = \ddot{x}_i + \frac{\Delta\ddot{x}_i}{\Delta t}(t - t_i) \qquad (2.47)$$

where $\Delta\ddot{x}_i$ is given by eqn.(2.43). Integrating eqn.(2.47) twice with respect to time between the limits t_i and t gives

$$\dot{x}(t) = \dot{x}_i + \ddot{x}_i(t - t_i) + \frac{1}{2}\frac{\Delta\ddot{x}_i}{\Delta t}(t - t_i)^2 \qquad (2.48)$$

and

$$x(t) = x_i + \dot{x}(t - t_i) + \frac{1}{2}\ddot{x}_i(t - t_i)^2 + \frac{1}{6}\frac{\Delta\ddot{x}_i}{\Delta t}(t - t_i)^3 \qquad (2.49)$$

Evaluating eqns. (2.48) and (2.49) at time $t = t_i + \Delta t$ yields

$$\Delta\dot{x}_i = \ddot{x}_i\Delta t + \tfrac{1}{2}\Delta\ddot{x}_i\Delta t \qquad (2.50\ a)$$

and

$$\Delta x_i = \dot{x}_i\Delta t + \frac{1}{2}\ddot{x}_i\Delta t^2 + \frac{1}{6}\Delta\ddot{x}_i\Delta t^2 \qquad (2.50\ b)$$

where Δx_i and $\Delta\dot{x}_i$ are given by eqns. (2.41) and (2.42) respectively. From eqn. (2.50) the incremental acceleration is

$$\Delta\ddot{x}_i = 6\frac{\Delta x_i}{\Delta t^2} - 6\frac{\dot{x}_i}{\Delta t} - 3\ddot{x}_i \qquad (2.51)$$

and substituting eqn.(2.51) into eqn. (2.50) yields

$$\Delta\dot{x}_i = \frac{3}{\Delta t} - 3\dot{x}_i - \frac{\Delta t}{2}\ddot{x}_i \qquad (2.52)$$

By substituting eqns.(2.51) and (2.52) into eqn.(2.46) the equation of motion can be rewritten as

$$m\left[\frac{6}{\Delta t^2}\Delta x_i - \frac{6}{\Delta t}\dot{x}_i - 3\ddot{x}_i\right] + c_i\left[\frac{3}{\Delta t}\Delta x_i - 3\dot{x}_i - \frac{\Delta t}{2}\ddot{x}_i\right] + k\,\Delta x_i = \Delta F \qquad (2.53)$$

or

$$\bar{k}_i \Delta x_i = \Delta\bar{F} \qquad (2.54)$$

where

$$\bar{k}_i = k_i + \frac{6m}{\Delta t^2} + \frac{3c_i}{\Delta t} \qquad (2.55)$$

and

$$\Delta\bar{F} = \Delta F + m\left[\frac{6}{\Delta t}\dot{x}_i + 3\ddot{x}_i\right] + c_i\left[3\dot{x}_i + \frac{\Delta t}{2}\ddot{x}_i\right] \qquad (2.56)$$

From eqn.(2.54) the incremental displacement can be determined as

$$\Delta x_i = \frac{\Delta\bar{F}}{\bar{k}_i} \qquad (2.57)$$

Substituting this value into eqn.(2.41) the displacement at time t_{i+1} is obtained as

$$x_{i+1} = x_i + \Delta x_i \qquad (2.58)$$

The incremental velocity $\Delta\dot{x}_i$ is obtained from eqn.(2.52) and the velocity at time t_{i+1} is obtained from eqn.(2.42) as

$$\dot{x}_{i+1} = \dot{x}_i + \Delta\dot{x}_i \qquad (2.59)$$

Finally the acceleration $\ddot{x}_{i+1}$ at time t_{i+1} is obtained directly from eqn.(2.36) i.e

$$\ddot{y}_{i+1} = \frac{1}{m}\left(F(t_{i+1}) - F_D(t_{i+1}) - F_S(t_{i+1})\right) \qquad (2.60)$$

After the displacement, velocity and acceleration have been determined at time $t_{i+1} = t_i + \Delta t$, the outlined procedure is repeated at the next time step $t_{i+2} = t_{i+1} + \Delta t$ and so on until the desired final value of time. Using this method two approximations have been made

1) The acceleration varies linearly within any time increment and

2) The stiffness and damping ratios remain constant within any time increment. To ensure that the errors produced by these two approximations are small the time increment Δt chosen should be sufficiently small.

Several suggestions have beeen made by different authors as to the choice of the time increment but for most cases a satisfactory value is obtained if the following criteria are taken into account.

1) The time increment used is smaller than one tenth of the natural period of the structure.

2) The time step should be small enough to take consideration of the changes of force with time.

3) The time step should be small enough to take consideration of any sudden variation in material properties such as a sudden change from linear elastic to plastic.

2.2.7 Nonlinear structural behaviour

When a structure is allowed to yield plastically, the force displacement curve is assumed to follow the pattern shown in fig.2−8(a). It can be seen that initially the material behaves linearly elastic in tension, after further loading plastic yielding takes place. When the structure is unloaded, the behaviour is again elastic until further loading produces plastic yielding in compression. The structure may be subjected to cyclic loading and unloading in this manner and the energy dissipated during each cycle is propotional to the area under the curve, such a loop is known as a hysterisis loop. This behaviour may be simplified by assuming a definite yield point beyond which the material displacement increases under the influence of a constant force. Such behaviour is known as *elastic−perfectly plastic* or *elastoplastic* behaviour and the forces at which yielding begins are known as the yield forces in tension and in compression (fig. 2−8(b)).

For a single degree of freedom system the yield forces can be determined

easily. The initial conditions are assumed to be zero ($x_0 = 0$, $\dot{x}_0 = 0$) for the unloaded structure. When the structure is initially loaded it follows an elastic behaviour along line E_0. The displacements x_t, at which plastic behaviour in tension is initiated and x_c at which the plastic behaviour in compression is initiated may be calculated as follows.

$$x_t = F_{yt}/k \tag{2.61}$$

and

$$x_c = F_{yc}/k \tag{2.62}$$

where F_{yt} and F_{yc} are the respective values of the forces which produce yielding in tension and compression and k is the stiffness of the structure. The structure will follow an elastic behaviour i.e it will remain on curve E_0 as long as

$$x_c < x < x_t \tag{2.63}$$

When the displacement x exceeds x_t then the structure behaves plastically along curve T (fig. 2–8(b)) as long as the velocity $\dot{x} > 0$. When $\dot{x} < 0$ the structure returns to behave elastically along a curve such as E_1. The new yielding limits are

$$x_t = x_{max} \tag{2.64}$$

and

$$x_c = x_{max} - (F_{yt} - F_{yc})/k \tag{2.65}$$

where x_{max} is the maximum displacement that occurs when $\dot{x} = 0$

On the same basis if x decreases to x_c the structure will behave plastically in compression along curve C as long as the velocity $\dot{x} < 0$. Elastic behaviour will be restored when when the velocity $\dot{x} > 0$ and the new yielding limits are given by

$$x_c = x_{min} \tag{2.66}$$

and

$$x_t = x_{min} + (F_{yt} - F_{yc})/k \tag{2.67}$$

where x_{min} is the minimum displacement that occurs when $\dot{x} = 0$. The condition specified in eqn. (2.63) is valid for elastic behaviour along any elastic curve such as E_0, E_1, E_2 etc. as shown in fig 2–8(b). To determine the

acceleration at the end of each cycle, the spring force F_S is initially estimated as follows

$$F_S = F_{yt} - (x_t - x).k \qquad (2.68)$$

in the elastic phase and

$$F_S = F_{yt} \qquad (2.69)$$

in the plastic phase in tension and

$$F_S = F_{yc} \qquad (2.70)$$

in the plastic phase in compression.

Having determined the spring force and acceleration at the end of each cycle, the response of a structure can be determined using the procedure outlined in the previous section.

2.2.7.1 Algorithm for step by step integration procedure

For a particular time increment Δt, the following steps are performed

1) Initial displacement and velocity values $x(t_i)$ *and* $\dot{x}(t_i)$ are read either from values at the end of the preceeding increment or as initial conditions of the problem.

2) Using these values and the specified non linear properties of the structure the damping and stiffness coefficients and forces are evaluated from

3) The initial acceleration is evaluated from eqn.(2.60)

4) The incremental load,stiffness and displacement values are evaluated using eqns.(2.55),(2.56) and (2.57) respectively.

5) The incremental velocity value is calculated using eqn.(2.52).

6) Finally the velocity and displacement at the end of the time step are obtained from eqns.(2.58) and (2.59)

The evaluations for the particular time step in consideration are now completed

and the values obtained from step (6) are used as initial values for the next time increment. The whole procedure is repeated until the complete response of the structure until the desired time is obtained.

2.3 DYNAMIC ANALYSIS OF MULTISTOREY SHEAR BUILDINGS

A shear building may be defined as a structure in which there is no rotation of a horizontal section at the level of the floors. The assumptions made are

1) The total mass of the structure is lumped at the floor levels.
2) The beams at the floor levels are infinitely rigid compared to the columns.
3) The deformation of the structure is independent of the axial forces in the columns.

Fig. 2−9 shows the layout of a shear building. The structure can have several bays each of the same configuration and constructed with the same material.

2.3.1 Free vibration of a shear building

Considering the shear frame shown in Fig. 2−10, it is clear that n independent coordinates ($x_1..x_n$) are required to define the configuration of the structure, i.e the structure can be assumed to have n degress of freedom. The stiffness method is used to develop the equations of motion. At a particular instant of time if the displacements at the various storeys are x ,x ,..xn respectively, then the equations of motions for the various masses are

$$M\ddot{x}_1 + k_{11}x_1 + k_{12}x_1 + ... + k_{1n}x_n = 0$$

$$M\ddot{x}_2 + k_{21}x_1 + k_{22}x_2 + ... + k_{2n}x_n = 0$$

.

.

$$M\ddot{x}_n + k_{n1}x_1 + k_{n2}x_2 + ... + k_{nn}x_n = 0 \qquad (2.71)$$

In matrix from these equations can be expressed as

$$M\ddot{x} + Kx = 0 \qquad (2.72)$$

where the mass matrix is defined as

$$M = \begin{bmatrix} M_1 & 0 & 0 & 0 & 0 & 0 \\ & M_2 & 0 & 0 & 0 & 0 \\ & & M_3 & 0 & 0 & 0 \\ & symmetric & & \cdot & 0 & 0 \\ & & & & \cdot & 0 \\ & & & & & M_n \end{bmatrix}$$

and the stiffness matrix K is defined as

$$K = \begin{bmatrix} k_{11} & k_{12} & \cdot & \cdot & \cdot & k_{1n} \\ k_{21} & k_{22} & \cdot & \cdot & \cdot & k_{2n} \\ k_{31} & k_{31} & \cdot & \cdot & \cdot & k_{3n} \\ \cdot & & & & & \\ \cdot & & & & & \\ \cdot & & & & & \\ k_{n1} & k_{n2} & \cdot & \cdot & \cdot & k_{nn} \end{bmatrix}$$

and the dispalcement and acceleration vectors are

$$x = \begin{bmatrix} x_1 \\ x_2 \\ x_3 \\ \cdot \\ x_n \end{bmatrix} \qquad \ddot{x} = \begin{bmatrix} \ddot{x}_1 \\ \ddot{x}_2 \\ \ddot{x} \\ \cdot \\ \ddot{x}_n \end{bmatrix}$$

Equation (2.72) is the equation of motion for the free vibration of an undamped multi degree of freedom system. Assuming that the free vibration motion is simple harmonic the solution takes the form

$$x_i = a_i \sin(\omega t+\alpha) \qquad i= 1..n \qquad (2.73)$$

or in matrix notation

$$x = a \sin(\omega t-\alpha) \qquad (2.74)$$

where a_i is the amplitude of motion of the i^{th} coordinate. Substituting eqn.(2.74) into eqn.(2.72) gives

$$-\omega^2 M\, a \sin(\omega t-\alpha) + K\, a \sin(\omega t-\alpha) = 0 \qquad (2.75)$$

rearranging this equation gives

$$[\, K - \omega^2 M \,]\, a = 0 \qquad (2.76)$$

Equation (2.76) is known as the frequency equation with respect to the circular

natural frequency ω and is essentially an eigenproblem. Nontrivial solutions for $\boldsymbol{a}$ exist only if the determinant

$$| K - \omega^2 M | = 0 \qquad (2.77)$$

i.e

$$| M (M^{-1}.K - \omega^2 I)| = 0 \qquad (2.78)$$

where I is an n x n unit matrix. Since the product of two matrices is equal to the product of the determinants of the two matrices. Hence eqn. (2.78) can be written as

$$| M || M^{-1}.K - \omega^2 I | = 0 \qquad (2.79)$$

Since M is a diagonal matrix whose elements are all non zero, M is non singular; hence for eqn. (2.79) to be valid

$$| M^{-1}.K - \omega^2 I | = 0 \qquad (2.80)$$

$\{M^{-1}.K\}$ is known as the *dynamic matrix*, if nontrivial solutions exist for eqn.(2.76) then the values of ω^2 are the eigenvalues of the dynamic matrix $M^{-1}\cdot K$, and the corresponding amplitude vectors $\boldsymbol{a}$ satisfying eqn.(2.76) are the eigenvectors of the dynamic matrix.

For a structure with n degrees of freedom, the dynamic matrix is of order n x n, and hence it will have n eigenvalues and n eigenvectors. The n eigenvalues will be

$$\omega_1^2,\ \omega_2^2,\ \ldots\ldots,\ \omega_n^2$$

where

$$\omega_1^2 < \omega_2^2 \ \ldots\ldots < \omega_n^2$$

and the corresponding eigenvectors are

$$a_1,\ a_2,\ \ldots\ldots\ a_n$$

where

$$\boldsymbol{a} = [\ a_1\ a_2\ \ldots\ a_n] = \begin{bmatrix} a_{11} & a_{12} & . & . & a_{1n} \\ a_{21} & a_{22} & . & . & a_{2n} \\ . & . & . & . & . \\ . & . & . & . & . \\ a_{n1} & . & . & . & a_{nn} \end{bmatrix} \quad etc.$$

Each of the n values of ω corresponds to a natural frequency ($\omega/2\pi$), the

smallest natural frequency $\omega_1/2\pi$, is called the first natural frequency, similarly $\omega_2/2\pi$ the second natural frequency and so on. Each of the amplitude vectors $\boldsymbol{a}$ is known as the normal mode shape, $\boldsymbol{a}_1$ is the first mode shape, $\boldsymbol{a}_2$ is the second mode shape etc. The solution to the above eigenproblem is achieved by using the *Generalised Jacobi method* which is briefly described in Appendix−1. A more detailed explanation is given by Bathe[1].

2.3.1.1 Orthogonality property of the modes

Mode shape vectors possess an orthogonality property which can be demonstrated as follows. Considering the i^{th} mode shape vector eqn.(2.76) can be written as

$$K.a_i - \omega_i^2.M.a_i = 0 \quad \text{i.e} \quad K.a_i = \omega_i^2.M.a_i \qquad (2.81)$$

Similarly for the j^{th} mode

$$K.a_j = \omega_j^2.M.a_j \qquad (2.82)$$

Transposing both sides of eqn.(2.81) gives

$$a_i^T.K^T = \omega_i^2.a_i^T.M^T \qquad (2.83)$$

Since the structural mass and stiffness matrices are symmetrical the above equation can be written as

$$a_i^T.K = \omega_i^2.a_i^T.M \qquad (2.84)$$

Post multiplying each side by a_j gives

$$a_i^T.K.a_j = \omega_i^2.a_i^T.M.a_j \qquad (2.85)$$

Pre multiplying each side of eqn.(2.82) by a_i^T gives

$$a_i^T.K.a_j = \omega_j^2.a_i^T.M.a_j \qquad (2.86)$$

Subtracting eqn.(2.86) from eqn.(2.81)

$$(\omega_i^2 - \omega_j^2).a_i^T.M.a_j = 0 \qquad (2.87)$$

For two different modes, $\omega_i^2 \neq \omega_j^2$. Therefore from eqn.(2.87)

$$a_i^T.M.a_j = 0 \qquad (2.88)$$

which means that the normal modes are orthogonal to one another with respect to the mass matrix. Substituting eqn.(2.88) into eqn.(2.85) gives

$$a_i^T.K.a_j = 0 \qquad (2.89)$$

This means that the normal modes are also orthogonal with respect to the stiffness matrix. This important property of orthogonality can be used to obtain the elastic response of multi degree of freedom systems subjected to external forces, by using the mode superposition technique. It is also used in the evaluation of the structural damping matrix which is described in section (2.3.2.1).

2.3.2 Forced vibration of shear buildings

In the previous section the free vibration of multi degree of freedom systems was described. In the determination of the natural frequencies the effect of structural damping was ignored as its effect is negligible. To obtain the response of structural systems to forced motion it is necessary to take account of the damping in the structure. The equation of motion for a damped structure is

$$M\ddot{x} + C\dot{x} + Kx = F(t) \qquad (2.90)$$

where C is the damping matrix, $F(t)$ is the applied forcing function which varies with time and the other symbols are as defined previously.

2.3.2.1 Determination of the damping matrix

The damping coefficient c_n for any node i is expressed as

$$C_i = 2.\xi_i.\omega_i.M_i \qquad (2.91)$$

where ξ_i is the damping ratio in the i^{th} natural mode of vibration.
The orthogonality property of the mode shape vectors with respect to the mass and stiffness matrices can be assumed to apply equally to the damping matrix, therefore the relationship can be expressed as

$$a_i^T.C.a_j = 0 \qquad (2.92)$$

Having established the above relationship, for mode i, eqn.(2.90) can be written as

$$M_i\ddot{x}_i + C_i\dot{x}_i + K_i x_i = F_i(t) \qquad (2.93)$$

or alternatively as

$$\ddot{x}_i + 2.\xi_i.\omega_i.\dot{x}_i + \omega_i^2.x_i = F_i(t)/M_i \qquad (2.94)$$

where

$$M_i = a_i^T.M.a_i \qquad C_i = a_i^T.C.a_i = 2.\xi_i.\omega_i.M_i$$
$$K_i = a_i^T.K.a_i \qquad F_i(t) = a_i^T.F(t) \qquad (2.95)$$

The damping matrix can now be evaluated as it terms of the damping coefficients. The procedure which is described in detail by Craig[15] can be briefly explained as follows.

Considering the complete diagonal matrix of damping coefficients, which can be obtained by pre and post-multiplying the damping matrix by the mode shape matrix, the following relationship may be established.

$$A = a^TCa \begin{bmatrix} 2\xi_1\omega_1M_1 & 0 & 0 & \cdot & \cdot & 0 \\ 0 & 2\xi_2\omega_2M_2 & 0 & \cdot & \cdot & \cdot \\ 0 & 0 & 2\xi_3\omega_3M_3 & \cdot & \cdot & \cdot \\ \cdot & \cdot & \cdot & \cdot & \cdot & \cdot \\ \cdot & \cdot & \cdot & \cdot & \cdot & \cdot \\ 0 & 0 & 0 & \cdot & \cdot & 2\xi_n\omega_nM_n \end{bmatrix} \qquad (2.96)$$

Therefore, for any specified set of modal damping ratios $\{\xi\}$, the matrix A can be evaluated from the above equation. The damping matrix may now be evaluated by performing the following matrix operation

$$C = [a^T]^{-1}.A.[a]^{-1} \qquad (2.97)$$

Since the inversion of the mode shape matrix is a large computational job, the orthogonality property of the mode shape vector relative to the mass matrix is made use of in determination of the damping matrix as shown below. The generalised mass matrix is obtained by pre and postmultiplying the mass matrix by the complete mode shape matrix

$$M_g = a^T.M.a \qquad (2.98)$$

Premultiplying this by the inverse of the generalised mass matrix

$$I = M_g^{-1}.M_g = [M_g^{-1}.a^T.M]a = a^{-1}.a \qquad (2.99)$$

Therefore the inverse of the mode shape matrix is

$$a^{-1} = M_g^{-1}.a^T.M \qquad (2.100)$$

Subsituting eqn.(2.100) into eqn.(2.97)

$$C = [M.a.M_g^{-1}].A.[M_g^{-1}.a^T.M] \qquad (2.101)$$

For any mode i since $A_i = 2\xi_i\omega_i M_i$, the product of the central diagonal matrices is

$$M_g^{-1}.A_i.M_g^{-1} = \zeta_i = 2\xi_i\omega_i/M_i \qquad (2.102)$$

Hence eqn.(2.101) can be written as

$$C = [M.a.\zeta.a^T.M] \qquad (2.103)$$

where ζ is the diagonal matrix of ζ_i

The total damping matrix is expressed as a summation of contribution of each of the modes where the damping coefficient for each mode is

$$C_i = [M.a_i.\zeta_i.a_i^T.M] \qquad (2.104)$$

Therefore the total damping matrix C is

$$C = \sum_{i=1}^{n} C_i = M.\left[\sum_{i=1}^{n} a_i.\zeta_i.a_i^T\right].M \qquad (2.105)$$

Substituting for ζ_i from eqn.(2.102)

$$C = M\left[\sum_{i=1}^{n} \frac{2\xi_i\omega_i}{M_i} . a_i.a_i^T\right] M \qquad (2.106)$$

In the above equation the contribution of each mode is propotional to the appropriate modal ratio, thus any undamped mode will not contribute anything to the damping matrix. The damping matrix will be used in the solution of the equation of motion using the direct integration technique.

2.3.2.2 Direct integration of the equation of motion

The method presented in this section for the solution of the equation of motion of multi degree of freedom systems subjected to external forces is basically an extension of numerical technique presented in section 2.2.6.1 for the nonlinear response of single degree of freedom systems. A modification to

the linear acceleration method which has been incorporated known as the *Wilson– θ method*[40] ensures numerical stability to the solution of the equation of motion irrespective of the magnitude of the time step chosen. The direct integration technique is used for both the linear and nonlinear response of multi degree of freedom systems. For linear systems the computational procedure is reduced significantly since it is not necessary to modify structural properties at each time step.

For non linear systems, a comparison is made at the end of each time step between the calculated displacement at each node and the displacement required to induce nonlinear material behaviour. A brief description of the Wilson– θ method and the algorithm for the direct integration technique is presented. For non linear behaviour the damping and stiffness coefficients are evaluated in a similar manner described previously.

The incremental equation of motion for a multi degree of freedom system is

$$M\Delta\ddot{x}_i + C\Delta\dot{x}_i + K_i\Delta x_i = \Delta F_i \qquad (2.107)$$

where

M = Mass matrix C = Damping matrix

K = Stiffness matrix $F(t)$ = Force vector

and the other symbols are as defined previously.

2.3.2.2.1 The Wilson-θ Method

The basic assumption of the Wilson– θ method is that the acceleration varies linearly over the time interval from t to $t + \theta\Delta t$ where $\theta \geq 1.0$. It has been shown by Wilson that for unconditional numerical stability θ should be ≥ 1.37. Fig.(2–11) shows the linear variation of acceleration for the extended time step.

The procedure is described by rewriting the basic relationships of the linear acceleration method described previously. By analogy with eqns.(2.49) and (2.50).The incremental velocity at any time t may be expressed as

$$\hat{\Delta}\dot{x}_i = \frac{\tau}{2}\hat{\Delta}\ddot{x}_i + \tau.\ddot{x}_i \qquad (2.108)$$

and

$$\hat{\Delta}x_i = \tau\dot{x}_i + \frac{\tau^2}{2}\ddot{x}_i + \frac{\tau^2}{6}\hat{\Delta}\ddot{x}_i \qquad (2.109)$$

where

$$\tau = \theta\Delta t \qquad (2.110)$$

The circumflex refers to the increment associated with the extended time step. Repeating the mathematical procedures described earlier for the linear acceleration method, the incremental acceleration for the extended time step τ is

$$\hat{\Delta}\ddot{x}_i = \frac{6}{\tau^2}\hat{\Delta}x_i - \frac{6}{\tau}\dot{x}_i - 3\ddot{x}_i \qquad (2.111)$$

From the next equation the incremental acceleration for the normal time step Δt is obtained by linear interpolation

$$\Delta\ddot{x}_i = \frac{1}{\theta}\hat{\Delta}\ddot{x}_i \qquad (2.112)$$

The incremental velocity $\Delta\dot{x}_i$ and the incremental displacement Δx_i are obtained by substituting the above value in eqns.(2.108) and (2.109) but written for the normal time step Δt. From these results, the initial acceleration for the next time step is obtained from the equation of motion at time $t + \Delta t$; thus

$$\ddot{x}_{i+1} = M^{-1}.[\, F_{i+1} - C_{i+1}.\dot{x}_{i+1} - K_{i+1}.x_{i+1} \,] \qquad (2.113)$$

where C_{i+1} and K_{i+1} represent the damping and stiffness coefficients evaluated at the end of the time step $ti+1 = t + \Delta t$. Once the displacement, velocity and acceleration vectors have been evaluated at the incremented time step, the outlined procedure can be repeated until any desired final time.

2.3.3 Algorithm for the direct integration technique

The algorithm presented herein was used to solve the equations of motion of shear buildings subjected to external forces and was incorporated in the

computer programs.

2.3.3.1 Linear analysis

For a particular extended time increment $\tau = \theta \Delta t$, the following steps are performed

1) Read the previously assembled structural stiffness matrix K, mass matrix M damping matrix C and read the excitation force vector.

2) Initial displacement – and velocity values $x(t_i)$ and $\dot{x}(t_i)$ are obtained either from values at the end of the previous time increment or as initial conditions of the problem.

3) The initial acceleration is evaluated from

$$M\ddot{x}_0 = F_0 - C\dot{x}_0 - Kx_0$$

4)* The incremental load and stiffness values are evaluated using eqns.(2.55) and (2.56).

5) Using these values calculate the incremental displacement and velocity values using eqns.(2.108) and (2.109).

6) Calculate the incremental acceleration for both the extended and normal time steps ($\hat{\Delta}\ddot{x}_i$ and $\Delta\ddot{x}_i$) using eqns.(2.111) and (2.112).

7) Evaluate the incremental velocity $\Delta\dot{x}_i$ and displacement Δx_i for the normal time step by substituting the value of $\Delta\ddot{x}_i$ into eqns.(2.108) and (2.109), note however that these two equations have to be modified appropriately for the normal time step Δt.

8)* Finally the velocity and displacement at the end of the time step are obtained from eqns.(2.58) and (2.59)

* – Note that the variables in these equations pertain to single degree of freedom systems. For this analysis they should be replaced by multi dimensional vectors of the same quantities of size n, where n is the number of degrees of freedom of the structure.

The calculations for the particular time step in consideration is completed and

the values obtained from step (8) are used as initial values for the next time increment. The whole procedure is repeated until the complete response of the structure until the desired time is obtained.

2.3.3.2 Nonlinear analysis

For the nonlinear analysis since the stiffness and damping properties of the structure are assumed to be changing with time, step (1) above is modified as follows:

1) Using the nonlinear properties of the structure assemble the stiffness matrix K and the damping matrix C. Read the excitation force vector

The rest of the procedure is as described for the linear analysis.

2.4 NUMERICAL EXAMPLES USING THE COMPUTER PROGRAMS

Computer programs were developed for the dynamic analysis of single and multi degree of freedom systems using the theory presented in this chapter. Four programs were written, two for the linear and nonlinear analysis of single degree of freedom systems and the other two for similar analysis of multi degree of freedom systems. In each of these programs the applied force to the structure could be input either as accelerations at the base of the structure or as forces at the storey levels.

The linear response of single degree of freedom systems was obtained by evaluating the Duhamel's integral at the given time intervals. The direct integration technique using the linear acceleration method was incorporated in the other programs to obtain the response. The algorithms used have been described in the previous sections. The programs were written to enable data to be input in any consistent system of units.

Two typical structures were analysed, the first one being a single storey shear frame, constructed of steel and carrying a flat concrete slab which was

rigidly attached to it at the roof level (Fig. 2−12). The structure was intentionally designed to be flexible thus enabling it to behave nonlinearly when subjected to large forces. The second structure was a three storey shear building (Fig. 2−13) which was designed to withstand relatively large forces. Both of these structures were subjected to the digitised accelerogram input of the Adak, Alaska earthquake of 1st May 1971 (See Appendix 2). The earthquake had a maximum intensity of approximately 0.06g in terms of acceleration. This earthquake was not a particularly strong one, it lasted for 20 seconds and large ground accelerations were existant even in its final seconds. This in effect would cause the analysed structures to undergo large displacements for almost its entire duration. To obtain nonlinear behaviour in both these structures they were subjected to three times the magnitude of the digitised accelerogram.

2.4.1 Structural details and results

The diagrams included at the end of the chapter show the configurations of the two structures analysed. The properties of the steel members were obtained from the Structural steel handbook[35]. The concrete slabs were assumed to have a density of 2400 kg/m^3. The results shown in graphical form are the comparison of displacements obtained using the linear and nonlinear analyses at each of the floor levels. For the three storey shear building the the natural frequencies and mode shapes calculated using the Jacobi method mentioned earlier are shown in a diagramatic form.

2.5 CONCLUSIONS

The concept of using two dimensional mathematical models to represent single or multistorey skeletal frames is a valid one provided that the behaviour of such frames is essentially two dimensional. The structures which were analysed using the computer programs were chosen to be symmetrical in their

plan view and the mass of the structures were effectively lumped at the floor levels. This in effect cancelled the effect of torsion in the structures and reduced the number of degrees of freedom.

From the results obtained using the computer programs the following points can be deduced.

1) Linear behaviour of structures is only valid when they are subjected to relatively small forces produced by minor earthquakes.

2) By using a nonlinear model the increase in displacements which will be encountered can be accounted for in the design procedure.

3) Comparison of the two curves in Fig. 2−14 shows that once the columns in the structure have yielded , the behaviour follows the same trend but the displacements pattern varies. As mentioned previously the magnitude of the input base acceleration was just sufficient to produce nonliner behaviour, which explains the small magnitude of variation in displacements between the two curves.

4) Figs. 2−16 show that only the third storey displacement was large enough to induce nonlinear behaviour in the columns at that level. In Fig. 2−16(c) the fact that the two curves follow the same pattern indicates that the only the first mode is dominant in obtaining the response. Contribution of the higher modes would result in a shift between the two curves.

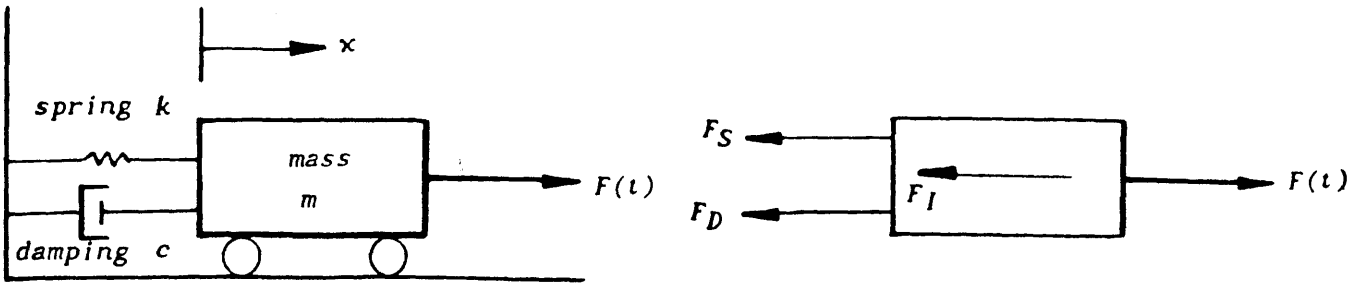

Fig.2-1 Mathematical model for a single degree of freedom system.

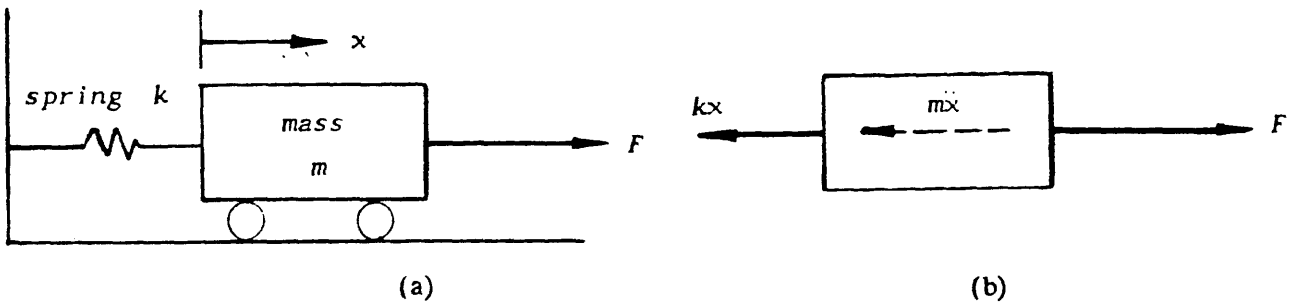

Fig. 2-2 (a) Mathematical model (b) Free body diagram

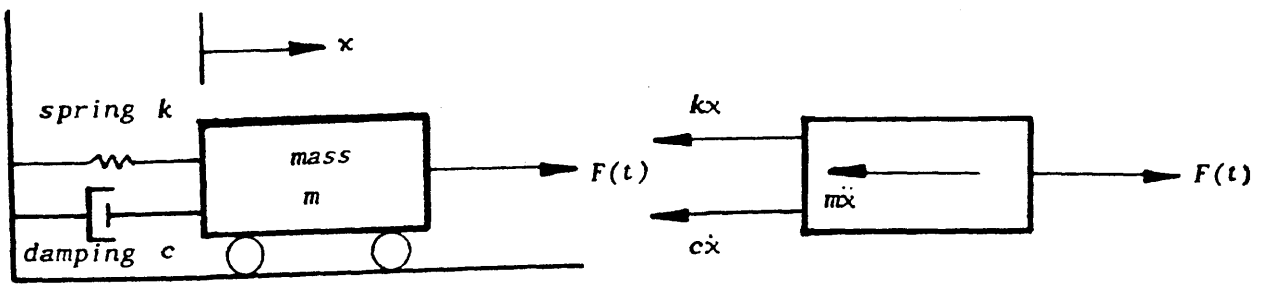

Fig. 2-3 (a) Mathematical model (b) Free body diagram

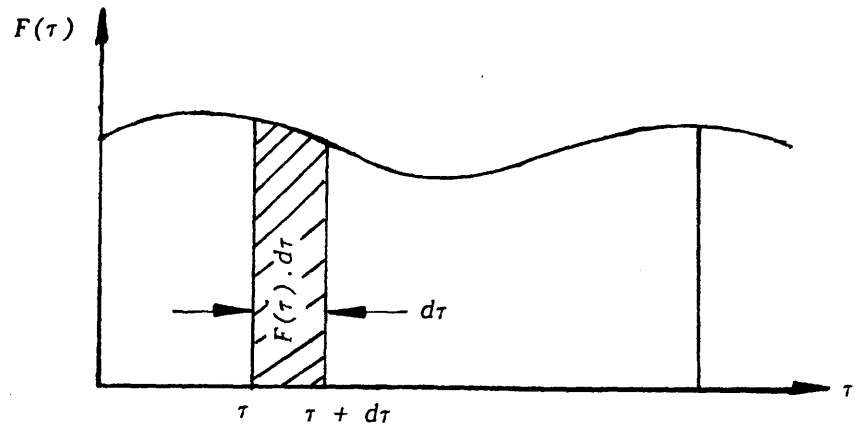

Fig. 2–4 General impulsive loading history

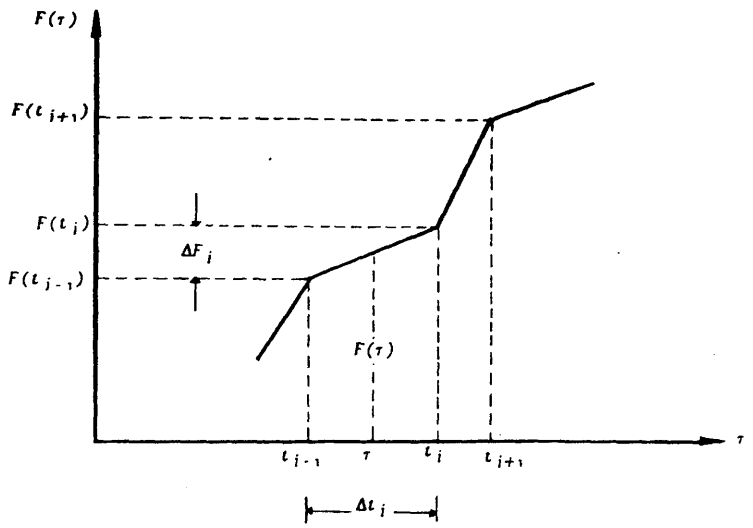

Fig. 2–5 Segmentally incremented loading function

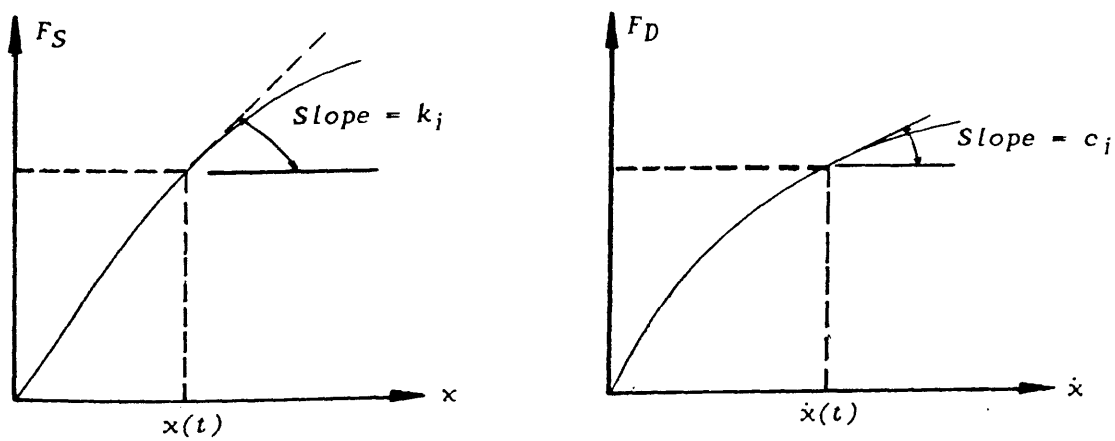

Fig. 2–6 Non linear stiffness and damping

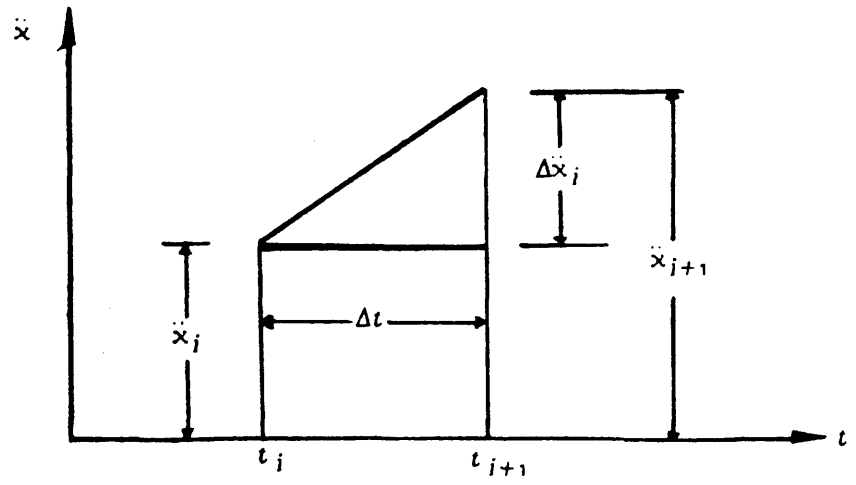

Fig. 2-7 Variation of acceleration within time step

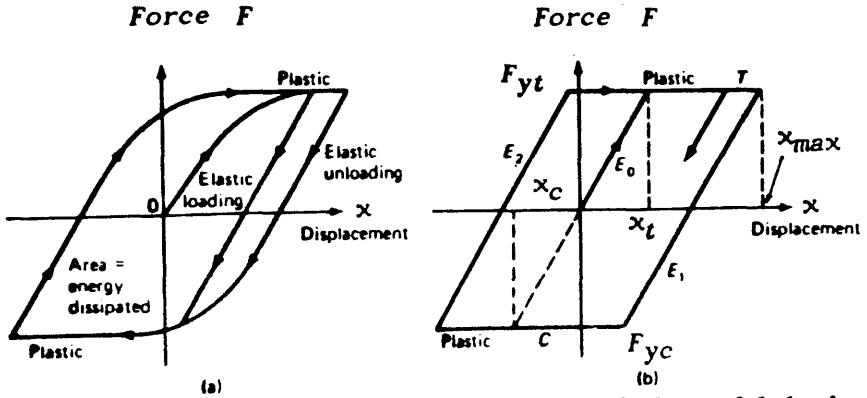

Fig.2– 8 Non linear load deformation curves (a) General behaviour

(b) Elastoplastic behaviour

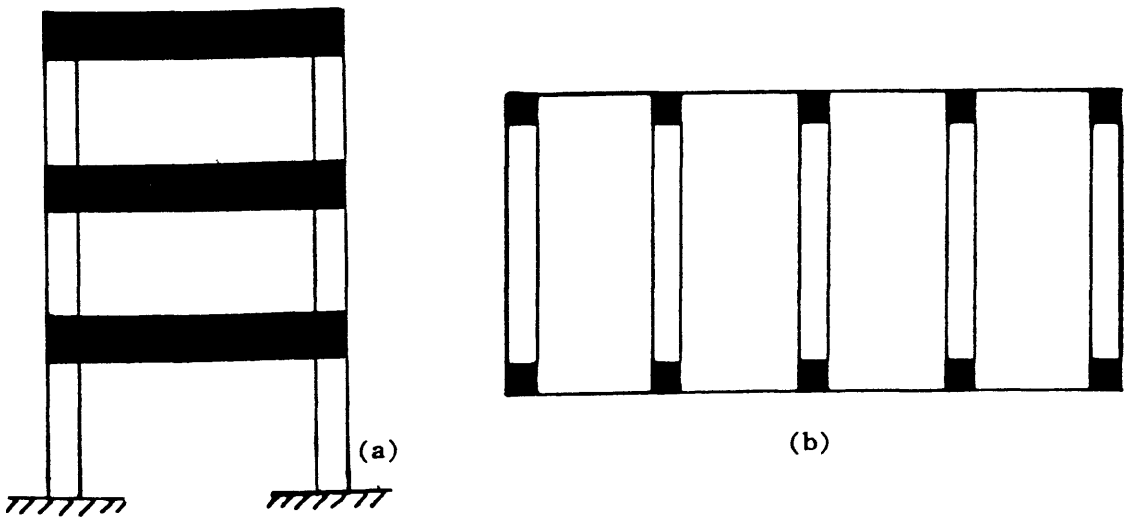

Fig.2-9 A typical shear building (a) A single bay (b) Plan view

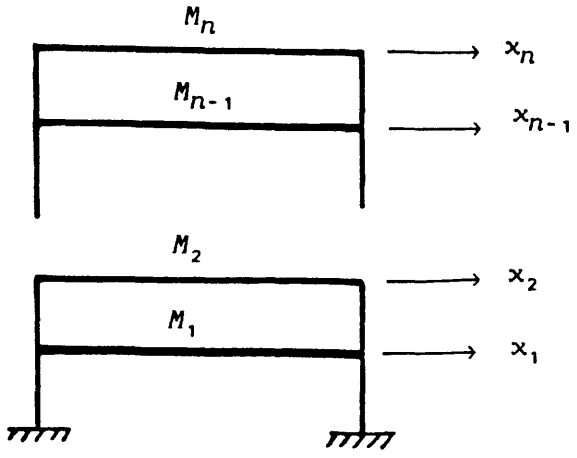

Fig.2—10 Single bay model of a shear building

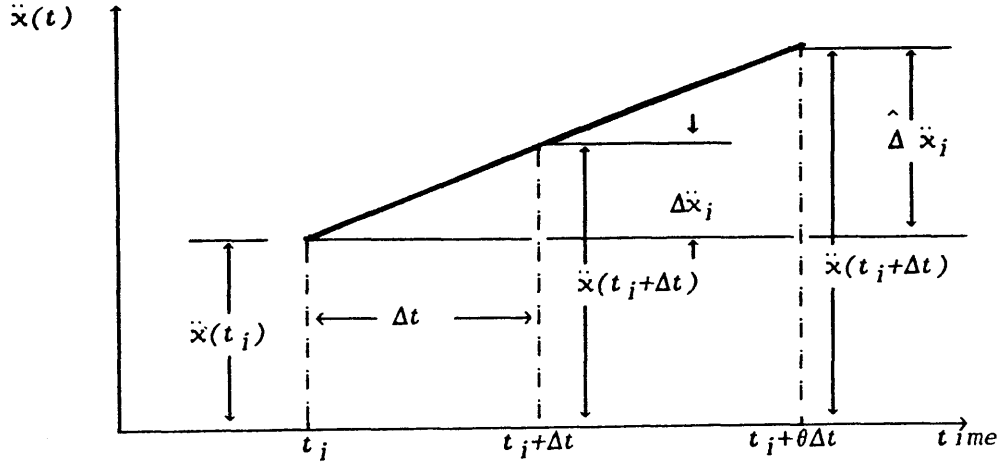

Fig.2-11 Variation of acceleration over the extended time step

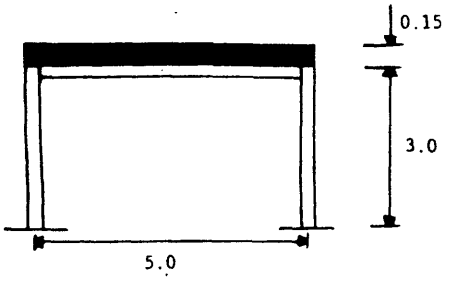

(a)

Column size 152 X 152 X 30 U.C

Beam size 203 X 133 X 30 U.B

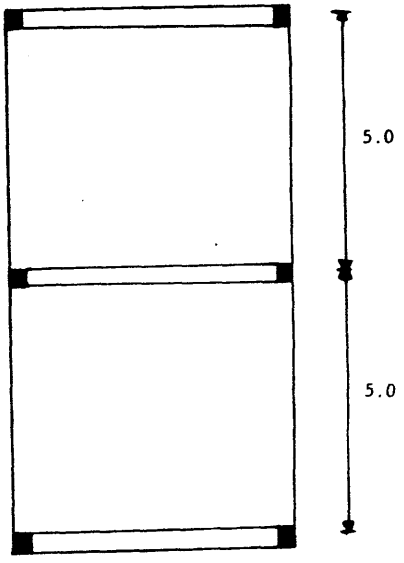

(b)

Fig. 2–12(a) Elevation of single storey shear frame.

Fig. 2–12(b) Plan view of the building

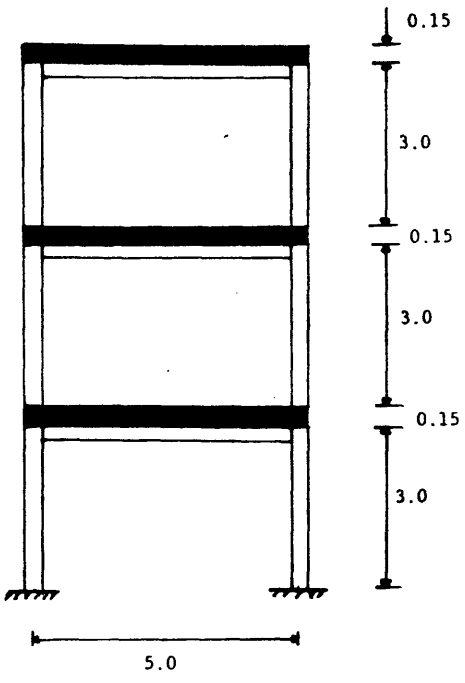

(a)

All columns 203 X 203 X 52 U.C

All beams 203 X 133 X 30 U.B

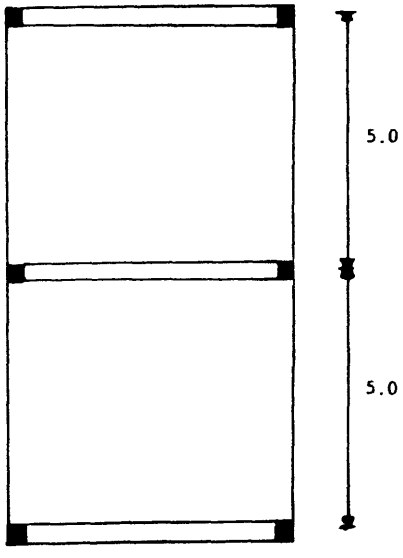

(b)

Fig. 2–13(a) Elevation of three storey shear building.

Fig. 2–13(b) Plan view of the building

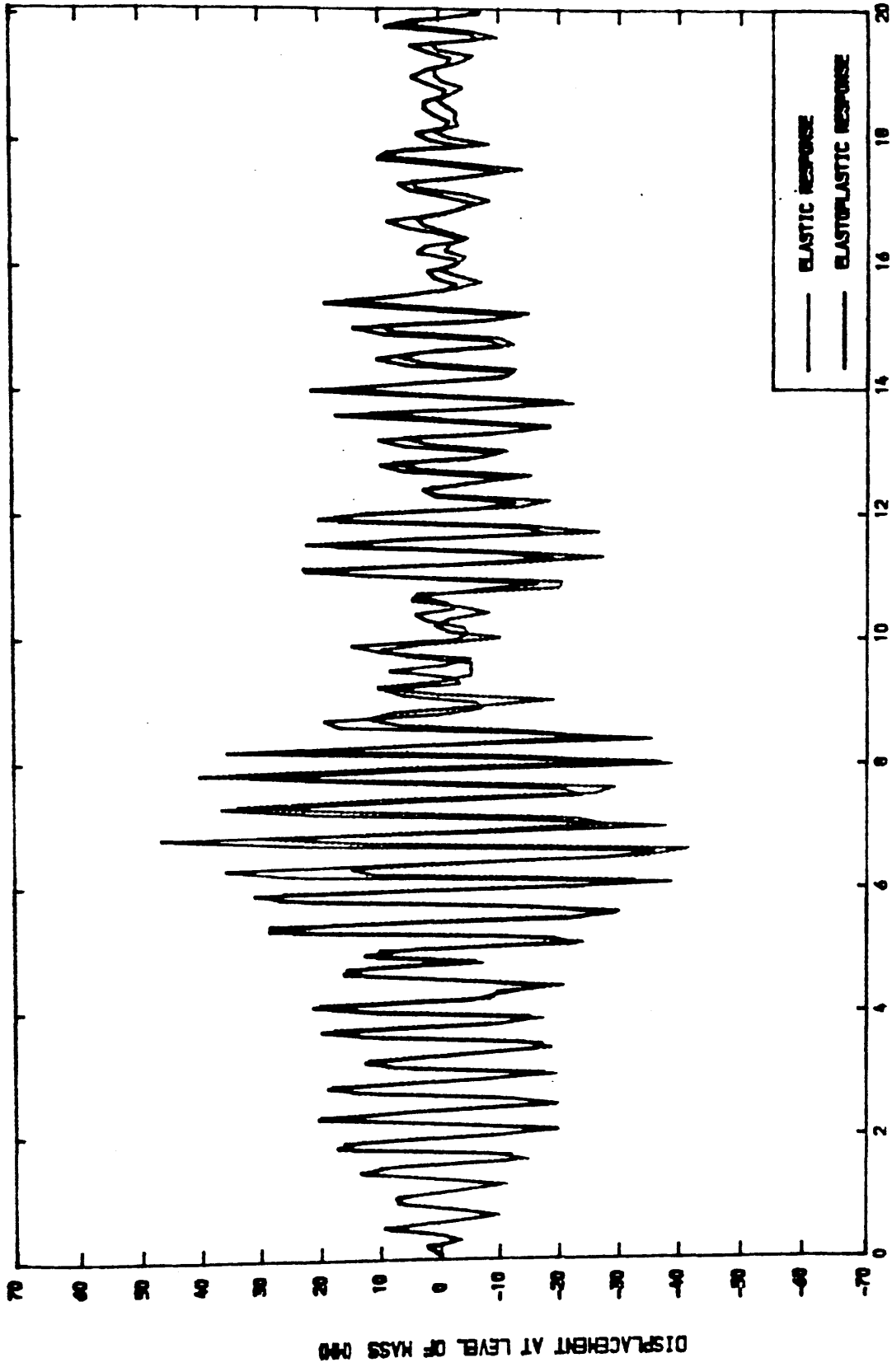

Fig. 2-14 DISPLACEMENT VS. TIME CURVE FOR S.D.O.F SYSTEM

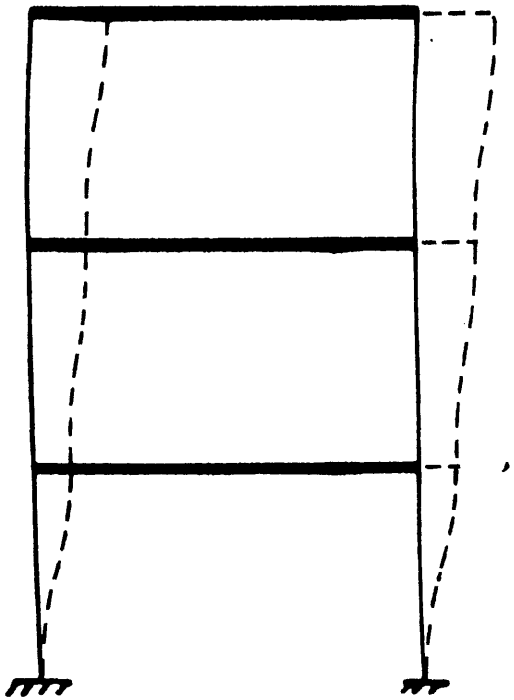

$f_1 = 1.60$ Hz.

Mode 1

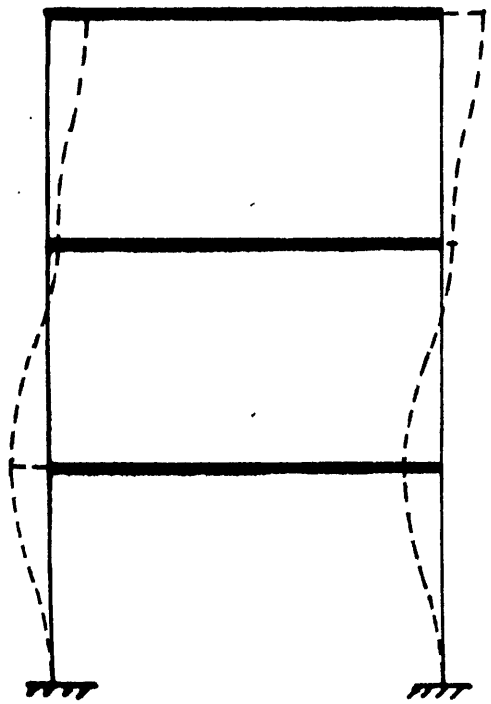

$f_2 = 3.97$ Hz.

Mode 2

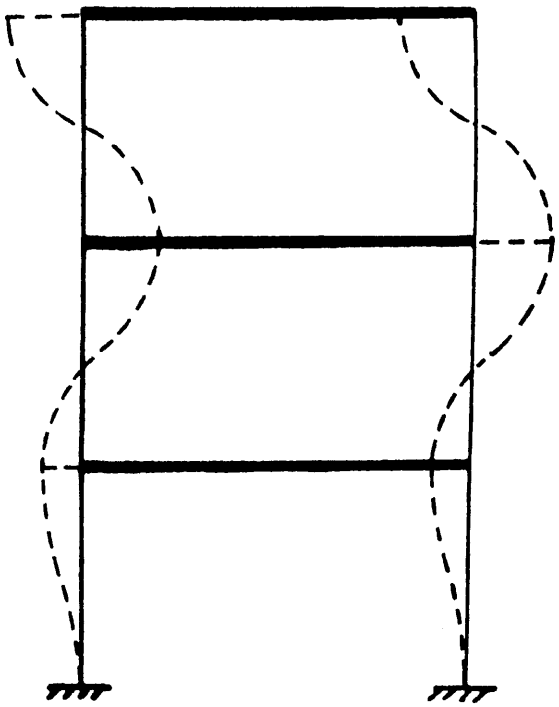

$f_3 = 6.09$ Hz.

Mode 3

Fig. 2.15 Mode shapes of the three storey shear frame

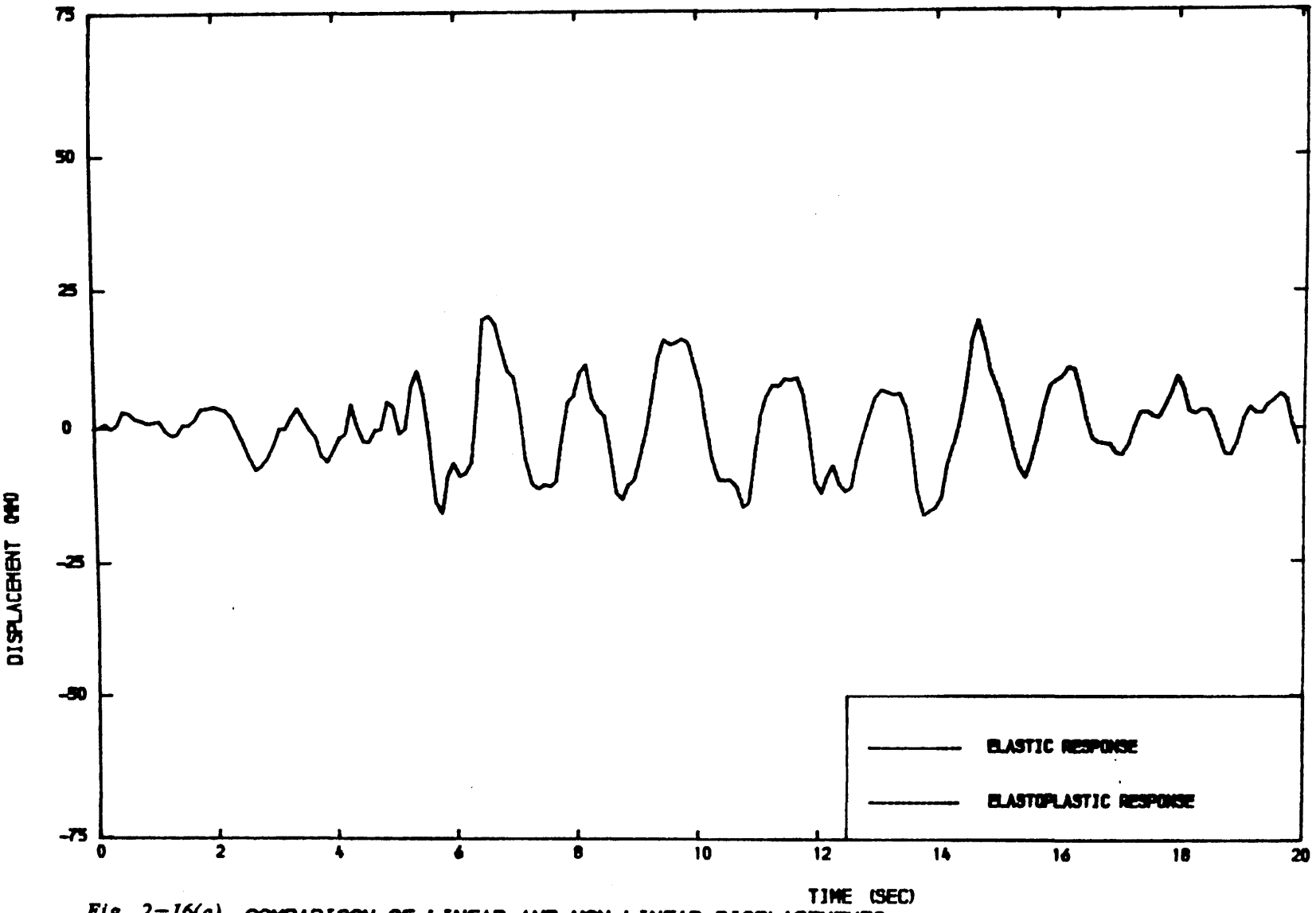

Fig. 2-16(a) COMPARISON OF LINEAR AND NON LINEAR DISPLACEMENTS LEVEL 1

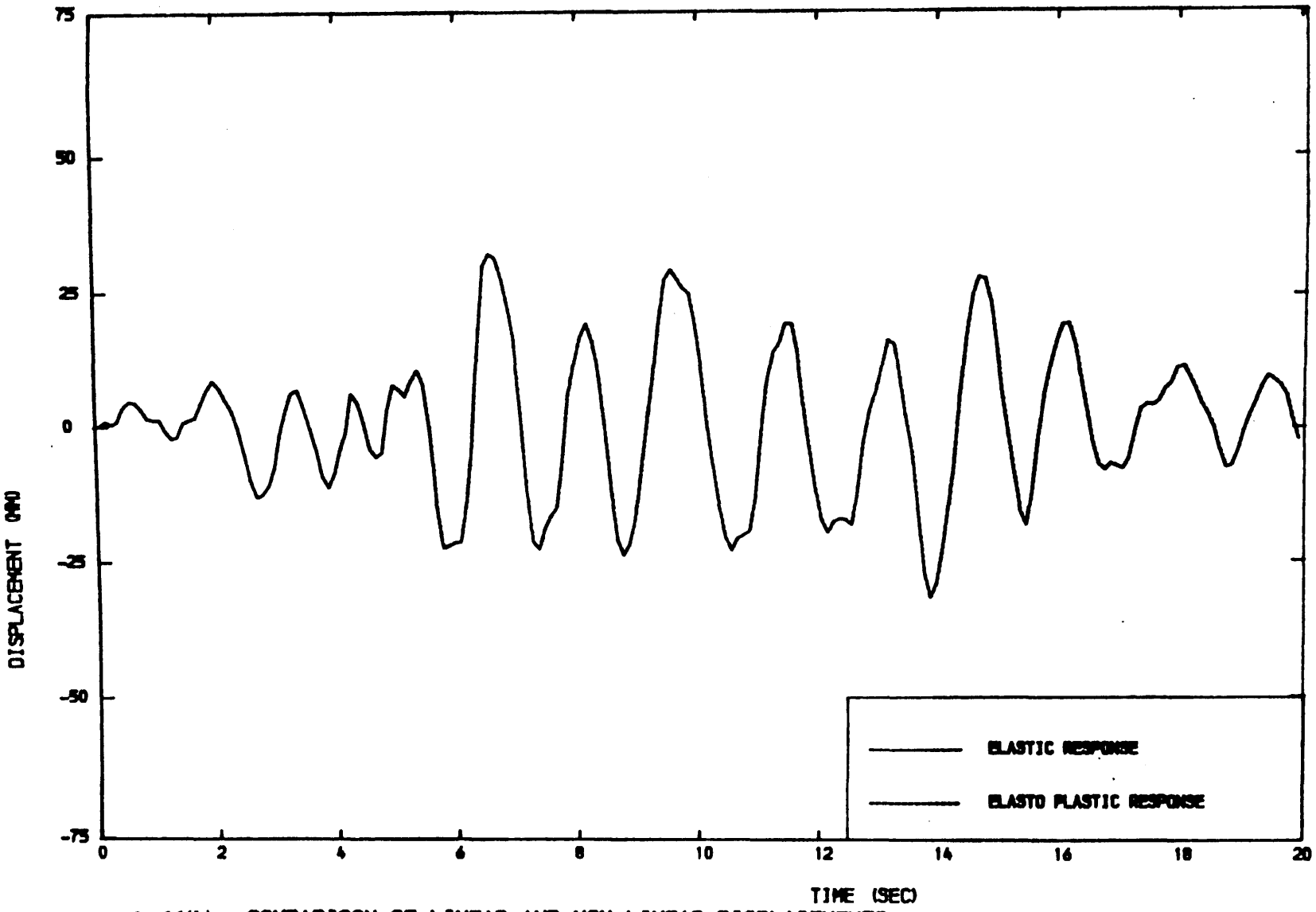

Fig. 2-16(b) COMPARISON OF LINEAR AND NON LINEAR DISPLACEMENTS LEVEL 2

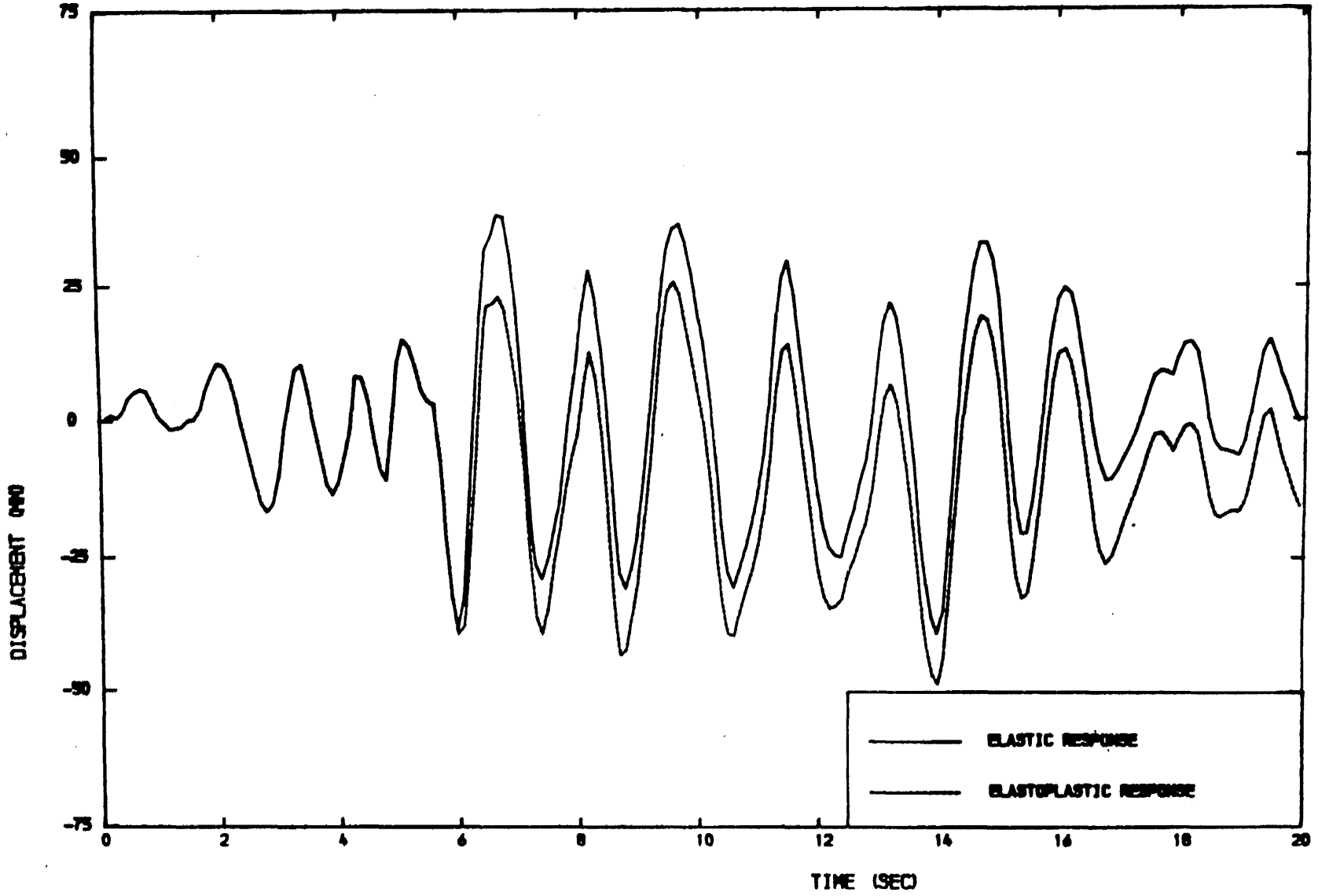

Fig. 2-16(c) COMPARISON OF LINEAR AND NON LINEAR DISPLACEMENTS LEVEL 3

CHAPTER 3 DYNAMIC ANALYSIS OF THREE DIMENSIONAL FRAMES

3.1 INTRODUCTION

In the previous chapter structures were analysed using two-dimensional mathematical models. Such analysis produces sufficiently accurate results provided the structural action is predominantly two dimensional and is applicable to structures which are symmetrical in plan and in which torsional behaviour is negligible.

In practice, however, the behaviour of most structural frameworks is essentially three dimensional and the structural analysis should be carried out using a three dimensional mathematical model. This chapter is concerned with such dynamic analysis of rigidly jointed skeletal frameworks. As in the previous chapters the stiffness method is used to analyse the dynamical behaviour. The 12 x 12 element stiffness and consistent mass matrices are used to assemble the overall stiffness and mass matrices.

Allowing all the degree of freedoms for each element leads to very large global stiffness and mass matrices even for a medium sized structure. The effort and cost involved in solving the resulting eigenproblem is high. To overcome this problem the size of these matrices is reduced using a technique known as *Dynamic Condensation*. The dynamic analysis of a typical skeletal framework using the full sized and condensed matrices is presented.

3.2 ELEMENT STIFFNESS AND MASS MATRICES

Fig. 3-1 shows a beam element of a three dimensional frame with its 12 degrees of freedom numbered consequently. The single arrow is used to indicate the translation components and the double arrow is used to indicate the rotational components of displacement. The notation of member axes

which will be used in the rest of the chapter is also shown.

- The element stiffness matrix shown below for a uniform prismatic beam element of a three dimensional frame is assembled by superpositioning the axial, flexural and torsional stiffness matrices.

$$k_e = \begin{bmatrix}
\frac{EA}{L} & 0 & 0 & 0 & 0 & 0 & -\frac{EA}{L} & 0 & 0 & 0 & 0 & 0 \\
 & \frac{12EI_z}{L^3} & 0 & 0 & 0 & \frac{6EI_z}{L^2} & 0 & -\frac{12EI_z}{L^3} & 0 & 0 & 0 & \frac{6EI_z}{L^2} \\
 & & \frac{12EI_y}{L^3} & 0 & -\frac{6EI_y}{L^2} & 0 & 0 & 0 & -\frac{12EI_y}{L^3} & 0 & -\frac{6EI_y}{L^2} & 0 \\
 & & & \frac{GJ}{L} & 0 & 0 & 0 & 0 & 0 & -\frac{GJ}{L} & 0 & 0 \\
 & & & & \frac{4EI_y}{L} & 0 & 0 & 0 & \frac{6EI_y}{L^2} & 0 & \frac{2EI_y}{L} & 0 \\
 & & & & & \frac{4EI_z}{L} & 0 & -\frac{6EI_z}{L^2} & 0 & 0 & 0 & \frac{2EI_z}{L} \\
 & & & & & & \frac{EA}{L} & 0 & 0 & 0 & 0 & 0 \\
 & & & & & & & \frac{12EI_z}{L^3} & 0 & 0 & 0 & -\frac{6EI_z}{L^2} \\
 & & \text{symmetric} & & & & & & \frac{12EI_y}{L^3} & 0 & \frac{6EI_y}{L^2} & 0 \\
 & & & & & & & & & \frac{GJ}{L} & 0 & 0 \\
 & & & & & & & & & & \frac{4EI_y}{L} & 0 \\
 & & & & & & & & & & & \frac{4EI_z}{L}
\end{bmatrix}$$

The consistent mass matrix shown below for a uniform beam element is assembled in a similar manner to the element stiffness matrix taking account

$$m_e = \rho AL \begin{bmatrix}
\frac{1}{3} & 0 & 0 & 0 & 0 & 0 & \frac{1}{6} & 0 & 0 & 0 & 0 & 0 \\
 & \frac{13}{35} & 0 & 0 & 0 & \frac{11}{210}L & 0 & \frac{9}{70} & 0 & 0 & 0 & -\frac{13}{420}L \\
 & & \frac{13}{35} & 0 & -\frac{11}{210} & 0 & 0 & 0 & \frac{9}{70} & 0 & \frac{13}{420}L & 0 \\
 & & & \frac{J}{3A} & 0 & 0 & 0 & 0 & 0 & \frac{J}{6A} & 0 & 0 \\
 & & & & \frac{L^2}{105} & 0 & 0 & 0 & -\frac{13}{420}L & 0 & -\frac{L^2}{140} & 0 \\
 & & & & & \frac{L^2}{105} & 0 & \frac{13}{420}L & 0 & 0 & 0 & -\frac{L^2}{140} \\
 & & & & & & \frac{1}{3} & 0 & 0 & 0 & 0 & 0 \\
 & & & & & & & \frac{13}{35} & 0 & 0 & 0 & -\frac{11}{210}L \\
 & & \text{symmetric} & & & & & & \frac{13}{35} & 0 & \frac{11}{210}L & 0 \\
 & & & & & & & & & \frac{J}{3A} & 0 & 0 \\
 & & & & & & & & & & \frac{L^2}{105} & 0 \\
 & & & & & & & & & & & \frac{L^2}{105}
\end{bmatrix}$$

3.3 COORDINATE TRANSFORMATION

The stiffness and mass matrices shown above are related to the local coordinate system. The x− axis is defined as coinciding with the centroidal line of the member. The local coordinate system may be different for different members. When a local coordinate system is used, the nodal degrees of freedom will also be taken in a convenient manner. In such a case before the element equations can be assembled, it is necessary to transform the element equations derived in local coordinates systems so that all the elemental equations are referred to a common global coordinate system. Fig. 3− 2(a) shows the two coordinate systems for an inclined member, the member axes are shown in lower case letters and the global axes are shown in capital letters, this will be the representation used in the rest of the chapter.

Using the stiffness method the element stiffness equations in a local coordinate system can be expressed in the standard form as

$$f_e = k_e . \delta_e \qquad (3\text{-}1)$$

where f_e is the force vector, k_e is the stiffness matrix and δ_e is the vector of nodal displacements of element e. Lower case letters and capital letters are used to represent the characterestics pertaining to the local and global coordinate systems respectively. Let a transformation matrix T_e exist, between the local and global coordinate systems such that

$$\delta_e = T_e . \Delta_e \qquad (3\text{-}2)$$

and

$$f_e = T_e . F_e \qquad (3\text{-}3)$$

By substituting eqns. (3− 2) and (3− 3) into eqn. (3− 1) we obtain

$$T_e . F_e = k_e . T_e . \Delta_e \qquad (3\text{-}4)$$

Premultiplying this equation throughout by T_e^{-1} yields

$$F_e = T_e^{-1} . k_e . T_e . \Delta_e \qquad (3\text{-}5)$$

or

$$F_e = K_e . \Delta_e \qquad (3\text{-}6)$$

where $$K_e = T_e^{-1} . k_e . T_e \qquad (3\text{-}7)$$

Since F_e and Δ_e are directional quantities, T_e will be the matrix of direction cosines relating to the two coordinate systems. In this case the transformation matrix will be orthogonal and hence

$$T_e^{-1} = T_e^T \qquad (3\text{-}8)$$

and $$K_e = T_e^T . k_e . T_e \qquad (3\text{-}9)$$

3.3.1 Transformation matrix

In the previous section the concept of coordinate transformation was introduced and in this section the assemblance of the transformation matrix will be described. This transformation matrix assembled here will correspond to the submatrices of the element and mass matrices. Figure 3–3 shows two reference systems shows two reference systems *x,y,z axes* representing the local axes and *X,Y,Z* axes representing the global system of coordinates. Also shown in the figure is a general vector $\bar{A}$ which may represent any force or nodal displacement. To obtain the components of vector $\bar{A}$ along one of the local axes *x,y* or *z*, it is necessary to add the projections of *X,Y* and *Z* components along that axis. For example, the component *x* of vector $\bar{A}$ along the *x* coordinate is given by

$$x = X \cos xX + Y \cos xY + Z \cos xZ \qquad (3\text{-}10a)$$

in which *cos xX* is the cosine of the angle between the *x* and *X* axes and corresponding definitions for the other cosines. Similarly the *y* and *z* components of $\bar{A}$ are

$$y = X \cos yX + Y \cos yY + Z \cos yZ \qquad (3\text{-}10b)$$

$$z = X \cos zX + y \cos zY + Z \cos zZ \qquad (3\text{-}10c)$$

These equations can be written in the matrix form as

$$\begin{bmatrix} x \\ y \\ z \end{bmatrix} = \begin{bmatrix} \cos xX & \cos xY & \cos xZ \\ \cos yX & \cos yY & \cos yZ \\ \cos zX & \cos zY & \cos zZ \end{bmatrix} \begin{bmatrix} X \\ Y \\ Z \end{bmatrix} \qquad (3\text{-}11)$$

or alternatively as

$$\begin{bmatrix} x \\ y \\ z \end{bmatrix} = \begin{bmatrix} l_x & m_x & n_x \\ l_y & m_y & n_y \\ l_z & m_z & n_z \end{bmatrix} \begin{bmatrix} X \\ Y \\ Z \end{bmatrix} = [T_m] \begin{bmatrix} X \\ Y \\ Z \end{bmatrix} \qquad (3\text{-}12)$$

where l_x, m_x and n_x are the direction cosines of the member 'x' axis. The problem is to find the remaining elements of the transformation matrix as l_x, m_x, and n_x define only the orientation of the member 'x' axis (i.e the member 'y' and 'z' axes can be rotated about the member 'x' axis to take up any orientation).It should be noted that the transformation matrix $[T_m]$ corresponds to the first three degrees of freedom i.e the translations at end 'i' of a member and the same matrix will apply for the three rotational degrees of freedom, therefore the complete transformation matrix for an element will be a 6 X 6 matrix.

The problem may be solved by using vector cross products. The vector cross product $\bar{C}$ of two vectors $\bar{A}$ and $\bar{B}$ is defined as follows

$$\bar{A} = \bar{I}\, x_a + \bar{J}\, y_a + \bar{K}\, z_a \qquad (3\text{-}13)$$

$$\bar{B} = \bar{I}\, x_b + \bar{J}\, y_b + \bar{K}\, z_b \qquad (3\text{-}14)$$

$$\bar{C} = \bar{A} \times \bar{B} = \begin{vmatrix} \bar{I} & \bar{J} & \bar{K} \\ x_a & y_a & z_a \\ x_b & y_b & z_b \end{vmatrix} \qquad (3\text{-}15)$$

where $\bar{C}$ is the third vector normal to the plane of $\bar{A}$ and $\bar{B}$ and is directed such that $\bar{A}$, $\bar{B}$ and $\bar{C}$ form a right hand system. The length of $\bar{C}$ is $|\bar{A}||\bar{B}||\sin \bar{A}.\bar{B}|$

$\sin \bar{A}.\bar{B}$ is the absolute value of the sine of the angle between $\bar{A}$ and $\bar{B}$.

$\bar{I},\bar{J},\bar{K}$ are unit vectors in the direction of the 'x','y' and 'z' axes respectively.

x_a, y_a, z_a are the magnitudes of the components of the vector $\bar{A}$ in the direction of the 'x','y' and 'z' axes respectively.

x_b, y_b, z_b are the magnitudes of the components of the vector $\bar{B}$ in the direction of the 'x','y' and 'z' axes respectively.

l_x, m_x, and n_x are effectively the components in the directions of the global 'x','y' and 'z' axes of a unit vector lying along the member 'x' axis. If the member 'y' axis, which is perpendicular to the member 'x' axis, lies in the global 'x,y', it must also be perpendicular to the global 'z' axis. Hence the cross product of unit vectors lying along the global 'z' and the member 'x' axes must result in a vector Z in the direction of the member 'y' axis.

$$Z = \begin{vmatrix} \bar{I} & \bar{J} & \bar{K} \\ 0 & 0 & 1 \\ l_x & m_x & n_x \end{vmatrix} = -\bar{I}\, m_x + \bar{J}\, l_x + \bar{K}\, 0 \qquad (3\text{-}16)$$

The length of Z is $|1||1||\sqrt{(1-n_x^2)}|$ as $\sin\theta = \sqrt{(1-\cos^2\theta)}$

l_y, m_y, and n_y are the components in the global axis system of a unit vector lying on the member 'y' axis. Hence the direction cosines of the member 'y' axis are found by scaling Z to make a unit vector.

$$Z/\sqrt{(1-n_x^2)} = -\bar{I}\, m_x/\sqrt{(1-n_x^2)} + \bar{J}\, l_x/\sqrt{(1-n_x^2)} + \bar{K}\, 0 \qquad (3\text{-}17)$$

i.e

$$l_y = -m_x/\sqrt{(1-n_x^2)} \qquad (3\text{-}18)$$

$$m_y = l_x/\sqrt{(1-n_x^2)} \qquad (3\text{-}19)$$

$$n_y = 0 \qquad (3\text{-}20)$$

A vector in the direction of the member 'z' axis is generated by taking the cross product of unit vectors lying along the member 'x' and 'y' axes

$$Z = \begin{vmatrix} \bar{I} & \bar{J} & \bar{K} \\ l_x & m_x & n_x \\ l_y & m_y & n_y \end{vmatrix} \qquad (3\text{-}21)$$

Using the same procedure as above the terms in the third row of the transformation matrix can also be expressed in terms of the direction cosines of the member 'x' axis as follows

$$l_z = -l_x n_x / \sqrt{(1-n_x^2)} \qquad (3\text{-}22)$$

$$m_z = -m_x n_x / \sqrt{(1-n_x^2)} \qquad (3\text{-}23)$$

$$n_z = \sqrt{(1-n_x^2)} \qquad (3\text{-}24)$$

As all the direction cosines have now been expressed in terms of l_x, m_x and n_x the transformation matrix becomes

$$[T_m] = \begin{bmatrix} l_x & m_x & n_x \\ -m_x/D & l_x/D & 0 \\ -l_x n_x/D & -m_x n_x/D & D \end{bmatrix} \qquad (3\text{-}25)$$

where $D = \sqrt{(1-n_x^2)}$

The transformation matrix shown in Eqn. (3−25) transforms the vectors of nodal forces , nodal masses and nodal displacements from the global axes system to the member axes system for an element 'i,j'. The inverse of the matrix shown below is used for the reverse transformation (i.e from the member to the global axes system)

$$[T_m]^{-1} = \begin{bmatrix} l_x & -m_x/D & -l_x n_x/D \\ m_x & l_x/D & -m_x n_x/D \\ n_x & 0 & D \end{bmatrix} \qquad (3\text{-}26)$$

In the full form the transformation matrix will be

$$[T_{ij}] = \begin{bmatrix} l_x & m_x & n_x & 0 & 0 & 0 \\ -m_x/D & l_x/D & 0 & 0 & 0 & 0 \\ -l_x n_x/D & -m_x n_x/D & D & 0 & 0 & 0 \\ 0 & 0 & 0 & l_x & m_x & n_x \\ 0 & 0 & 0 & -m_x/D & l_x/D & 0 \\ 0 & 0 & 0 & -l_x n_x/D & -m_x n_x/D & D \end{bmatrix} \qquad (3\text{-}27)$$

$[T_{ij}]^{-1}$ will be the inverse of the above matrix.

3.3.1.1 Rotation of element about member 'x' axis

In the previous section in obtaining the transformation matrix the member 'y' axis was forced to lie in the global 'x,y' plane, however this restriction means that the member 'y' and 'z' axes will not necessarily coincide with the principal axes (x^*,y^*) of the section. Fig. 3−2(b) illustrates the general case, where the member is viewed at from end 'i'. The principal 'x' axis and the member 'x' axis are always coincident and β is the anticlockwise rotation which will make the principal axes coincide with the member axes.

The transformation required of member end displacements and rotations form the member axes to the principal axis system is as follows

$$[T_{ij}^*] = \begin{bmatrix} 1 & 0 & 0 & 0 & 0 & 0 \\ 0 & \cos\beta & \sin\beta & 0 & 0 & 0 \\ 0 & -\sin\beta & \cos\beta & 0 & 0 & 0 \\ 0 & 0 & 0 & 1 & 0 & 0 \\ 0 & 0 & 0 & 0 & \cos\beta & \sin\beta \\ 0 & 0 & 0 & 0 & -\sin\beta & \cos\beta \end{bmatrix} \qquad (3\text{-}28)$$

The reverse transformation is

$$[T_{ij}^*]^{-1} = \begin{bmatrix} 1 & 0 & 0 & 0 & 0 & 0 \\ 0 & \cos\beta & -\sin\beta & 0 & 0 & 0 \\ 0 & \sin\beta & \cos\beta & 0 & 0 & 0 \\ 0 & 0 & 0 & 1 & 0 & 0 \\ 0 & 0 & 0 & 0 & \cos\beta & -\sin\beta \\ 0 & 0 & 0 & 0 & \sin\beta & \cos\beta \end{bmatrix} \qquad (3\text{-}29)$$

In Eqns. (3−27) and (3−28) β the anticlockwise rotation required to make the principal and member axes to coincide has to be determined, this rotation cannot always be assessed by inspection and the following section describes a general method for its determination.

3.3.1.1.1 Third node method

This method as its name suggests involves using a third node which would enable the principal 'x,y' plane to be defined. This point 'p' may lie

anywhere on the principal 'x,y' plane except on the principal 'x' axis. Consider the member shown in Fig. 3−3, the three points 'i','j' and 'p' define the principal 'x,y' plane.

The cross product of two independent vectors lying on the principal 'x,y' plane will result in a vector normal to that plane i.e in the direction of the principal 'z' axis. The nodes 'i' and 'j' provide one vector and the nodes 'i' and 'p' provide the other. Hence

$$\bar{Z} = \begin{vmatrix} \bar{I} & \bar{J} & \bar{K} \\ (x_j - x_i) & (y_j - y_i) & (z_j - z_i) \\ (x_p - x_i) & (y_p - y_i) & (z_p - z_i) \end{vmatrix} \qquad (3\text{-}30)$$

$$\bar{Z} = \bar{I}\, X_Z^* + \bar{J}\, Y_Z^* + \bar{K}\, Z_Z^* \qquad (3\text{-}31)$$

The length of this vector is

$$L = \sqrt{\left(X_Z^{*2} + Y_Z^{*2} + Z_Z^{*2} \right)} \qquad (3\text{-}32)$$

and the direction cosines are

$$l_Z^* = X_Z^*/L \qquad (3\text{-}33)$$

$$m_Z^* = Y_Z^*/L \qquad (3\text{-}34)$$

$$n_Z^* = Z_Z^*/L \qquad (3\text{-}35)$$

l_Z^*, m_Z^* and n_Z^* are the components in the global axes system of a unit vector lying on the principal 'z' axis and l_Z, m_Z and n_Z are the components of a unit vector lying on the member 'z' axis. The angle between these unit vectors (β) can be found using the cosine rule

$$\beta = \cos^{-1} ((a^2 + b^2 - c^2)/ 2ab) \qquad (3\text{-}36)$$

but since 'a' and 'b' are unit vectors

$$\beta = \cos^{-1} ((1 - c^2)/2) \qquad (3\text{-}37)$$

where

$$c^2 = (l_Z^* - l_Z)^2 + (m_Z^* - m_Z)^2 + (n_Z^* - n_Z)^2 \qquad (3\text{-}38)$$

In the case where the angle between the member 'y' axis and the principal 'z' axis is less than 90° ,then the value of β found would be wrong and would have to be set equal to $(360 - \beta)^\circ$. This is due to the fact that

the vector cross product always produces a right hand system.

3.4 ELEMENT STIFFNESS MATRIX IN THE GLOBAL AXES SYSTEM

An element stiffness matrix is normally divided into submatrices to take account of the contributions of the two ends of the elements as follows:

$$k_e = \begin{bmatrix} k^i_{ii} & k_{ij} \\ k_{ji} & k^i_{jj} \end{bmatrix} \qquad (3\text{-}39)$$

Now that the transformation matrices from the principal axes to the member axes ($[T^*_{ij}]^{-1}$) and from the local axes to the global axes ($[T_{ij}]^{-1}$) have been assembled each of the global submatrices may be assembled in the following manner. Using eqn. (3–9)

$$K^j_{ii} = [T_{ij}]^{-1}.[T^*_{ij}]^{-1}\cdot k^{j*}_{ii}.[T^*_{ij}].[T_{ij}] \qquad (3\text{-}40)$$

$$K_{ij} = [T_{ij}]^{-1}.[T^*_{ij}]^{-1}\cdot k^*_{ij}.[T^*_{ij}].[T_{ij}] \qquad (3\text{-}41)$$

$$K_{ji} = [T_{ij}]^{-1}.[T^*_{ij}]^{-1}\cdot k^*_{ji}.[T^*_{ij}].[T_{ij}] \qquad (3\text{-}42)$$

and $$K^i_{jj} = [T_{ij}]^{-1}.[T^*_{ij}]^{-1}\cdot k^{i*}_{jj}.[T^*_{ij}].[T_{ij}] \qquad (3\text{-}43)$$

Since k_{ij} and k_{ji} are transposes of each other and since k^j_{ii} and k^i_{jj} are the same with only the non diagonal terms negative of each other expanding eqns. (3–40) and (3–41) will enable the whole element stiffness matrix to be assembled.

From the above equations it can be seen that for the evaluation of one global submatrix five, 6 x 6 matrices have to be multiplied. This involves a lot of multiplications and additions, and even though programming a computer to handle the task is straightforward, the time taken for the evaluation of global element stiffness matrix can become unacceptably long as the number of elements increases. Significant savings in computer time and memory can be made by expanding the multiplication of the transformation matrices

$$[T_{ij}]^{-1}.[T_{ij}^{*}]^{-1} = \begin{bmatrix} T_1 & T_2 & T_3 & 0 & 0 & 0 \\ T_4 & T_5 & T_6 & 0 & 0 & 0 \\ T_7 & T_8 & T_9 & 0 & 0 & 0 \\ 0 & 0 & 0 & T_1 & T_2 & T_3 \\ 0 & 0 & 0 & T_4 & T_5 & T_6 \\ 0 & 0 & 0 & T_7 & T_8 & T_9 \end{bmatrix} \qquad (3\text{-}44)$$

where

$T_1 = l$ (0)

$T_2 = -(m\cos\beta + ln\sin\beta)/D$ ($-n\sin\beta$)

$T_3 = (m\sin\beta - ln\cos\beta)/D$ ($-n\cos\beta$)

$T_4 = m$ (0)

$T_5 = (l\cos\beta - mn\sin\beta)/D$ ($\cos\beta$)

$T_6 = -(l\sin\beta + mn\cos\beta)/D$ $-(\sin\beta)$

$T_7 = n$ (n)

$T_8 = D\sin\beta$ (0)

$T_9 = D\cos\beta$ (0)

The values in brackets are those used for the special case where the member lies parallel to the global 'z' axis.

$$[T_{ij}^{*}].[T_{ij}] = [[T_{ij}]^{-1}.[T_{ij}^{*}]^{-1}]^{-1} \qquad (3\text{-}45)$$

which is the transpose of the matrix shown in eqn. (3−44).

In eqns. (3−40) and (3−41) the submatrices k_{ii}^{j*} and k_{ij}^{*} can be written in terms of stiffness coefficient terms or 'k' terms as follows:

$$k_{ii}^{j*} = \begin{bmatrix} K_1 & 0 & 0 & 0 & 0 & 0 \\ 0 & K_2 & 0 & 0 & 0 & K_7 \\ 0 & 0 & K_3 & 0 & K_8 & 0 \\ 0 & 0 & 0 & K_4 & 0 & 0 \\ 0 & 0 & K_9 & 0 & K_5 & 0 \\ 0 & K_{10} & 0 & 0 & 0 & K_6 \end{bmatrix} \qquad (3\text{-}46)$$

and

$$k_{ij}^{*} = \begin{bmatrix} -K_1 & 0 & 0 & 0 & 0 & 0 \\ 0 & -K_2 & 0 & 0 & 0 & K_7 \\ 0 & 0 & -K_3 & 0 & K_8 & 0 \\ 0 & 0 & 0 & -K_4 & 0 & 0 \\ 0 & 0 & -K_9 & 0 & -K_5/2 & 0 \\ 0 & -K_{10} & 0 & 0 & 0 & -K_6/2 \end{bmatrix} \qquad (3\text{-}47)$$

where

$K_1 = EA/L$ $\qquad$ $K_2 = 12\ EI_z/L^3$

$K_3 = 12\ EI_y/L^3$ $\qquad$ $K_4 = GJ/L$

$K_5 = 4\ EI_y/L$ $\qquad$ $K_6 = 4\ EI_z/L$

$K_7 = 6\ EI_z/L^2$ $\qquad$ $K_8 = -6\ EI_y/L^2$

$K_9 = -6\ EI_y/L^2$ $\qquad$ $K_{10} = 6\ EI_z/L^2$

The global stiffness submatrix can now be expressed in the expanded form, the first submatrix will be expanded in full, and the same expanded matrix may be used to assemble the other submatrices by making a few alterations to some of the terms. This procedure may be adopted due to the similarity in the arrangement of terms in the submatrices.

$$K_{ij} = [T_{ij}]^{-1} \cdot [T^*_{ij}]^{-1} \cdot k^*_{ij} \cdot [T^*_{ij}] \cdot [T_{ij}] = \begin{bmatrix} A & B \\ C & D \end{bmatrix} \quad (3\text{-}48)$$

The submatrices A,B,C and D are shown below

$$\begin{bmatrix} (K_1T_1^2 + K_2T_2^2 + K_3T_3^2) & (K_1T_1T_4 + K_2T_2T_5 + K_3T_3T_6) & (K_1T_1T_7 + K_2T_2T_8 + K_3T_3T_9) \\ (K_1T_4T_1 + K_2T_5T_2 + K_3T_6T_3) & (K_1T_4^2 + K_2T_5^2 + K_3T_6^2) & (K_1T_4T_7 + K_2T_5T_8 + K_3T_6T_9) \\ (K_1T_7T_1 + K_2T_8T_2 + K_3T_9T_3) & (K_1T_7T_4 + K_2T_8T_5 + K_3T_9T_6) & (K_1T_7^2 + K_2T_8^2 + K_3T_9^2) \end{bmatrix} \quad (3\text{-}49$$

$$\begin{bmatrix} (K_7T_2T_3 + K_8T_3T_2) & (K_7T_2T_6 + K_8T_3T_5) & (K_7T_2T_9 + K_8T_3T_8) \\ (K_7T_5T_3 + K_8T_6T_2) & (K_7T_5T_6 + K_8T_6T_5) & (K_7T_5T_9 + K_8T_6T_8) \\ (K_7T_8T_3 + K_8T_9T_2) & (K_7T_8T_6 + K_8T_9T_5) & (K_7T_8T_9 + K_8T_9T_8) \end{bmatrix} \quad (3\text{-}50$$

$$\begin{bmatrix} (K_9T_2T_3 + K_{10}T_3T_2) & (K_9T_2T_6 + K_{10}T_3T_5) & (K_9T_2T_9 + K_{10}T_3T_8) \\ (K_9T_5T_3 + K_{10}T_6T_2) & (K_9T_5T_6 + K_{10}T_6T_5) & (K_9T_5T_9 + K_{10}T_6T_8) \\ (K_9T_8T_3 + K_{10}T_9T_2) & (K_9T_8T_6 + K_{10}T_9T_5) & (K_9T_8T_9 + K_{10}T_9T_8) \end{bmatrix} \quad (3\text{-}51$$

$$\begin{bmatrix} (K_4T_1^2 + K_5T_2^2 + K_6T_3^2) & (K_4T_1T_4 + K_5T_2T_5 + K_6T_3T_6) & (K_4T_1T_7 + K_5T_2T_8 + K_6T_3T_9) \\ (K_4T_4T_1 + K_5T_5T_2 + K_6T_6T_3) & (K_4T_4^2 + K_5T_5^2 + K_6T_6^2) & (K_4T_4T_7 + K_5T_5T_8 + K_6T_6T_9) \\ (K_4T_7T_1 + K_5T_8T_2 + K_6T_9T_3) & (K_4T_7T_4 + K_5T_8T_5 + K_6T_9T_6) & (K_4T_7^2 + K_5T_8^2 + K_6T_9^2) \end{bmatrix} \quad (3\text{-}52$$

Taking advantage of the symmetry of the global element stiffness matrix only the upper triangle needs to be evaluated. By using the expansion described above the arithmetic for the evaluation of one global element submatrix is reduced to to 180 multiplications and 54 additions as opposed to 3456 multiplications and 2880 additions which would be required if the matrix multiplication of the five 6 x 6 matrices was carried out.

3.5 ELEMENT MASS MATRIX IN THE GLOBAL AXES SYSTEM

The element mass matrix is also subdivided into submatrices in a similar fashion as the element stiffness matrix

$$m_e = \begin{bmatrix} m_{ii}^{j} & m_{ij} \\ m_{ji} & m_{jj}^{j} \end{bmatrix} \qquad (3\text{-}53)$$

Using the same transformation matrices each of the global mass submatrices may be assembled in a similar manner as the global element stiffness submatrices. Using eqn (3–9)

$$M_{ii}^{j} = [T_{ij}]^{-1}.[T_{ij}^{*}]^{-1}\cdot m_{ii}^{j*}.[T_{ij}^{*}].[T_{ij}] \qquad (3\text{-}54)$$

$$M_{ij} = [T_{ij}]^{-1}.[T_{ij}^{*}]^{-1}\cdot m_{ij}^{*}.[T_{ij}^{*}].[T_{ij}] \qquad (3\text{-}55)$$

$$M_{ji} = [T_{ij}]^{-1}.[T_{ij}^{*}]^{-1}\cdot m_{ji}^{*}.[T_{ij}^{*}].[T_{ij}] \qquad (3\text{-}56)$$

and $$M_{jj}^{j} = [T_{ij}]^{-1}.[T_{ij}^{*}]^{-1}\cdot m_{jj}^{j*}.[T_{ij}^{*}].[T_{ij}] \qquad (3\text{-}57)$$

In the case of the element mass matrix as well, m_{ij} and m_{ji} are transposes of each other, but unlike the element stiffness matrix where simple mathematical relationships exist between the terms of k_{ii} and k_{ij} (see eqns. 3–46 and 3–47), the terms of m_{ii} and m_{ij} vary more widely . This leads to more hand expansions of the transformation matrices so as to achieve the same efficiency as for the element stiffness matrix case.The transformation matrices are the same shown in eqns. (3–44) and (3–45).

To enable eqns. (3–54) and (3–55) to be expanded m_{ii}^{j*} and m_{ij}^{*} are expressed in terms of mass coefficients as follows:

$$m_{ii}^{j*} = \rho AL \begin{bmatrix} M_1 & 0 & 0 & 0 & 0 & 0 \\ 0 & M_2 & 0 & 0 & 0 & M_7 \\ 0 & 0 & M_3 & 0 & M_8 & 0 \\ 0 & 0 & 0 & M_4 & 0 & 0 \\ 0 & 0 & M_9 & 0 & M_5 & 0 \\ 0 & M_{10} & 0 & 0 & 0 & M_6 \end{bmatrix} \qquad (3\text{-}58)$$

and

$$m_{ij}^{*} = \rho AL \begin{bmatrix} \frac{M_1}{2} & 0 & 0 & 0 & 0 & 0 \\ 0 & \frac{9M_2}{26} & 0 & 0 & 0 & \frac{-13M_7}{22} \\ 0 & 0 & \frac{9M_3}{26} & 0 & \frac{-13M_8}{22} & 0 \\ 0 & 0 & 0 & \frac{M_4}{2} & 0 & 0 \\ 0 & 0 & \frac{13M_9}{22} & 0 & \frac{-3M_5}{4} & 0 \\ 0 & \frac{13M_{10}}{22} & 0 & 0 & 0 & \frac{-M_6}{4} \end{bmatrix} \qquad (3\text{-}59)$$

where

$M_1 = 1/3$ $\qquad$ $M_2 = 13/35$

$M_3 = 13/35$ $\qquad$ $M_4 = J/3\ A$

$M_5 = L^2/105$ $\qquad$ $M_6 = L^2/105$

$M_7 = 11\ L/210$ $\qquad$ $M_8 = -11\ L/210$

$M_9 = -11\ L/210$ $\qquad$ $M_{10} = 11\ L/210$

The global element submatrices M_{ii}^{j} and M_{ij} will be expanded in full, using these two expanded matrices the upper triangle of the global element mass matrix can be assembled. M_{ii}^{j} will take the same form as K_{ii}^{j} (see eqns. (3−48)−(3−52)), but to enable M_{ij} to be assembled in terms of M_{ii}^{j}, each of the terms used for the assemblance of M_{ii}^{j} will be assigned seperately as follows

$F_1 = M_1T_1T_1$ $\qquad$ $F_2 = M_2T_2T_2$ $\qquad$ $F_3 = M_3T_3T_3$

$F_4 = M_1T_1T_4$ $\qquad$ $F_5 = M_2T_2T_5$ $\qquad$ $F_6 = M_3T_3T_6$

$F_7 = M_1T_1T_7$ $\qquad$ $F_8 = M_2T_2T_8$ $\qquad$ $F_9 = M_3T_3T_8$

$F_{10} = M_7T_2T_3$ $\qquad$ $F_{11} = M_8T_3T_2$ $\qquad$ $F_{12} = M_7T_2T_6$

$F_{13} = M_8T_3T_5$ $\qquad$ $F_{14} = M_7T_2T_9$ $\qquad$ $F_{15} = M_8T_3T_8$

$F_{16} = M_1T_4T_4$ $F_{17} = M_2T_5T_5$ $F_{18} = M_3T_6T_6$

$F_{19} = M_1T_4T_7$ $F_{20} = M_2T_5T_8$ $F_{21} = M_3T_6T_9$

$F_{22} = M_7T_5T_3$ $F_{23} = M_8T_6T_2$ $F_{24} = M_7T_5T_6$

$F_{25} = M_8T_6T_5$ $F_{26} = M_7T_5T_9$ $F_{27} = M_8T_6T_8$

$F_{28} = M_1T_1T_7$ $F_{29} = M_2T_8T_8$ $F_{30} = M_3T_9T_9$

$F_{31} = M_7T_8T_3$ $F_{32} = M_8T_9T_2$ $F_{33} = M_7T_8T_6$

$F_{34} = M_8T_9T_5$ $F_{35} = M_7T_8T_9$ $F_{36} = M_8T_9T_8$

$F_{37} = M_4T_1T_1$ $F_{38} = M_5T_2T_2$ $F_{39} = M_6T_3T_3$

$F_{40} = M_4T_1T_4$ $F_{41} = M_5T_2T_5$ $F_{42} = M_6T_3T_6$

$F_{43} = M_4T_1T_7$ $F_{44} = M_5T_2T_8$ $F_{45} = M_6T_3T_9$

$F_{46} = M_4T_4T_4$ $F_{47} = M_5T_5T_5$ $F_{48} = M_6T_6T_6$

$F_{49} = M_4T_4T_7$ $F_{50} = M_5T_5T_8$ $F_{51} = M_6T_6T_9$

$F_{52} = M_4T_7T_7$ $F_{53} = M_5T_8T_8$ $F54 = M_6T_9T_9$

Using these factors the global submatrices M_{ii}^{j} and M_{ij} can be assembled easily, even though this involves more coding substantial savings in computer time and memory are made. The complete assemblence of these submatrices is shown Fig. 3–4. Using these two submatrices the element mass matrix may be assembled in the usual fashion.

3.6 FREE VIBRATION ANALYSIS

The dynamic analysis of three dimensional frames is performed in a manner which is entirely parallel to that described for two dimensional shear buildings. The equation of motion may be expressed as

$$M\ddot{x} + Kx = 0 \qquad (3.60)$$

The solution to this equation is achieved by solving the eigenproblem

$$| K - \omega^2 M | = 0 \qquad (3.61)$$

Jacobi's method which is described in Appendix 1 or other eigenvalue solving routines could be used for solving this eigenproblem. Since six degrees of freedom are allowed at every node, the resulting stiffness and mass matrices for a skeletal framework tend to be quite large. The solution to this problem requires the use of a computer with a large storage

memory and takes a fairly long time.

In such cases it is desirable to reduce the size of these matrices by condensation techniques in order to make the solution of the eigenproblem more managable and economical.

3.6.1 Dynamic Condensation

The method of Dynamic Condensation is a recently proposed technique by Paz[29], for the reduction of the eigenvalue problem in dynamic analysis. The algorithm for this method begins by assigning an approximate value (e.g zero) to the first eigenvalue ω_1^2, applying dynamic condensation to the matrix $[D_1] = [K]-\omega_1^2[M]$ and then solving the reduced eigenvalue problem to determine the first and second eigenvalues ω_1^2 and ω_2^2. Next, dynamic condensation is applied to the matrix $[D_2] = [K]-\omega_2^2[M]$ to reduce the problem and calculate the second and third eigenvalues, ω_2^2 and ω_3^2. The process continues in this manner, with one virtually exact eigenvalue and an approximation of the next order eigenvalue calculated at each step.

The Dynamic Condensation method does not require matrix inversion nor series expansion. To illustrate the method more clearly the following eigenvalue problem is considered. A structural system for which it is desired do reduce the secondary degrees of freedom $\{x_s\}$ and retain the primary degrees of freedom $\{x_p\}$. In this case the equations of free motion may be written in the partioned form as

$$\begin{bmatrix} [M_{ss}] & [M_{sp}] \\ [M_{ps}] & [M_{pp}] \end{bmatrix} \begin{Bmatrix} \{\ddot{x}_s\} \\ \{\ddot{x}_p\} \end{Bmatrix} + \begin{bmatrix} [K_{ss}] & [K_{sp}] \\ [K_{ps}] & [K_{pp}] \end{bmatrix} \begin{Bmatrix} \{x_s\} \\ \{x_p\} \end{Bmatrix} = \begin{Bmatrix} \{0\} \\ \{0\} \end{Bmatrix} \quad (3.62)$$

The substitution of $\{x\} = \{X\}\ sin\ \omega_i t$ in eqn. (3.62) results in the general eigenvalue problem

$$\begin{bmatrix} [K_{ss}]-\omega_i^2[M_{ss}] & [K_{sp}]-\omega_i^2[M_{sp}] \\ [K_{ps}]-\omega_i^2[M_{ps}] & [K_{pp}]-\omega_i^2[M_{pp}] \end{bmatrix} \begin{Bmatrix} \{X_s\} \\ \{X_p\} \end{Bmatrix} = \begin{Bmatrix} \{0\} \\ \{0\} \end{Bmatrix} \qquad (3.63)$$

where ω_i^2 is the approximation of the i^{th} eigenvalue which was calculated in the preceding step of the process. To start the process an approximation or a value of zero is taken for the first eigenvalue ω_1^2.

The following three steps are executed to calculate the i^{th} eigenvalue ω_i^2 and the corresponding eigenvector $\{a\}_i$ as well as an approximation of the next eigenvalue ω_{i+1}.

Step 1 The approximation of ω_i^2 is introduced in eqn. (3.63). Gauss– Jordan elimination of the secondary coordinates $\{X_s\}$ is then used to reduce eqn. (3.63) to

$$\begin{bmatrix} [I] & -[\bar{T}_i] \\ [0] & [\bar{D}_i] \end{bmatrix} \begin{Bmatrix} \{X_s\} \\ \{X_p\} \end{Bmatrix} = \begin{Bmatrix} \{0\} \\ \{0\} \end{Bmatrix} \qquad (3.64)$$

The first equation in eqn. (3.64) can be written as

$$\{X_s\} = [\bar{T}_i]\ \{X_p\} \qquad (3.65)$$

Consequently, $\{X\}$ can be expressed as

$$\{X\} = [T_i]\ \{X_p\} \qquad (3.66)$$

where

$$[T_i] = \begin{bmatrix} [\bar{T}_i] \\ [I] \end{bmatrix} \qquad \{X\} = \begin{Bmatrix} \{X_s\} \\ \{X_p\} \end{Bmatrix} \qquad (3.67)$$

Step 2 The reduced mass matrix $[\bar{M}_i]$ and the reduced stiffness matrix $[K_i]$ are calculated as

$$[\bar{M}_i] = [T_i]^T\ [M]\ [T_i] \qquad (3.68)$$

and

$$[K_i] = [\bar{D}_i] + \omega_i^2 . [\bar{M}_i] \qquad (3.69)$$

where the transformation matrix $[T_i]$ is given by eqn. (3.67) and the reduced matrix $[\bar{D}_i]$ is defined by eqn. (3.64).

Step 3 The reduced eigenvalue problem

$$[[\bar{K}_i] - \omega^2[\bar{M}_i]]\{X_p\} = \{0\} \qquad (3.70)$$

is solved to obtain an improved eigenvalue ω_i^2, its corresponding eigenvector $\{X_p\}_i$, and also an approximation for the next higher eigenvalue ω_{i+1}^2.

This three step process may be applied iteratively, i.e, the value of ω_i^2 obtained in step 3 may be used as an improved approximate value in step 1 to obtain a further improved value of ω_i^2 in step 3. Once an eigenvalue $\{X_p\}_i$ for the reduced system is found, the i^{th} modal shape of the complete structural system is determined as $\{X\}_i = \{T_i\}.\{X_p\}_i$ using eqn.(3.66)

3.7 FORCED VIBRATION ANALYSIS

The analysis is performed in a similar fashion as for two dimensional multi degree of freedom systems which was described in the previous chapter. The direct integration technique is a suitable method to solve the resulting differential equation especially when the forcing function varies with time as is the case for earthquake loading. It also has the advantage that it does not employ an iterative procedure to obtain the solution at any particular time step. Thus the solution to even large sets of equations can be obtained fairly rapidly using this technique.

3.8 DESCRIPTION OF THE COMPUTER PROGRAMS

Two computer programs were developed for the dynamic analysis of three dimensional framed structures using the theory presented in this chapter. In the first program the element structure and mass matrices are computed initially, from which the overall structural stiffness and mass matrices are evaluated. The matrix multiplication procedures which are required to perform the coordinate transformations required were input in the expanded form shown. The advantage in terms of reduction in the number of

arithmetical operations required has been mentioned before, this in effect enables the program to be run on powerful microcomputers. Since the concept of consistent mass matrices was made use of, the mass of all the elements of the structure were taken into account, thus making the mathematical model more realistic. Every node was allowed six degrees of freedom, hence the degree of fixity at any node could be altered to suit requirements. The nodes at the base of the structure could thus be considered to be pinned or fixed as required, additional restraints at other nodes could also be defined.

The assumption of rigid floor slabs in structures and the contributions of self loads and design superimposed loads at the floor levels are taken into account by including additional members linking the columns at the floor levels. These members are given very high values of modulii of elasticity and shear (10^6 times the values input for other structural elements), thus imparting very high axial, flexural and torsional rigidity in these members. The value given for the density of these members was such that it would take account of the mass of the floor slab and any additional superimposed load.

Figure 3–5 will illustrate the point more clearly. Assuming a 150 mm concrete floor slab is rigidly fixed to a steel framework arranged on a 3 m grid and carrying a 3 kN/m^2 superimposed load, the equivalent structural set up which would be incorporated into the computer program is as follows. The mass of the floor slab = 3300 kg ($\rho_{conc.}$ = 2400 kg/m^3) and the total mass = 6050 kg.

Assuming two 100 x 200 mm members are used to simulate the floor slab, the value of density given to these members is 35650 kg/m^3.

Once the overall stiffness and mass have been computed and stored in a banded form, the natural frequencies are evaluated by solving the eigenvalue

problem by using a NAG subroutine[16] (F02BFF) which uses the Householder reduction method. The reason for not using Jacobi's method was due to the fact that the subroutine for the method from Bathe[1] required the stiffness and mass matrices to be input in the full form. It was thought that for large eigenproblems storing the matrices in full form would occupy large amounts of computer memory and that the Jacobi subroutine would take a relatively long time to solve the eigenproblem as it is an iterative procedure.Once the eigenvalues and eigenvectors are computed, the seismic analysis is performed using the direct integration technique described in the previous chapter.

The second program basically incorporated the dynamic condensation technique to reduce the size of the eigenvalue problem to be solved. The structural stiffness and mass matrices are computed in the normal fashion. The degrees of freedom which are considered as primary values i.e those which are regarded as effectively defining the behaviour of the structure, are input. The reduced eigenvalue problem which results from the condensation procedure is solved using the Jacobi method (Appendix 1).

3.9 NUMERICAL EXAMPLE

Dynamic analysis was performed on the four storey steel framed structure shown in Fig. 3– 6 . The structure was assumed to be rigidly fixed at the base level. All the other nodes defining the structure were allowed six degrees of freedom. The structure was designed to carry typical loadings for offices (Fig. 3– 7). Cross bracing was provided at appropriate positions to counter wind loading (Fig.3– 8) . The structure was intentionally chosen to have an L shape in plan, to enhance the torsional behaviour. The floors were assumed to be 100 mm concrete slabs which were rigidly connected to the steel framework, thus acting as integral parts of the structure. Free

vibration analysis of this strucuture was performed and for the forced vibration analysis a damping ratio of 5 percent was assumed. The structure was then subjected to the digitised accelerogram input of the Adak, Alaska earthquake of 1st May 1971, and the linear response was obtained.

In the second program the eigenvalue problem was reduced using the technique of Dynamic Condensation. The primary degrees of freedom which were chosen included two translation degrees of freedom for each node (relating to the global 'x' and 'z' directions), and one rotational degree of freedom (relating to rotation about the global 'y' direction). Thus three degrees of freedom were allowed for every node instead of the normal six.

The results obtained for the evaluation of the first six natural frequencies is shown in table 3−1

3.9.1 Discussion of results

From the free vibration analysis performed the first four mode shapes are shown in Figs. 3−9 − 3−12 . The deformed shapes are shown in an isometric view and to give a clear view of the nature of the modes a plan view of each mode is included. The first mode is a purely bending one about the weaker axis of the structure. The second mode is essentially a bending mode about the other axis but a slight effect of torsion is shown to manifest itself. The third mode is a purely torsional mode and the fourth mode was a combination of bending about both the axes and torsion of the structure . At higher frequencies, the effect of torsion plays a significant part in determining the behaviour of this structure, this is to be expected as the structure is unsymmetrical in plan about both the major axes.

From the forced vibration analysis carried out, graphs showing the average displacement for every storey in the global 'x' and 'z' directions are plotted (Figs. 3−13 and 3−14). The values plotted were obtained by

averaging the displacements at the fourteen nodes which define the boundary of each storey. The values of displacement at any two nodes connected by the rigid members simulating the floor slab were found to be close, thus validating the assumptions made in their choice. The displacement at any interior node at any particular time was found to be equal to the average of the displacement values of the two adjacent nodes, thus indicating that the structure behaved linearly throughout the period of application of the external loading.

The resulting displacement for any particular node can be obtained by vectorial addition of the displacements in the 'z' and 'x' directions. The displacements in the 'z' direction are seen to be significantly larger than corresponding values in the 'x' direction. This shows that the structure vibrates more freely and violently about the weaker axis and is to be expected. The behaviour of the four storeys in the 'z' direction follows a fairly uniform pattern indicating increasing bending with height about the weaker axis. The displacement in the 'x' direction shows rather erratic behaviour indicating that, rather than pure bending about the stronger axis torsional behaviour plays a small but significant part in determining the overall behaviour of the structure.

From the results shown in Table 3−1 it can be seen that the first two natural frequencies values calculated using the Dynamic Condensation method are very close and are acceptable, however the higher values vary considerably . Although the results shown are for Dynamic condensation with one iteration, the process was tried with two and three iterations, but the results produced were much the same. This discrepancy could be attributed to the choice made in selecting the primary degrees of freedom. The choice of primary degrees of freedom was made after examining the eigenvectors obtained by solving the full size problem, which indicated very

small displacements (of the order of 1/50 of the horizontal displacements) in the vertical direction, and negligible rotational deformations.

3.10 CONCLUSIONS

1) In framed structures which are unsymmetrical, three dimensional mathematical models are essential to portray the effects of torsional behaviour on the structure and the overall behaviour of the whole system.

2) By allowing six degrees of freedom at every node the fixity at the nodes can be altered as necessary,i.e nodes can be taken to be fixed, free or pinned as the case may be. This gives a better representation of real structures.

3) By using consistent mass matrices the mass of all the structural elements are taken into consideration. In vibration analysis since the mass of the system needs to be assessed accurately, it seems realistic to take account of the mass of all the structural elements.

4) The inclusion of additional members to simulate the effect of floor slabs and to take account of the mass contributions due to the superimposed loads has been shown to be valid by the fact that the displacements at nodes connected by these members are very close, this would be expected when the rigid floor slabs form an integral part of the structural system.

5) In the structure analysed the mode shapes indicate the effect of torsion and its contribution to vibrational behaviour of structures. The structure was deliberately chosen to accentuate this effect, but for most structures, after the bending modes, torsional behaviour is found to have large contributions in the higher modes.

6) The seismic analysis performed once again illustrates the erratic movement of the structure in the 'x' direction due to torsioanl behaviour. Although bending about the weaker axis caused high deformations, the

effects of cross axis movement is essential to determine the overall behaviour of the complete system.

7) The Dynamic Condensation method has been shown to be a useful technique for evaluating the natural frequencies only when the structure is encountering pure bending. Although each node was allowed three degrees of freedom, rather than the complete six, the torsional effects could not be effectively accounted for in the reduced eigenvalue problem. The choice of the degrees of freedom made seem to the most appropriate after examining the eigenvectors obtained by performing a full dynamic analysis. Inclusion of another degree of freedom at each node would have considerably reduced the efficiency of the technique and not led to a substantial saving in computer memory and time.

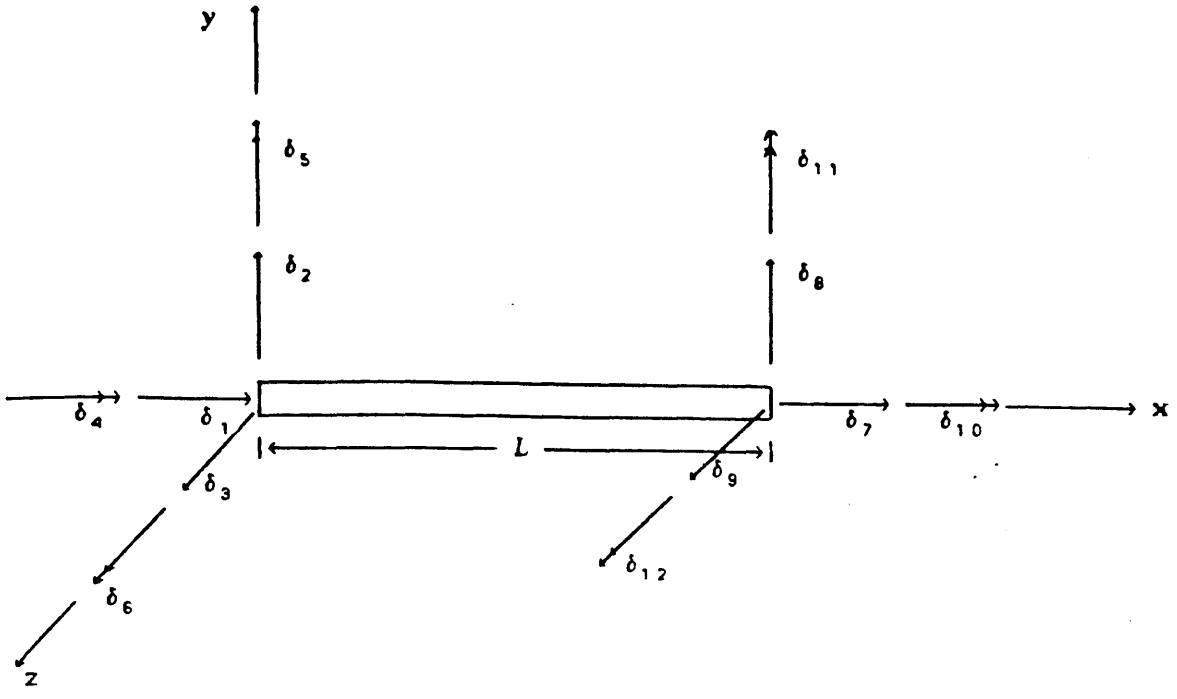

Fig. 3-1 Member axes and nodal freedoms for a three dimensional frame element.

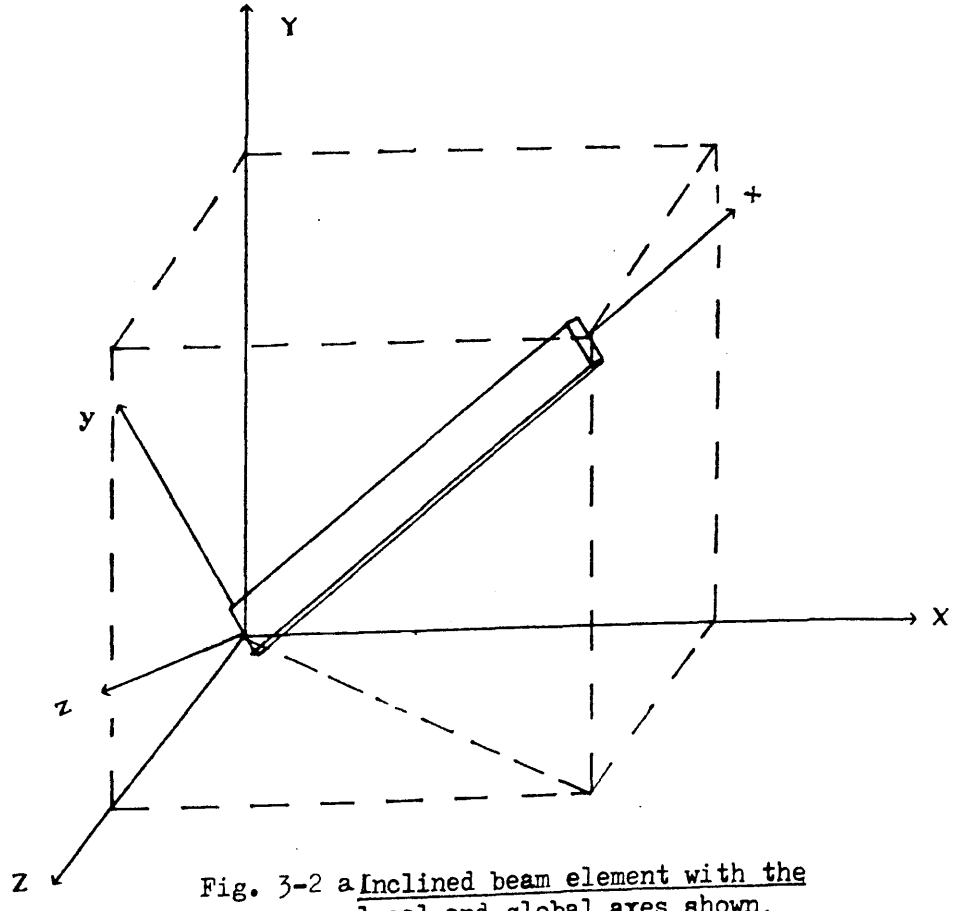

Fig. 3-2 a Inclined beam element with the local and global axes shown.

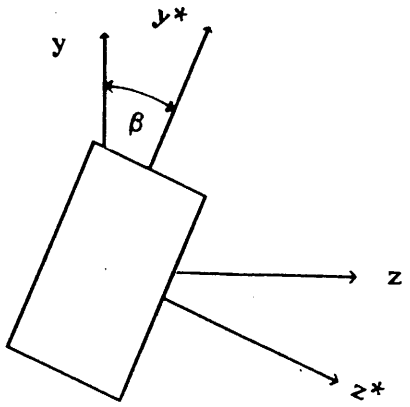

Fig. 3-2 b Principal and member axes.

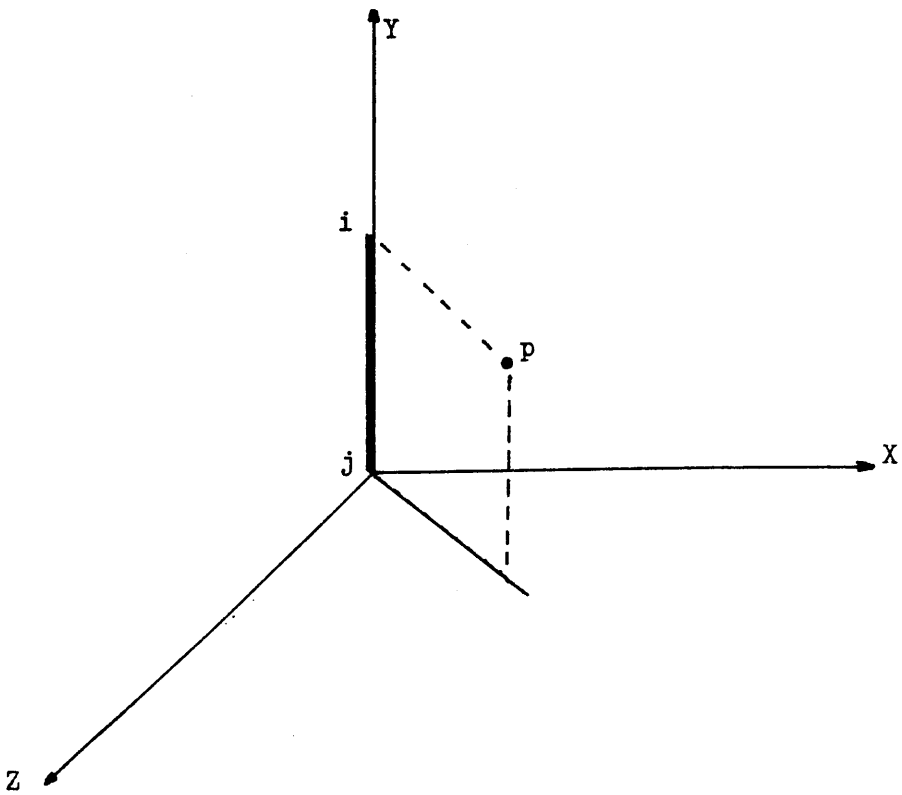

Fig. 3-3 Three nodes used to define principal 'x,y' plane.

$$M_{ii} = \begin{bmatrix} F_1+F_2+F_3 & F_4+F_5+F_6 & F_7+F_8+F_9 & F_{10}+F_{11} & F_{12}+F_{13} & F_{14}+F_{15} \\ & F_{16}+F_{17}+F_{18} & F_{19}+F_{20}+F_{21} & F_{22}+F_{23} & F_{24}+F_{25} & F_{26}+F_{27} \\ & & F_{28}+F_{29}+F_{30} & F_{31}+F_{32} & F_{33}+F_{34} & F_{35}+F_{36} \\ & \textit{symmetric} & & F_{37}+F_{38}+F_{39} & F_{40}+F_{41}+F_{42} & F_{43}+F_{44}+F_{45} \\ & & & & F_{46}+F_{47}+F_{48} & F_{49}+F_{50}+F_{51} \\ & & & & & F_{52}+F_{53}+F_{54} \end{bmatrix}$$

$$M_{ij} = \begin{bmatrix} \frac{1}{2}.F_1+\frac{9}{26}(F_2+F_3) & \frac{1}{2}.F_4+\frac{9}{26}(F_5+F_6) & \frac{1}{2}.F_7+\frac{9}{26}(F_8+F_9) & -\frac{13}{22}(F_{10}+F_{11}) & -\frac{13}{22}(F_{12}+F_{13}) & -\frac{13}{22}(F_{14}+F_{15}) \\ & \frac{1}{2}.F_{16}+\frac{9}{26}(F_{17}+F_{18}) & \frac{1}{2}.F_{19}+\frac{9}{26}(F_{20}+F_{21}) & -\frac{13}{22}(F_{22}+F_{23}) & -\frac{13}{22}(F_{24}+F_{25}) & -\frac{13}{22}(F_{26}+F_{27}) \\ & & \frac{1}{2}.F_{28}+\frac{9}{26}(F_{29}+F_{30}) & -\frac{13}{22}(F_{31}+F_{32}) & -\frac{13}{22}(F_{33}+F_{34}) & -\frac{13}{22}(F_{35}+F_{36}) \\ & & & \frac{1}{2}.F_{37}-\frac{3}{4}(F_{38}+F_{39}) & \frac{1}{2}.F_{40}-\frac{3}{4}(F_{41}+F_{42}) & \frac{1}{2}.F_{43}-\frac{3}{4}(F_{44}+F_{45}) \\ & \textit{symmetric} & & & \frac{1}{2}.F_{46}-\frac{3}{4}(F_{47}+F_{48}) & \frac{1}{2}.F_{49}-\frac{3}{4}(F_{50}+F_{51}) \\ & & & & & \frac{1}{2}.F_{51}-\frac{3}{4}(F_{53}+F_{54}) \end{bmatrix}$$

Fig. 3-4 Global mass submatrices.

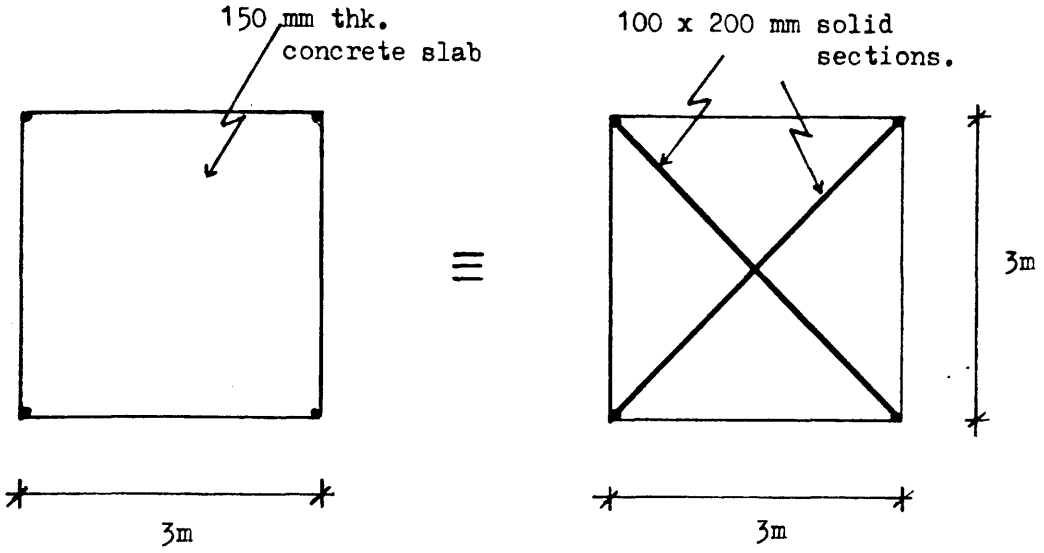

Fig. 3-5 Equivalent system for simulating the effect of a rigid floor slab.

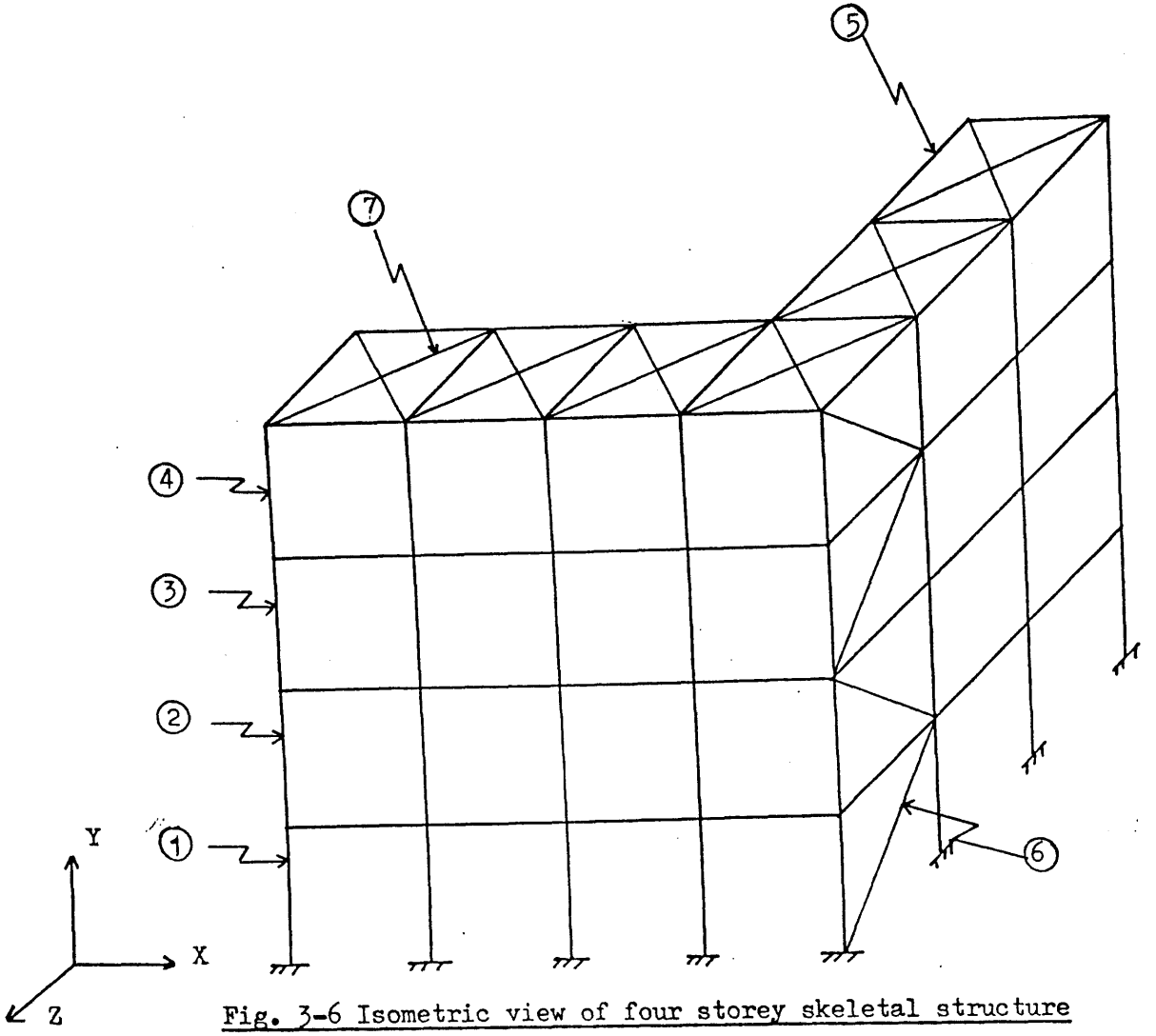

Fig. 3-6 Isometric view of four storey skeletal structure

DIMENSIONS OF STRUCTURAL ELEMENTS

(1)	COLUMNS AT BASE LEVEL	:- 356 x 406 x 634 U.C
(2)	COLUMNS AT LEVEL NO.1	:- 356 x 406 x 467 U.C
(3)	COLUMNS AT LEVEL NO.2	:- 356 x 406 x 287 U.C
(4)	COLUMNS AT LEVEL NO.3	:- 356 x 368 x 153 U.C
(5)	ALL FLOOR BEAMS	:- 203 x 133 x 30 U.B
(6)	BRACING MEMBERS	:- 2/ 150 x 90 x 10 L's
(7)	ASSUMED SIZE FOR MEMBERS SIMULATING LOADING, THE DENSITY VALUES INPUT FOR THESE MEMBERS ARE VARIED AS REQUIRED.	:- 100 x 200 SOLID SECTION.

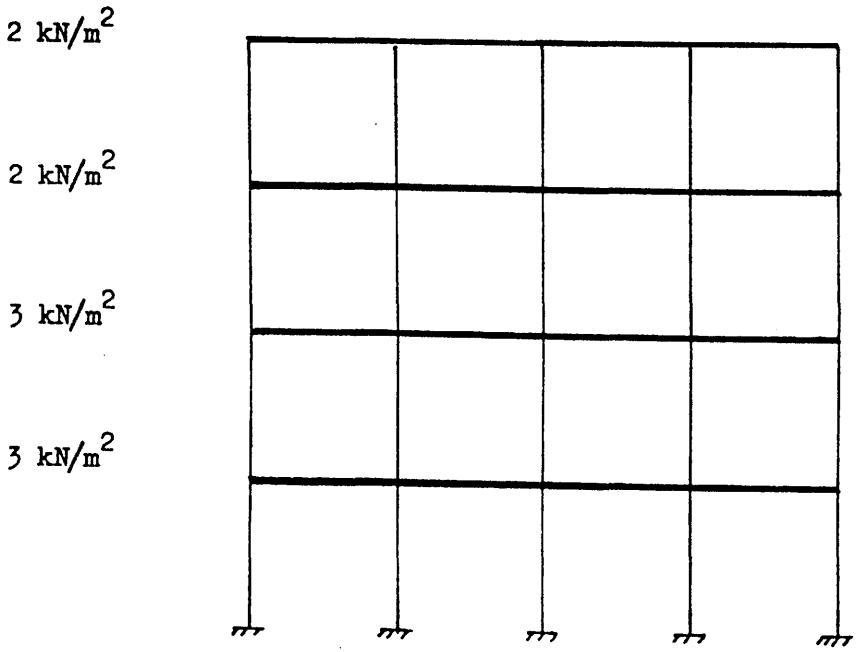

Fig. 3-7 Superimposed loadings on different levels

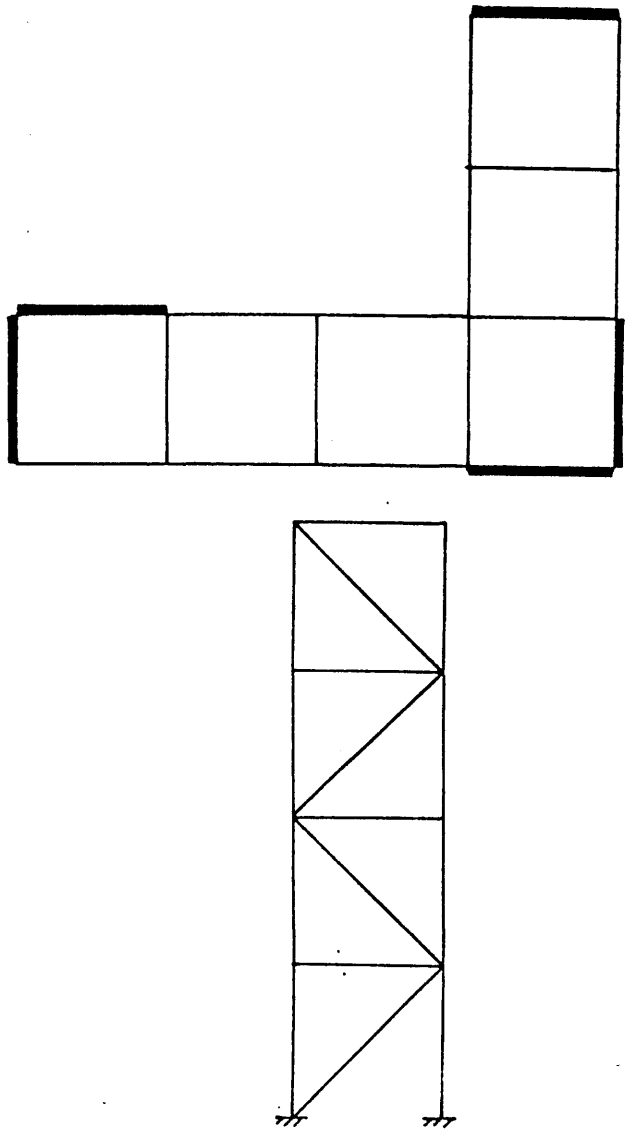

Fig. 3-8 a) Locations of cross braced bays
b) Typical cross bracing for a single bay

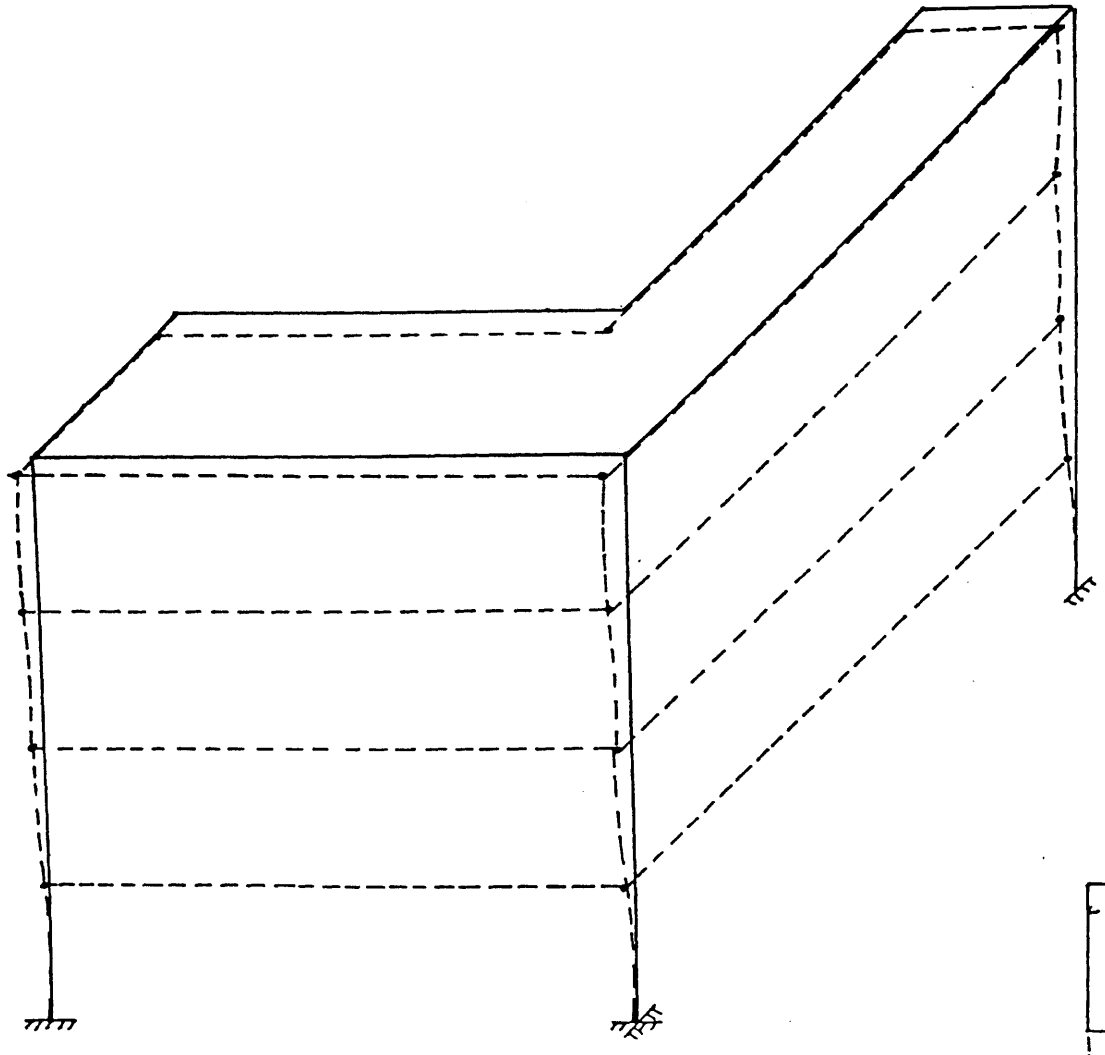

FREQUENCY NO. 1 :- 8.6927 Hz.

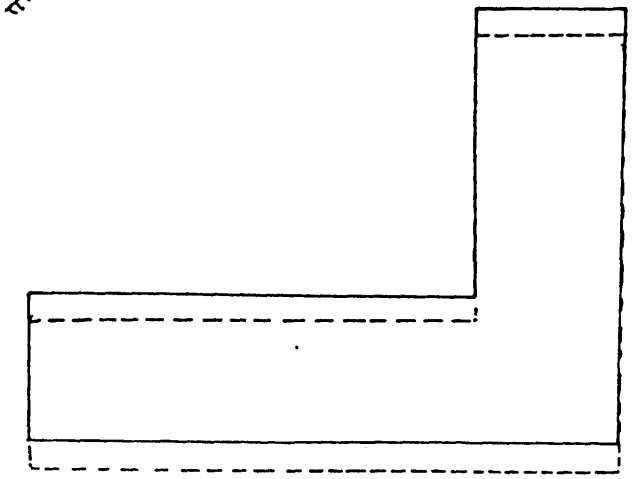

Fig. 3-9 Mode shape for the first natural frequency

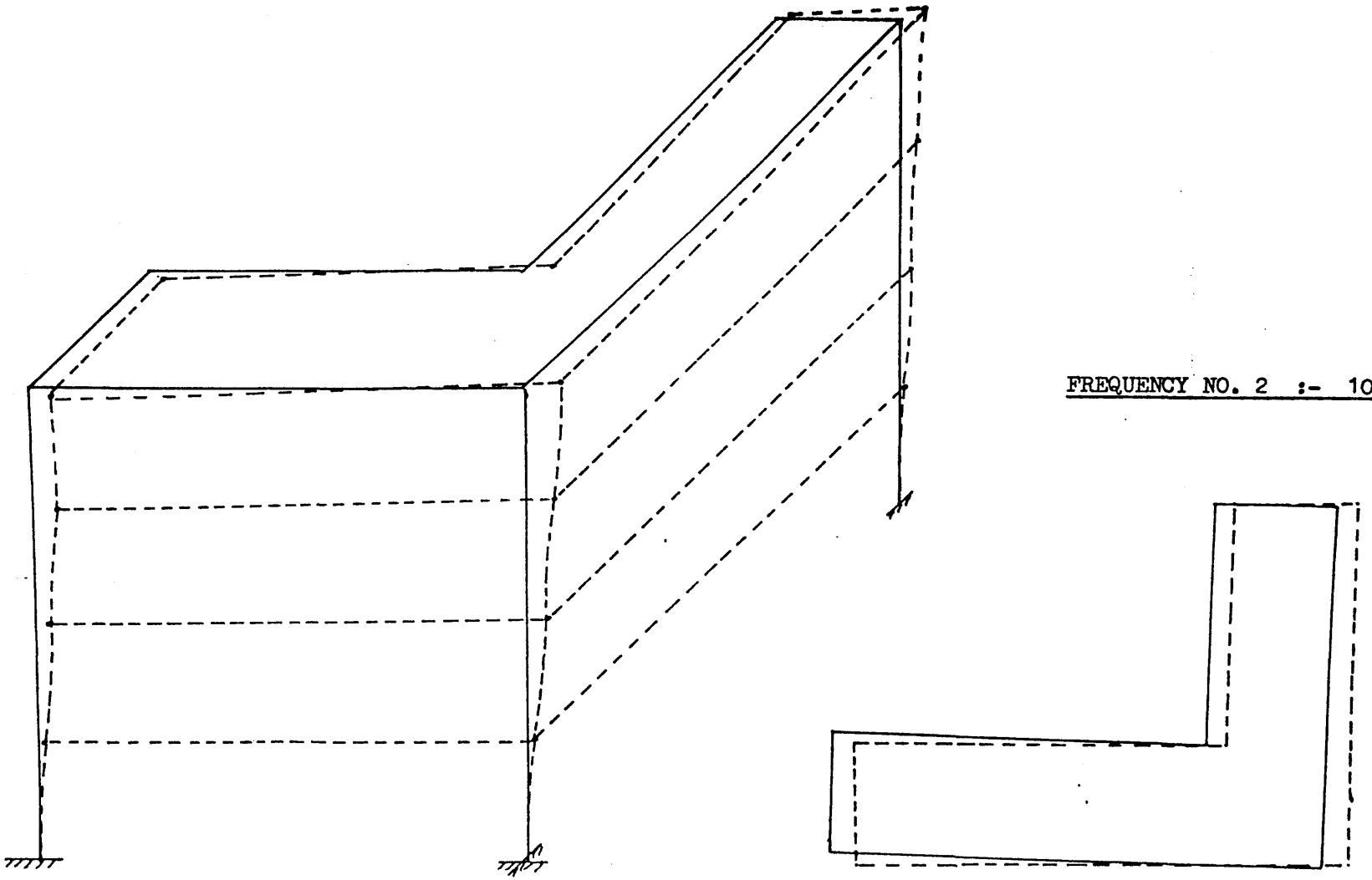

FREQUENCY NO. 2 :- 10.6867 Hz.

Fig. 3-10 Mode shape for the second natural frequency

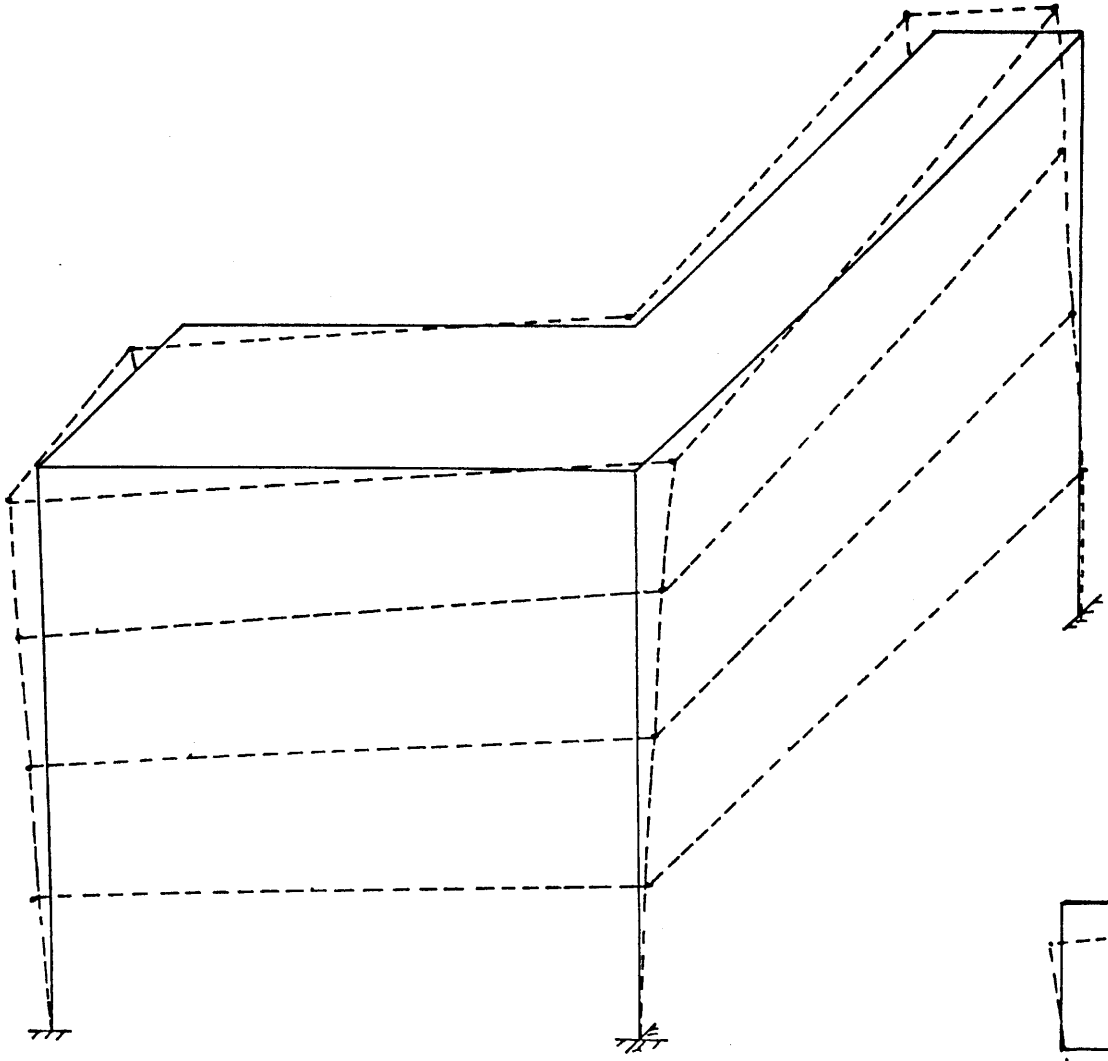

FREQUENCY NO. 3 :- 12.4554 Hz.

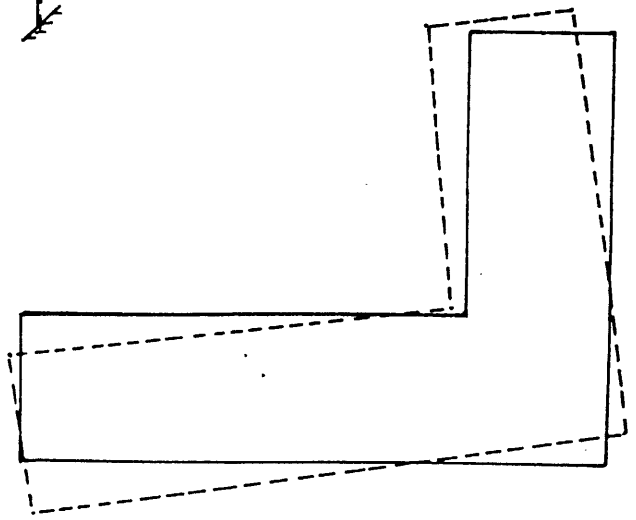

Fig. 3-11 Mode shape for the third natural frequency

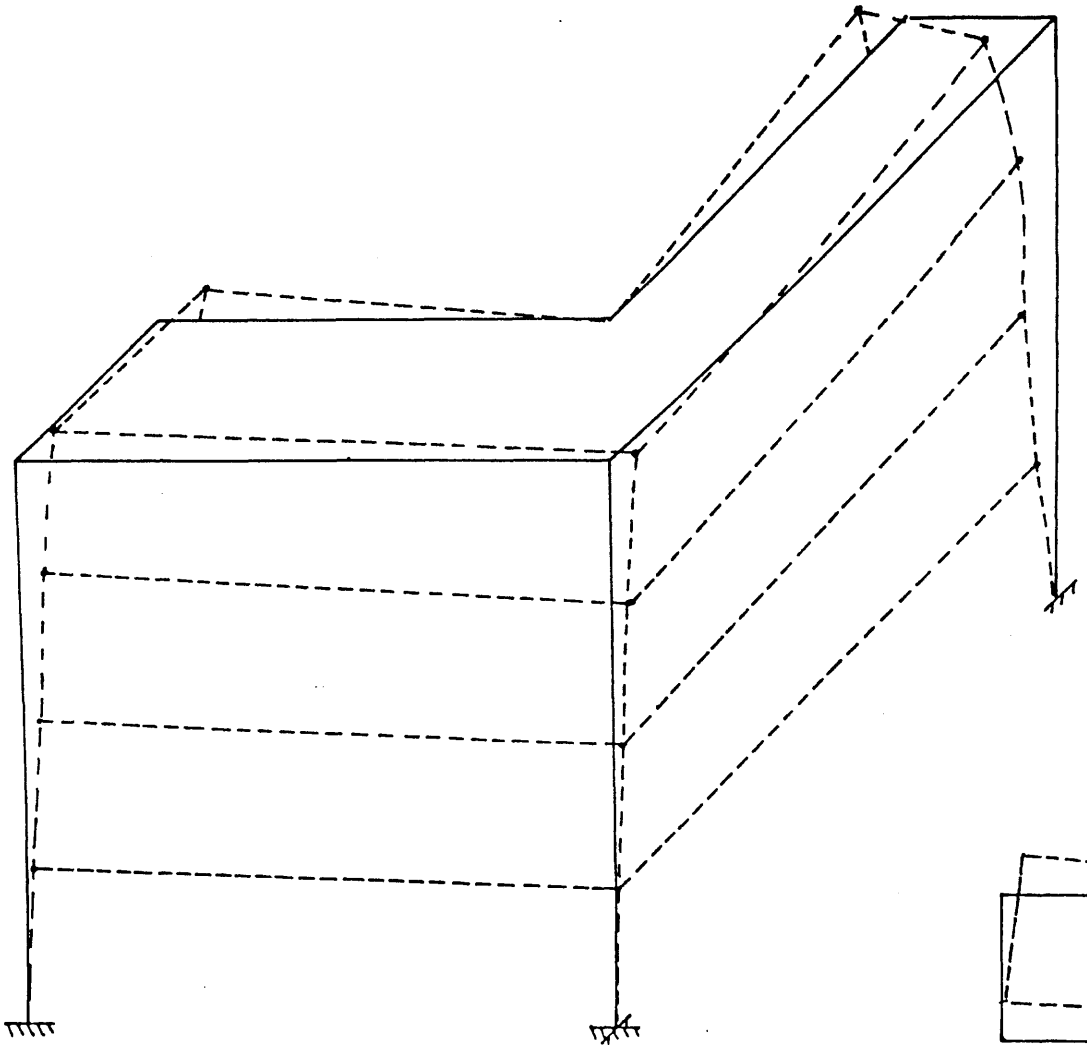

FREQUENCY NO. 4 :- 20.7951 Hz.

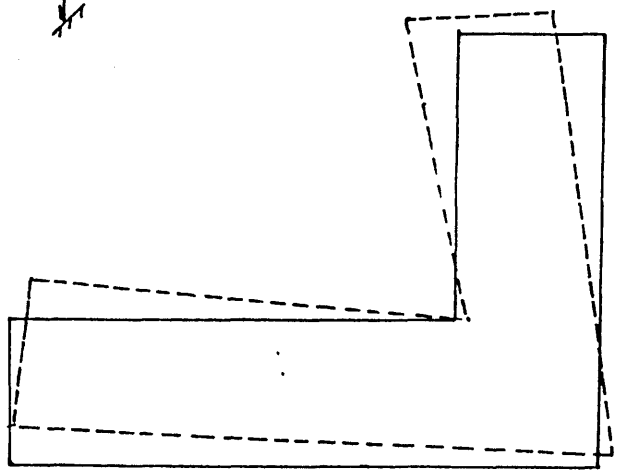

Fig. 3-12 Mode shape for the fourth natural frequency

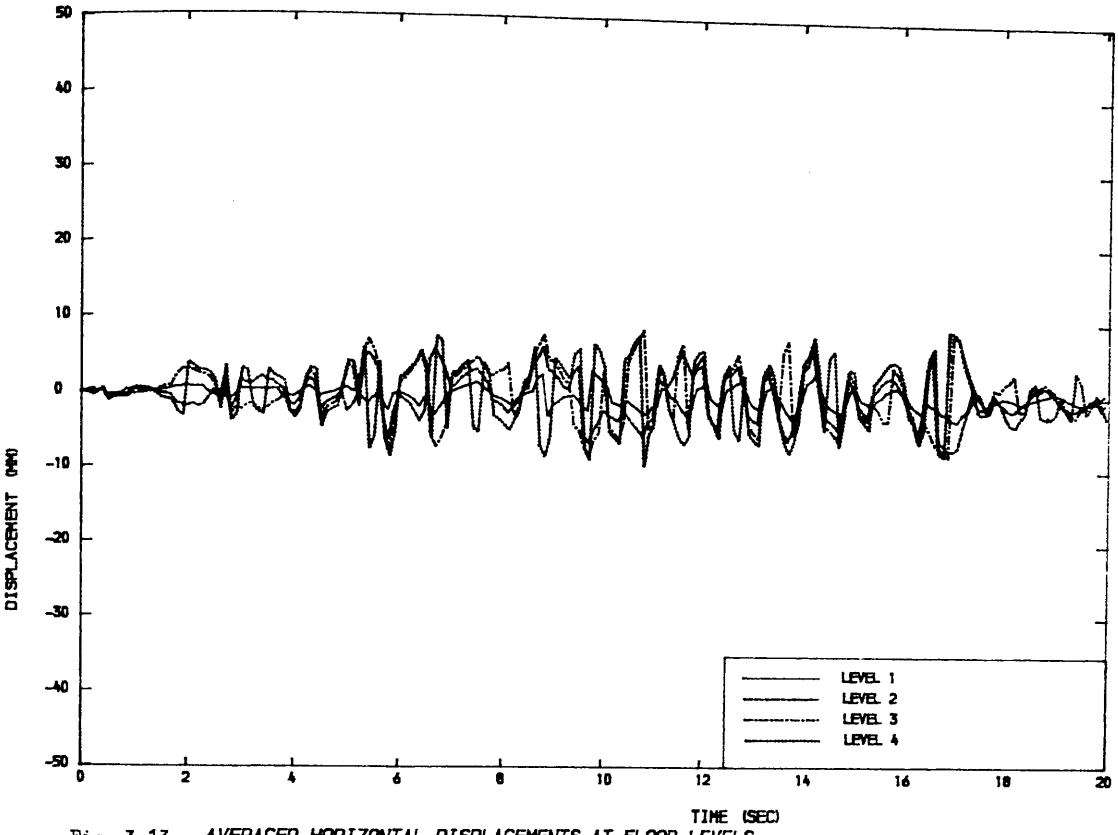

Fig. 3-13 AVERAGED HORIZONTAL DISPLACEMENTS AT FLOOR LEVELS IN THE ' X ' DIRECTION

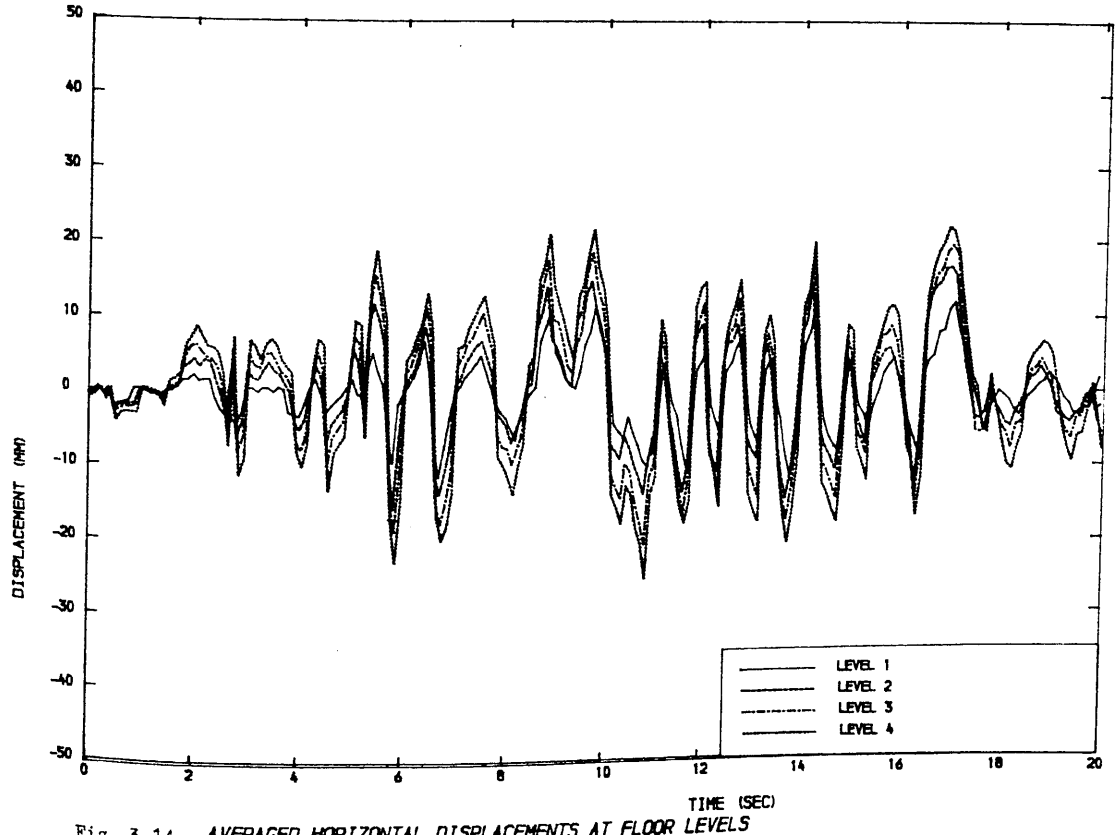

Fig. 3-14 AVERAGED HORIZONTAL DISPLACEMENTS AT FLOOR LEVELS IN THE ' Z ' DIRECTION

TABLE 3-1 COMPARISON OF NATURAL FREQUENCY VALUES

FREQUENCY NO.	EXACT VALUE	DYNAMIC CONDENSATION WITH ONE ITERATION	PERCENTAGE ERROR
1	8.6927	8.6023	1.04
2	10.6867	10.9583	2.54
3	12.4554	13.4556	8.03
4	20.7951	22.8761	10.01
5	21.1855	23.8795	12.72
6	27.6374	31.6502	14.52

CHAPTER 4 DYNAMIC MODELLING THEORY

4.1 INTRODUCTION

The purpose of model analysis in earthquake engineering is the prediction of dynamic response of a prototype structure from laboratory tests on physical models. This prediction may include all relevent response parameters or it may be limited to selected parameters such as natural frequencies and mode shapes. The desired range of prediction may be limited to linear elastic response or it may comprise the complete response history to failure including material and geometric non– linearities.

In this chapter modelling theory is discussed in a general sense initially, and is then applied to specific cases which are most useful in seismic investigation. Modelling theory establishes the rules according to which geometry, material properties, initial conditions, boundary conditions and loading effects of the model and the prototype have to be related so that the behaviour of one can be expressed as a function of the behaviour of the other. The theory which leads to the development of a complete set of scaling laws defining the model prototype correspondence is that of similitude.

The theory of similitude, upon which model design and analysis is based, may be developed by dimensional analysis. Dimensional analysis is based on the consideration of the dimensions in which each of the relevant quantities involved in a physical phenomenon is expressed. The principles of dimensional analysis are well established in the literature and are summarised in Section 4.3 as far is needed for the development of a general modelling theory.

4.2 BASIC MODELLING THEORY

To develop the necessary mathematical relationships between the characteristics of a prototype and its model, consider the basis that every physical phenomenon can be expressed by a dimensionally homogeneous equation of the type

$$q_1 = f(q_2, q_3, \ldots, q_n) \qquad (4.1)$$

where n is the total number of physical quantities involved in the phenomenon. In this expression q_1 is the dependent quantity and q_2 to q_n are the variables and parameters on which q_1 depends. According to Buckingham's Pi theorem (Sect. 4.3), every dimensionally homogeneous equation can be written in the form

$$\pi_1 = f(\pi_2, \pi_3, \ldots, \pi_{n-N}) \qquad (4.2)$$

where π_1 to π_{n-N} are dimensionless products of powers of the physical quantities q_1 to q_n. The number N is the rank of the dimensional matrix which is usually equal to the number of basic units needed to describe the physical quantities.

Since equation 4.2 is identical to equation 4.1, it describes the same physical phenomenon and, because of its dimensionless form, must be equally valid for the prototype and the model if similitude is to be achieved.

A sufficient condition for complete similitude is therefore

$$(\pi_1)_p = (\pi_1)_m \qquad (4.3)$$

and

$$(\pi_2)_p = (\pi_2)_m$$

$$\vdots$$

$$(\pi_{n-N})_p = (\pi_{n-N})_p \qquad (4.4)$$

Equation (4.3) is often referred to as the prediction equation and equations

(4.4) constitute the design conditions for the model. Methods for deriving the dimensionless products are summarised in section 4.3.

There are two major difficulties which have to be faced. Firstly extreme care has to be exercised in specifying the right number of physical quantities which enter equation (4.1). Quantities which have insignificant effect on the response parameters of interest will impose unnecessary restraints on the model, while neglecting a significant quantity can yield incorrect results. Secondly problems will be encountered when trying to reproduce at scales the design conditions posed by equation (4.4). In particular, the simulation of material properties and loading conditions may be an extremely difficult task. The latter often leads to the design of distorted models in which one or more of the design conditions are violated. Nevertheless, such models may still be adequate if the prediction can be corrected to account for the violation in the design conditions.

The specification of all important quantities on the right hand side of equation (4.1) requires some insight into the physical problem under study. In general, the more that is known about the behaviour of the prototype and of the laws which describe it, the easier it is to design the model. Models are most useful when the general features of the prototype behaviour are known but specifics such as complex geometry or material non–linearities render it difficult to obtain quantitative information by analytical means.

The physical quantities which may enter a structural problem are difficult to enumerate in their entirety but are for most cases contained in one of the following four groups:

4.2.1 Geometric Properties

Geometry includes all the space relationships which may influence the

results. All distances or lengths and all angles that are relevant must be represented. For geometrically similar models a location vector is sufficient to describe any point in the structure. In dynamic problems the vector will depend not only on the space coordinates but also on the time t.

4.2.2 Material Properties

In general, these properties may vary from point to point in space and with time and temperature. A material has thermal, mechanical, electrical and magnetic properties, although the latter two can usually be neglected in structural problems. Thermal properties of interest may be specific heat, coefficients of thermal conductivity and linear expansion, and emmisivity. The mechanical properties are stress and strain in the material. These properties may be time and temperature dependent (e.g creep and relaxation), vary from point to point (inhomogeneity), and be direction dependent (anisotropy). They also describe the interaction between different directions (Poisson's ratio) and the interaction between neighbouring points (e.g strain gradient effects).

4.2.3 Initial Conditions

These conditions can be described by initial stress and temperature functions, σ_0 and T_0, at time t_0. In many cases, the specification and simulation of σ_0 and T_0 will be an extremely difficult task due to their dependence on fabrication and construction procedures and previous loading histories. In the design of models this will necessitate an accurate reproduction of fabrication and construction procedures whenever those have a significant effect on the initial conditions. In reinforced concrete structures initial conditions may be strongly affected by creep and shrinkage effects, while in steel structures residual stresses due to welding and erection stresses

have to be considered. For steel as a prototype material it may be necessary to trace the history back to member fabrications which is usually the source of significant residual stresses.

4.2.4 External Influences

Such influences may be prescribed displacements which may be time dependent as in the case of seismic ground motions, prescribed temperature variations, surface forces on the boundaries of the structure, and body forces caused by the gravitational field of the earth or generated by artificial means such as magnetic fields.

For most structural problems the relevant physical quantities can be selected from these four groups. Based on a physical understanding of the problem, quantities which will significantly affect the response quantities to be measured during the model experiment , have to be chosen.

To aid in selecting model design and response quantities, an extensive list of physical quantities and their dimensional description is presented in Table. 4−1. Before equations (4.1) and (4.2) can be utilized to derive appropriate similitude relationships for dynamic model studies, it is necessary to briefly summarise the fundamentals of dimensional analysis.

4.3 DIMENSIONAL ANALYSIS

Dimensional analysis is an analytical method by which a dimensionally homogeneous equation, containing physical quantities and describing a physical phenemenon is converted to an equivalent equation containing only dimensionless products (π − factors of powers of the physical quantities). Since these dimensionless products describe the same physical phenomenon and are independent of the units of measurement, they must be equal in the prototype and the model if complete similitude is to be achieved.

Dimensional analysis is based on Buckingham's Pi theorem which states that a dimensionally homogeneous equation can be reduced to a functional relationship between a complete set of independent dimensionless products (π– factors). The number of independent dimensionless products is equal to the total number of physical quantities involved minus the number of fundamental quantities needed to describe the dimensions of all physical quantities.

The simple rule for the determination of the number of independent dimensionless products has been reformulated in more formal mathematical terms as: the number of dimensionless products in a complete set is equal to the the total number of physical quantities involved minus the rank of their dimensional matrix (The rank of a matrix is the order of the largest submatrix whose determinant is non zero). In order to determine a complete set of dimensionless products it should be noted that the units of any physical quantity can be expressed as a combination of units of basic or fundamental quantities. The choice of basic quantities is largely an arbitrary one but is governed by practical considerations of physical phenomena and simplicity of measurement.

In engineering , the most common sets of basic quantities are those of masss M, length L, time T and temperature Θ (called MLTΘ system) of force F, L , T and Θ (called the FLTΘ system).

The basic quantities can be used as building blocks since the dimensions of all other physical quantities can be expressed as products of powers of basic quantities. When the dimensions of physical quantities are properly arranged in a dimensional matrix it is reasonably simple to extract dimensionless products by comparing inidvidual quantities as to their dimensional dependence. Systematic methods for generating a complete set of dimensionless products can be achieved by inspection if the following

rules and guidelines are considered:

i) The dimensionless products are composed of products of powers of the physical quantities and should not involve more than N−1 quantities in any one product, where N is the number of basic quantities.

ii) The dimensionless products must be independent, i.e none of the products can be obtained as a product of power of other products.

iii) Independence is easy to verify if the dimensionless products are generated such that each product involves a quantity which does not appear in any other product.

iv) The dimensional matrix should be arranged such that the response quantity of interest (dependent variable) is listed first, followed by independent variables and then parameters.

v) Dimensionless products should be generated such that quantities are eliminated from left to right in the dimensional matrix.

Guidelines (iv) and (v) are important for the design and control of the experiment. Since complete sets of dimensionless parameters are not unique, one will be more useful than others in model analysis. These two guidelines are also important for the design and control of the experiment.

4.4 SIMILITUDE RELATIONSHIPS AND TYPES OF MODELS

The necessary conditions for complete similitude between model and prototype can be derived through the following procedure

i) Write down all physical quantities on which the solution of the phenomenon under study depends significantly.

ii) Develop a suitable and complete set of independent dimensionless products from these physical quantities (eqn. 4.2)

iii) Establish equality between prototype and model for each of the independent dimensionless products (eqns. 4.2 & 4.4).

The third step defines the design conditions for the model and the prediction equation(s) for the dependent response quantity (or quantities) which relates the measured model response to the prototype behaviour. As such, this step establishes the scaling laws for all physical quantities or products of physical quantities. Usually, these scaling laws are expressed as ratios of the numbers of units needed to describe identical quantities in model versus prototype. These ratios are designated with a subscript r added to the description of the physical quantity, i.e $l_r = l_m/l_p = 0.1$ means that one unit of length measurement (e.g mm) in the model corresponds to ten equal units of length measurement in the prototype.

One important observation can be made from the fact that all physical quantities can be expressed in terms of basic or fundamental quantities (e.g FLTΘ or MLTΘ) . Since these basic quantities are independent of each other, it is evident that as many scales can be selected arbirtarily as there are basic quantities needed to describe a problem. For instance in a static problem which has F and L as basic quantities, two scales can be selected arbitrarily. In a dynamic problem which may be described by M , L and T three scales can be selected arbitrarily, however, in this case it is usually necessary to select $g_r = 1$ (g is the acceleration due to gravity) which reduces the choice of arbitrary scales to two. The scales of all other physical quantities are then expressed in terms of the arbitrarily selected ones and can be obtained from the dimensionless products.

It should be noted that the choice of arbitrary scales is not limited to basic quantities; any set of independent quantities may be selected for this purpose. The number of independent quantities is always equal to the number of basic ones. In many practical situations the fulfillment of all design conditions will be an impossible task. Under those circumstances it is a matter of judgement and experience to isolate those features which may

be altered such that the model construction becomes feasible but the response prediction is not hindered by an excessive amount of error.

4.5 PHYSICAL MODELS FOR SHAKE TABLE STUDIES

4.5.1 True Replica Model

A model that fulfills all similitude requirements is called a true replica model. Suppose the task is to reproduce, at model scale, the time history of stress components $\sigma_{ij}(\mathbf{r},t)$ in a replica model subjected to a time history of vector imposed acceleration a(t). Recognising that the distributions of stress and of material in the prototype and model must be identical, dimensional analysis can be applied by calling σ a typical stress, ρ a typical density, and E some representative stiffness property. then the stress distribution may be written as

$$\sigma_{ij} = \sigma S_{ij}(\mathbf{r},t) \qquad i,j = 1,2,3$$

where S_{ij} is dimensionless.

With the greatest degree of simplification, the typical stress can be expressed through a functional relationship of the form

$$\sigma = f(\mathbf{r},t;\rho,E,a,g,l,\sigma_0,\mathbf{r}_0) \qquad (4.5)$$

where σ_0 and $\mathbf{r}_0$ refer to initial conditions. Evidently, the ommision of all material properties with the exception of E implies that similarity of material properties is implicitly assumed.

Utilising dimensional analysis, a complete set of dimensionless products can be generated from the dimensional matrix of the quantities in equation (4.5). The products presented in Table 4.1 should be useful for this task. The resulting dimensionless relationship could be of the following form

$$\frac{\sigma}{E} = \left\{ \frac{r}{l} \; , \frac{t}{l} \left[\frac{e}{\rho} \right]^{\frac{1}{2}} ; \frac{a}{g} \; ; \; \frac{gl\rho}{E} \; , \frac{\sigma_0}{E} \; , \frac{r_0}{l} \right\} \qquad (4.6)$$

If gravitational contributions to stress histories must be accounted for, the two terms containing the gravitational acceleration g restrict the freedom in selecting model materials and scale factors. Since there is almost no practical way that g can be changed between model and prototype, the value of g_r usually must be taken equal to one. Consequently, from the dimensionless product a/g (also known as Froude's number and usually written as v^2/lg) it follows that

$$a_r = g_r = 1 \qquad (4.7)$$

If this relationship is substituted into the design condition $(gl\rho/E)_r = 1$ it follows that

$$\left[\frac{E}{\rho} \right]_r = l_r \qquad (4.8)$$

This scaling law places a severe limitation on the choice of suitable model materials. Equation (4.8) is sometimes expressed in terms of one dimensional wave propogation velocities as follows

$$v_r = \left[\frac{E}{\rho} \right]_r = (l_r)^{\frac{1}{2}} \qquad (4.9)$$

and is referred to as the Cauchy's condition (based on Cauchy's number $\rho v^2/E$)

The ratio between Froude's and Cauchy's number produces a parameter $E/l\rho g$. If it is required that a replica model reproduces the full scale values of those numbers, for fixed g, equations (4.7) & (4.8) can be derived. Thus eqn. (4.8) is a necessary condition for simultaneous replication of restoring forces, inertia forces and gravitational forces.

Additional design conditions are obtained from the other dimensionless terms of eqn. (4.6). For instance, it follows from the second term on the right hand side that

$$t_r = \frac{l_r}{\left[\frac{E}{\rho}\right]_r^{\frac{1}{2}}} = (l_r)^{\frac{1}{2}} \qquad (4.10)$$

Since elastic and plastic strains are dimensionless, they must be instantaneously equal in the prototype and model structures. From this observation it follows that typical structural displacements are related by

$$\delta_r = l_r$$

This relation ensures that geometrical non−linearity in structural behaviour is properly simulated.

Table 4−2 shows in column (4) the scaling laws for several physical quantities for a true replica model. In this case the independent quantities are chosen to be l,E and g, and g_r is taken equal to one. However, one major difficulty exists in this true replica modelling, namely, the selection of a suitable model material. Exact material simulation goes far beyond simulation of modulus of elasticity (E), Poisson's ratio (υ) and strain; theoretically it should include all relevant material properties discussed in section 4−2. Since no two materials in nature are exactly alike, material simulation will always introduce errors in the prediction values.

In the simplest case, similarity is necessary for the uniaxial stress strain curve for the range of strains in interest. Since true replica modelling requires that $\epsilon_r = 1$ (since ϵ is dimensionless), the stress−strain curves for model and prorotype materials should be identical except for a constant stretching by the ratio E_p/E_m in the ϵ direction (fig. 4−1).

Materials with shape similar $\sigma - \epsilon$ diagrams are difficult to find, particularly if nodistortion in the ϵ direction ($\epsilon_r = 1$) is permitted. Under certain conditions, strain distortion ($\epsilon_r \neq 1$) may provide an interesting

alternative to true replica modelling, an idea discussed in section 4.5.2.

True replica models are extremely difficult to realise because of problems in material simulation. Nevertheless, for certain length scale factors ($l_r = E_r/\rho_r$), suitable materials for the modelling of metallic structures are available.

In many cases it is possible to find acceptable alternatives to true replica modelling which are based on compromises that minimise the errors in rewponse prediction. The next section deals with an alternative method which will not solve all the problems encountered in dynamic modelling but is suitable for certain types of model studies concerned with particular parameters and structural configurations.

4.5.2 Adequate Models

All physical models which violate any of the design conditions discussed in the previous section could be called distorted models. However if the effect of distortion in one dimensionless product is such that it does not require an adjustment of other dimensionless products or of the prediction equation, then it seems appropriate to seperate such models from truly distorted models. Such models are known as adequate models.The need for such models is based on the desire to use the same materials as in the prototype.

There are two distinct distortions leading to two types of models which should prove very useful for model studies of certain classes of structures on shaking tables.

4.5.2.1 Model Tests With Artificial Mass Simulation

Equation (4.9) for true replica modelling requires that model materials have a small modulus or large mass density or both. Since such materials

are difficult to find, it appears attractive to supplement the density of the structurally effective material with additional material which is structural not effective. This can easily be achived in lumped mass systems as discussed below.

(a) Lumped Mass Systems – For many types of typical building structures it is acceptable to represent the seismically effective mass by a series of masses concentrated at the floor levels (lumped masses). In this case the seismically effective mass can be decoupled from the density of the structurally effective material which relaxes the dimensional requirement that $(E/\rho)_m$ must be equal to l_r.

Cauchy's requirement for proper simulation of internal forces and restoring forces can be written as

$$\left[\frac{gM}{l^2 E} \right]_m = \left[\frac{gM}{l^2 E} \right]_p \qquad (4.11)$$

which for $g_r = 1$ becomes

$$M_r = E_r l_r$$

In this equation M represents the lumped masses at the floor levels . It must be emphasised that " lumped masses " are those which are seismically but not structurally effective. In reality any mass, which is attached to structural components will affect the structural response. Masses at floor levels, such as a concrete slab system, will certainly affect the stress distribution in the structutal elements and in many cases will be part of the structural system. Great care must be taken in positioning such lumped masses in models to simulate the effects of gravitational and inertia forces. In many cases the distributed mass simulation discussed in (b) is preferable.

When the structurally effective mass is small and a representation of the seismically effective mass by lumped masses is feasible, the structural model may be made of prototype material ($E_r = 1$) and lumped masses are

scaled in the ratio $M_r = l_r^2$. For small scale model tests this often requires excessive weights which may render such tests impractical. However, the weight requirements may be reduced when the model materials used have small stiffness properties (see eqn. 4.11).

(b) Distributed Mass Systems :– For many types of structures a correct simulation of the mass distribution in space is essential and a simplified lumped mass system cannot be accepted. A simple way of testing adequate models of such structures would be to decouple the mass density ρ_0 of the structurally effective material from an additive ρ_1, which is to be built into the model but has no counterpart in the prototype. Thus the full scale density and stiffness would be represented by $(\rho_0)_p$ and E_p whereas those for the model would be $(\rho_0)_m + \rho_1$ and E_m respectively. This modification would alter the Cauchy's requirement as follows

$$\left[\frac{gl(\rho_0 + \rho_1)}{E} \right]_m = \left[\frac{gl\rho_0}{E} \right]_p$$

with one g testing this relation leads to

$$(\rho_0)_r + \frac{\rho_1}{(\rho_0)_p} = \frac{E_r}{l_r}$$

or

$$\rho_1 = \left[\frac{E_r}{l_r} - (\rho_0)_r \right] \qquad (4.12)$$

For instance,for a $1/20^{th}$ scale model using prototype material ($E_r = (\rho_0)_r = 1$) the density will have to be increased by a factor of 19. In a small scale model, the incorporation of the material that increases the density ρ_1 has to carefully thought out.

It is very difficult to effectively seperate the seismically effective mass from the structurally effective material. This method is practical for instance in structures consisting of slender load carrying mambers, the method for

adding mass could be to attach to each member suitable amounts of lead or other soft high density materials, arranged in such a way that it contributes negligibly to the strength and stiffness but supplements the weight and inertia. The spacing of these added masses should be maximised, so as to facilitate the manufacture while still approximating a distributed inertia.

The modelling law for such distributed masses can be obtained by replacing the mass per unit volume ρ_0 with some representative mass per unit length μ_0. When lead or other material with runnung mass μ_1 is attached to the model members, Cauchy's requirement is altered to

$$\left[\frac{g\ (\ \mu_0 + \mu_1\ )}{EI} \right]_m = \left[\frac{g\mu_0}{EI} \right]_p$$

With one g testing this leads to

$$(\mu_0)_r + \frac{\mu_1}{(\mu_0)_p} = E_r l_r$$

or

$$\mu_1 = [\ E_r l_r - (\mu_0)_r\ ](\mu_0)_p \qquad (4.13)$$

Using the same material in the model and prototype would make $E_r = 1$ and $(\mu_0)_r = l_r^2$ (from $\rho_0 = \mu_0/l^2$). This leads to the requirement

$$\mu_1 = (l_r - l_r^2\ )(\mu_0)_p \qquad (4.14)$$

This law may not be practical because it calls for adding a lot of mass. For instance for linear elements of a 1/20 scale model of identical structurally effective material, $(\mu_0)_m$ is 1/400 of $(\mu_0)_p$ whereas μ_1 is 1/21 of $(\mu_0)_p$, hence 19 times as massive per unit length as the basic model structure.

It appears that the practical realisation of this scale for small scale models in many cases will call for using reduced E/ρ_0 model materials. The use of such materials , which need not obey the requirement $(E/\rho)_r = l_r$ will require a lesser amount of added μ_1 which might lead to desirable compromises in the choice of materials and added weights.

The modelling laws summarised in column (1) of Table 4−2 apply to

the cases discussed in (a) and (b) with the exception of the requirement $(E/\rho)_r = l_r$. For the case of identical prototype and model material ($E_r = 1$) the modelling laws are shown in column (2) of the table.

Models with artificial mass simulation particularly suit the model study of multistorey and bridge structures. Such model studies are expected to result in a good prediction of prototype behaviour provided that mass distribution is properly simulated, the ground motion is reproduced according to the laws of similitude, model design and construction is done according to prototype procedures, and last perhaps most important, a thorough material study has proven the adequacy of material simulation. Model tests with artificial mass simulation is a very important source of information on structures whose stress and displacement histories have to be simulated in the elastic and inelastic range and whose materials are difficult to simulate by other than prototype like materials, such as in the case of reinforced concrete.

4.5.2.2 Model Tests Without Simulation Of Gravity Forces

Considering only multistorey structures, it appears that for certain types of structural configurations (e.g frame and shear wall structures) the stresses induced by gravity loads are small and maybe negligible compared to stress histories generated by seismic motions. In this case (a/g_r) need not be equal to unity, which allows considerably more freedom in selecting model materials and scaling parameters.

The scaling laws can be derived from the remaining dimensionless products of eqn. (4.6) with g in $gl\rho/E$ replaced by a. If l and E as well as ρ of a specific model material are selected as the independent quantities, the scale factors shown in column (3) of Table 4–2 can be derived. If prototype material is used (i.e $E_r = \rho_r = 1$), all scale factors can be

expressed in terms of l_r. (column (4) in Table 4–2)

It is important to note that the scale factors for many physical quantities are different from those for true replica models which will affect the shaking table input, the model design and the response prediction. For instance, when prototype material is used (column (4) in Table 4–2) with $t_r = l_r$ and $a_r = 1/l_r$, a reproduction of actual seismic motions on shaking tables may cause problems. This makes the use of other than prototype materials with $(E/\rho)_r$ smaller than one more feasible. For instance if brass is used for the simulation of steel (with $(E/\rho)_r \simeq 0.5$) results in $t_r = 1.41 l_r$, $v_r = 0.71$ and $a_r = 0.5/l_r$. With these values, seismic motions become more easily reproducable on shaking tables.

A building system which may be suitable for this type of model testing is a structural system where the lateral load resisting system consists primarily of shear walls which carry little vertical loads except through boundary elements. In slender shear walls the level of stress due to vertical loads in the boundary elements will be small and will not affect the response of the shear walls to a significant degree.

Now consider a mutistorey steel braced frame without moment resisting connections. In most type of bracing systems the stresses in the bracing members due to vertical loads will be negligible compared to those induced by lateral loads. A simulation of the load – deformation response of the structure will require proper modelling of the vertical elements of the braced bays.

4.5.3 Distorted Models

Models in which deviations from complete similarity exist and linear extrapolation from model to prototype would not be valid are known as distorted models. Distortion can be due to dissimilarity in boundary and

initial conditions , geometry or material properties.

In structural problems a distortion in boundary and initial conditions or in geometry is not usually necessary. Distortion in the reproduction of prototype stress strain characteristics is of greater significance. The requirement of identical strains in model and prototype ($\epsilon_r = 1$, see fig.4.1) is difficult to achieve in terms of availibility of suitable model materials. Materials which follow the stress _ strain pattern shown in Fig. 4.2 are more easily available.

If a model material which conformed to Fig. 4_2 was used the strains in the model would be larger than those in the prototype, hence the displacements in the model would not be similar to those in the prototype.

If a model material which conformed to Fig. 4_2 was used the strains in the model would be larger than those in the prototype, hence the displacements in the model would not be similar to those in the prototype. If the structural behaviour is dependent on the displacements such a distortion would not be suitable. However, if the displacements are sufficiently small such that they do not affect the equilibrium conditions, they may be acceptable. Since the ratio of correspondence between the model and the prototype is known strains, displacements, velocities and accelerations which occur in the model would vary by a factor which indicates the magnitude of strain deformation (ϵ_r in Fig 4_2).

Another type of material property distortion occurs when the Poisson's ratio of the model material and the prototype material are not the same. If the structural behaviour is dependent on the plane stress, a Poisson's ratio variation may distort the model strains. If however, the Poisson's ratio ν is not of prime importance materials having dissimilar Poisson's ratio may be used leading to only a small percentage of error.

4.6 CONCLUSIONS

Dimensional analysis has to be used to derive modelling laws for various types of model tests of structures subjected to seismic motion. It has to be realised that an exact reproduction of all parameters affecting the response of structures under dynamic actions can rarely be achieved. The emphasis here has beeen directed towards identification of important parameters and possible types of model tests which allow, as exact as possible, replication of these important parameters.

The choice of the right type of model for the intended purpose and the degree of approximation that must be accepted are of primary concern. In the most general case of a complex three dimensional structure where gravity and inertia effects are equally important, a true replica model is the ideal choice provided that a suitable model material can be found. If this is not possible, adequate accuracy in model tests can often be achieved by means of model tests with artificial mass simulation. In cases where prior knowledge shows that gravitational effects are small compared to seismic effects, model tests without simulation of gravity forces are feasible alternatives. These three types of model studies are the most suitable ones for seismic response phenomenon by means of small shaking tables.

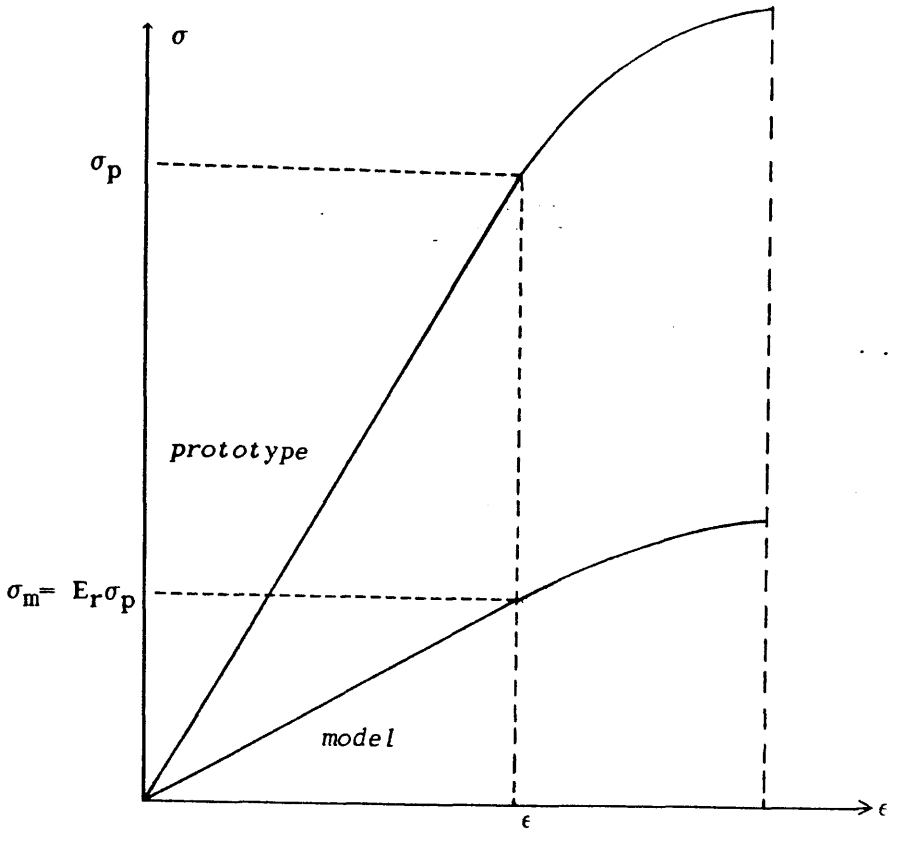

Fig. 4-1 Stress strain similitude requirements.

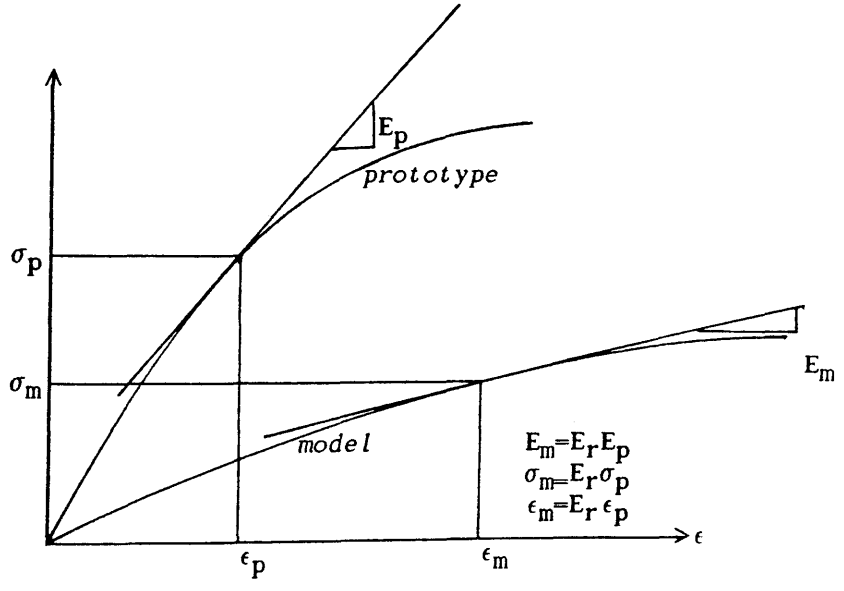

Fig. 4-2 Stress strain diagram indicating strain distortion.

TABLE 4-1 PHYSICAL QUANTITIES AND THEIR DIMENSIONS

PHYSICAL QUANTITY	SYMBOL	DESCRIPTIONS IN TERMS OF OTHER PHYSICAL QUANTITIES	DIMENSIONS IN FLTθ SYSTEM				DIMENSIONS IN MLTθ SYSTEM			
			F	L	T	θ	M	L	T	θ
Strain	ϵ	σ/E	0	0	0	0	0	0	0	0
Poisson's ratio	ν		0	0	0	0	0	0	0	0
Length	l		0	1	0	0	0	1	0	0
Time	t		0	0	1	0	0	0	1	0
Frequency	ω	$(k/m)^{\frac{1}{2}}$	0	0	-1	0	0	0	-1	0
Elastic restoring force	F_E	$k\delta, \sigma l^2, \epsilon E l^2$								
Gravitational force	F_G	$\gamma l^3, \rho g l^3$	1	0	0	0	1	1	-2	0
Inertia force	F_I	$ma, \rho l^3 a$								
Viscous damping force	F_D	cv								
Modulus of elasticity	E	$\sigma/\epsilon, F_E/\epsilon l^2$								
Shear modulus	G	$E/2(1+\nu)$	1	-2	0	0	1	-1	-2	0
Stress	σ	$\epsilon E, F_E/l^2$								
Displacement	δ	$\epsilon l, F_E/l^2$	0	1	0	0	0	1	0	0
Elastic stiffness	K	$\epsilon E l, F_E/\delta$								
Axial stiffness	K_a	AE/l								
Shear stiffness	K_s	$A_s G/l$	1	-1	0	0	1	0	-2	0
Flexural stiffness	K_f	EI/l^3								
Moment	M	Fl	1	1	0	0	1	2	-2	0
Mass	m	ρl^3	1	-1	2	0	1	0	0	0
Velocity	v		0	1	-1	0	0	1	-1	0
Acceleration	a		0	1	-2	0	0	1	-2	0
Coefficient of viscous damping	c	F_D/v	1	-1	1	0	1	0	-1	0

TABLE 4-2 BASIC SIMILTUDE REQUIREMENTS

MODEL TYPE / SCALING PARAMETERS	TRUE REPLICA	ARTIFICIAL MASS SIMULATION	GRAVITY FORCES NEGLECTED		STRAIN DISTORTION
			ANY MATERIAL	PROTOTYPE MATERIAL	
	(1)	(2)	(3)	(4)	(5)
Length l_r	l_r	l_r	l_r	l_r	l_r
Time t_r	$l_r^{\frac{1}{2}}$	$l_r^{\frac{1}{2}}$	$l_r(E/\rho)_r^{-\frac{1}{2}}$	l_r	$(\epsilon_r l_r)^{\frac{1}{2}}$
Frequency ω_r	$l_r^{-\frac{1}{2}}$	$l_r^{-\frac{1}{2}}$	$l_r^{-1}(E/\rho)_r^{\frac{1}{2}}$	l_r^{-1}	$(\epsilon_r l_r)^{-\frac{1}{2}}$
Velocity v_r	$l_r^{\frac{1}{2}}$	$l_r^{\frac{1}{2}}$	$(E/\rho)^{\frac{1}{2}}$	1	$(\epsilon_r l_r)^{\frac{1}{2}}$
Gravitational acceln. g_r	1	1	neglected	neglected	1
Acceleratn. g_r	1	1	$l_r^{-1}(E/\rho)_r$	l_r^{-1}	1
Mass density ρ_r	E_r/l_r	-	ρ_r	1	$\epsilon_r E_r l_r^{-1}$
Strain ϵ_r	1	1	1	1	ϵ_r
Stress σ_r	E_r	E_r	E_r	1	$E_r\epsilon_r$
Modulus of elasticity E_r	E_r	E_r	E_r	1	E_r
Specific stiffness $(E/\rho)_r$	l_r	-	$(E/\rho)_r$	1	$l_r\epsilon_r^{-1}$
Displacement δ_r	l_r	l_r	l_r	l_r	$l_r\epsilon_r$
Force F_r	$E_r l_r^2$	$E_r l_r^2$	$E_r l_r^2$	l_r^2	$E_r l_r^2 \epsilon_r$
Energy $(EN)_r$	$E_r l_r^3$	$E_r l_r^3$	$E_r l_r^3$	l_r^3	$E_r l_r^3 \epsilon_r^2$

CHAPTER 5 EXPERIMENTAL STUDY

5.1 INTRODUCTION

The literature review of Chapter 1 examined a few case studies where experimental techniques have been used to verify analytical results for the dynamic analysis of skeletal frames. The use of small scale models however has been limited partially due to the difficulties involved in modelling and in the interpretation of results. The main problem of accurate scale modelling involves the simulation of the mass of the structure i.e as the section sizes of the members are reduced to the appropriate scale, the mass is not reduced accordingly. To overcome this problem, in the last few years the technique of artificial mass simulation, where additional material of a non structural nature is attached to the structure to simulate the required scaled density of the model, has been used quite successfully by several researchers[20,23].

To examine the feasibility of using small scale models to depict the seismic behaviour of the skeletal framed structures, it was decided to build a simple unidirectional shaking table upon which small scale models could be tested. Two models were tested on the shaking table. The models were subjected to simple sinusoidal loading to determine the natural frequency and completely random vibrations covering a large frequency spectrum which simulated an artificial earthquake.

5.2 DESIGN AND CONSTRUCTION OF THE SHAKING TABLE

5.2.1 Modification of existant supporting framework

A supporting framework, which had been used by Burns[7] to study the dynamic behaviour of model bridge decks, was modified to enable the mounting of the vibrator and shaking table. Basically this involved the addition of extra members on which the vibrator and shaking table itself could rest.

Fig. 5−1 shows the side elevation of the whole system where the double frame arrangement was isolated from one another using steel coil springs. The frequencies of the springs isolating the two frames were selected so that the value of transmissibility was as low as possible. Transmissibility is a measure of the amount of vibration transmitted through an isolation system. It is a function of damping and the ratio of the fundamental frequency of the element being isolated and of the fundamental frequency of the isolation system. For satisfactory isolation of the two systems a minimum value of two, for the frequency ratio, is recommended.

For frame 'A' the calculated fundamental frequency was 465 Hz. Forcing frequencies thus had to be below 465 Hz. to avoid frame resonance. The natural frequency of the complete set up was found to be 4 Hz. These two values defined the upper and lower bounds of the allowable excitable frequencies. By ensuring that the minimum exciting frequency would be 10 Hz. and assuming a damping ratio of 0.2, the value of transmissibility was found to be less than 0.5 (Fig.5−2)

5.2.2 Design of the shaking table

The size and material used for the shaking table were limited by two factors

1) The dimensions of the supporting framework.

2) The operational capability of the electromagnetic vibrator.

The supporting framework consisted of two parallel frames (Fig. 5−3), 430mm apart, which were rigidly connected together by two cross members. The usable working space between the two cross members was approximately 1m, within which both the vibrator and the supporting system for the shaking table had to accomodated. As the vibrator was approximately 350mm long, it was decided that the shaking table should occupy the remaining space available to enable reasonably sized models to be tested in the future if necessary. A dimension of 710mm X 680mm was chosen.

The elctromagnetic vibrator used had a maximum throw of 16mm (± 8mm). The mass of the table had to be chosen such that it would not adversely affect this capability. Mild steel which was the first choice of material was found to be too heavy and considerable problems were encountered due to the distortion of the supplied plate, which had been cut to size by oxy–acetelyene burning. Aluminium was chosen as an alternative material. It had the advantage of being lighter in weight and no distortions were produced when cut to the required size. Table support rollers were made of mild steel and, to overcome the problem of possible rapid wear at the contact positions with the aluminium table, thin pieces of stainless steel strips were attached at the appropriate roller positions (Figs. 5–3,5–5). In order to maintain a low mass and yet have a high rigidity the thickness of the aluminium table was chosen to be 10mm.

5.2.3 Design of the table support mechanisms

To evenly distribute the load from the shaking table to the supporting framework, it was to rest on bearing at the four corners of the table. The bearings had to carry the load and simultaneously allow movement of the table in one horizontal direction. The supporting mechanism for each corner was made up of three mild steel rollers which were fitted with ball races at each end and were mounted together in a single bracket (Fig.5–4). A similar inverted double roller system was used on the top surface of the table to prevent possible table "chatter". This upper mechanism could be moved up or down in order to position it accurately against the surface of the table (Figs.5–5, 5–19). A substantial reduction in the amount of vibration in the table could be felt when these upper rollers were in contact with the table, as opposed to when they were raised from the contact position.

Two additional pairs of PTFE (Polytetrafluoroethene) rollers (Figs.5–19,5–20) which were mounted on vertical shafts were located against

two sides of the shaking table. These were used to ensure that the table encountered no torsional or lateral movement which would inevitably have caused damage to springs within the body of the vibrator.

5.2.4 Performace of the shaking table

To determine the capability of the shaking table, sinusoidal signals in the frequency range of 2 Hz.– 100 Hz. were fed through the vibrator connected to the bare table. The amplifier (PA 1000) maximum power was produced at an output current of 16.5 Amps. (rms) and was controlled by adjusting the 'sine' output control potentiometer on the Random Spectrum Generator (RSG 30). To obtain the overall response characteristics, bare table accelerations over the frequency spectrum of 2 Hz.– 100 Hz. were recorded when maintaining the output current fixed at 5, 10 and 15 Amps. (rms) in turn. Fig. 5–6 is a four way logarithmic plot showing the characteristics of the bare table, from which the displacement and accelerations can be read for a particular frequency at any of the three designated values of output current.

5.3 THE EXPERIMENTAL PROCEDURE

The two models tested were subjected to both sinusoidal and random excitations. By applying a sinusoidal input the natural frequencies of the models and the associated maximum displacements at these frequencies were determined. These values were also evaluated using simple mathematical relationships. Comparison of these experimental and analytical results served as a basic check to the accuracy and performance of the models.

The models were then subjected to random base excitations. The excitation was tailored to simulate an artificial earthquake by enveloping a wide frequency spectrum. The response of the models to these excitations was obtained and compared to the results obtained by using the computer programs.

5.3.1 Experimental Apparatus

The experimental equipment for testing each of the models can be broadly divided into two basic component systems namely the excitation system and the data aquisition and signal conditioning system.

The vibration input system comprised of :

a) A Farnell sine–square oscillator with a frequency range of 1 Hz.– 1 MHz.

b) A Ling Dynamics Systems Random Spectrum Generator (RSG 30) which could provide a random input in the frequency range of 2 Hz. – 2 kHz.

c) A Ling Dynamics Systems Random Spectrum Analyser (RSA 30) which was used in combination with the RSG 30 to give a visual display of the frequency spectrum in histogram form.

d) A Ling Dynamics Systems Amplifier (PA 1000) which provided the input current to the vibrator. Its maximum output power of 1000 W was achieved at an output current of 16.5 Amps. (rms).

d) A cooling fan, used to protect the moving coil assembly of the vibrator from overheating.

e) A Ling Dynamics Systems Vibrator (Model no. 455). The peak thrust force with air cooling and bare table was 490 N.

The data aquisition apparatus which were directly located at appropriate positions in the shaking table and the models comprised of :

a) Birchall general purpose piezoelectric accelerometers which were used to measure accelerations by attaching them at the required positions on the shaking table and the models.

b) Linear Variable Differential Transducers (LVDTs) were positioned against appropriate locations on the shaking table and the models. The output from the LVDTs was used to evaluate the displacements at these locations.

To determine the response of the table and the models, the following signal conditioning equipment was used. For the accelerometers :–

a) The signals were passed through high impedence microdot cables. These high impedence cables were reduced to low impedence cables by using voltage amplifiers. The reason for this impedence transfer is that if long cables are required on site where low impedence is necessary, the loss of signal power would not be great.

b) The output from the voltage amplifiers were fed through an oscilloscope, which was used to check resonant frequencies of the models by associating them with the maximum signal amplitude on the oscilloscope screen.

c) The signals from the voltage amplifiers were passed through an attenuator/amplifier.

d) Permanent records of the accelerometers' signals were made on photographic paper using an S.E Laboratories Oscillograph (Type S.E 3000).

The signals obtained using the LVDT's were

a) Fed into a voltage calibrator and amplifier. The voltage calibrator was used to control the voltage change induced by movement of the plunger by a fixed amount. The output signal was then amplified to 24 mv before it could be compatible with other instrumentation being used.

b) The signals from the voltage amplifiers were passed through an attenuator and an amplifier which were used to decrease or increase the LVDT's signals respectively.

c) Permanent records of the accelerometers' signals were made on photographic paper using an Bell and Howell light pen Oscillograph.

5.4 EXPERIMENTAL STUDY OF MODEL 'A'

Model 'A' was chosen to be the prototype, this was mainly to ascertain the performance of the experimental equipment and model behaviour without having to get involved with the complications of scale modelling. The results obtained from the experimental study could be directly compared to analytical results without actually having to scale them in any way.

5.4.1 Description of model 'A'and instrumentation used

In order to check the validity of assumptions made in modelling a structure as a shear building, this model was basically a single bay of a single storey shear building. It was composed of two mild steel columns with the mass lumped at the top of the columns. As can be seen in Fig. 5–7 the columns were rigidly fixed at the base and at the level of the mass. The lumped mass was taken as an infinitely rigid beam and as such was a structural component. For simplicity bolted connections were used both at the base and at the upper level. The exterior plates at the upper level were used to ensure that the positions of the points of contraflexure at the top of each column would remain fixed when the model swayed about its equilibrium position.

One accelerometer was attached to the shaking table from which continuous recordings of the base acceleration was made. When the model was subjected only to sinusoidal vibrations the response of the lumped mass was obtained from the output of the accelerometer attached at this level. However, when the model was subjected to random excitations, the response of the lumped mass could not be obtained from the accelerometer trace as it was necessary to know the frequency content at any particular instant before the accelerations could be related to displacement. To obtain a direct reading of the displacement one LVDT was attached at the centre level of the mass. The LVDT was mounted on a rigid member which was secured to the clamping supports on the shaking table. This effectively ensured that the absolute

displacement readings were being monitored. Continuous readings from both aceelerometers and LVDT's were fed into the light pen oscillograph from which acceleration and displacement traces were obtained. Fig. 5–8 shows a line diagram of the instrumentation used for this model.

5.4.2 Determination of damping ratio

From free vibration experiments the damping ratio for a single storey structure was determined by the following procedure

a) The structure was disturbed from its equilibrium position through some initial displacement x_0 and then released.

b) The free vibrations of the structure were recorded and an acceleration– time plot was obtained from which :

c) Two peak values of accelerations $\ddot{x}_i$ and $\ddot{x}_{i+j}$, that were several cycles apart were measured.

d) The logarithmic decrement $\delta = 1/j \; [\; \ln(u_i / u_{i+j}) \;]$ was computed.

e) The damping ratio ξ, for the structure was evaluated as $\xi = \delta / 2\pi$

For this particular model the free vibration acceleration– time plot is shown in Fig. 5–9 . By measuring the peak values for the 2^{nd} and 7^{th} cycles the logarithmic decrement δ, was computed as 0.1353. The corresponding value for the damping ratio ξ, was evaluated as 0.0215.

5.4.3 Determination of the natural frequency of the model

Although free vibration measurements are sometimes easily accomplished by pulling on the structure, then releasing quickly and measuring the free motions of the structure, in the laboratory tests it was simpler to force the structure to

vibrate in one of its natural frequencies and then measure the response. By attaching the model to the shaking table and changing the frequency of the forcing signal, occurence of resonance was observed on the oscilloscope. When resonance occured, since the displacement at the level of the mass was maximum, the output from the accelerometer attached at that level produced a point of maximum amplitude on the oscilloscope. The output signals were also examined through the oscillograph traces obtained at this particular frequency. The results were measured from the oscillograph traces as follows :

The photographic paper used to record the traces was fed through the oscillograph at a known speed, so that by measuring the distance along the trace for say 20 cycles, the time for 1 cycle, and hence the frequency could be calculated.

Table 5—1 shows the comparison of the experimental and theoretically computed values. The sinusoidal oscillator was used to to generate the required frequency, the frequency of motion of the table was estimated by obtaining an oscillograph trace of the output from the accelerometer attached to the table and counting the number of sine waves plotted for a period of 5 seconds. The theroretical value for the frequency of the model was computed by considering it as a single degree of freedom system.

5.4.4 Response to harmonic excitation

The response of the model when subjected to harmonic excitation was studied to provide a further check on the behaviour of the model. The input signal to the table was fine tuned to produce a frequency of 20 Hz. This was checked by obtaining an oscillograph trace for 5 seconds and counting the number of sine waves. From this trace the base acceleration was computed using the following formula :—

$$\hat{a} = \frac{A_T}{G_S \cdot G_A \cdot A_O} \qquad (5.1)$$

where $\hat{a}$ - Peak acceleration in terms of 'g'

A_T - Trace amplitude (peak value) (mm)

G_A - Amplifier gain

G_S - Galvanometer sensitivity (mm/mv)

A_O - Accelerometer output (mv/g)

For the experiments performed in this study each accelerometer was calibrated with a 3m. length of microdot cable connected to a voltage amplifier and the average peak outputs were found to be 26.77 mv/g. The fluid damped galvanometers had a sensitivity of 14 mv/mm for a 1v input with the amplifier gain set to unity. To obtain reasonably sized traces from the oscillograph the amplifier gain was set to 10.

Since the model was considered to be a single degree of freedom system, the static and maximum dynamic displacement at a particular forcing frequency was computed by following the procedure indicated in Fig. 5–23. Experimentally the value of the acceleration at the level of the mass was obtained from the output of the accelerometer attached at this level. For harmonic loading the equation of motion can be written as

$$x = A \sin \omega t \qquad (5.2)$$

differentiating this equation twice gives

$$\ddot{x} = - \omega^2 . A \sin \omega t \qquad (5.3)$$

hence the peak accelaration is

$$\tilde{\ddot{x}} = \omega^2 . A \qquad (5.4)$$

By substituting the experimental value of the peak mass acceleration into eqn. (5.4), the displacement at this position was computed.

5.4.5 Response to random vibration

Having examined the response of the model to harmonic excitation, it was subjected to random excitations. Since the model was effectively a single degree of freedom system, the frequency content of the random excitations had to be composed of mainly those frequency bandwidths which included the

natural frequency of the model. The frequency control potentiometer in the 10 – 20 Hz. range of the Random Spectrum Generator was used to provide the major component of the random signal. However, due to overlap of adjacent frequency ranges, the generator produced vibrations in the 20 – 30 Hz. and 30 – 40 Hz. ranges. These signals had smaller intensities but could not be altogether isolated as shown in Fig. 5–11.

The model was vibrated continuously for a period of 10 seconds and base accelerations and mass displacements were recorded. The values of the base accelerations were later digitised and used as data for the mathematical analysis using the computer program. The comparison of response of the model using the theoretical and experimental results was made and is shown in Fig. 5–13.

5.4.6 Discussion of results

The predicted and actual values for the natural frequency correspond very well. The response to harmonic excitation also shows that the behaviour of the model to sinusoidal behaviour can be predicted quite accurately. The supporting blocks did not provide absolute fixity, this was clear as slight lifting of the supports could be noticed, and hence the actual stiffness of the structure was possibly lower than the calculated value. This would certainly result in a lower value for the natural frequency of the structure. Losses which were encountered in the transmission of signals from the accelerometer could also be one of the contributing factors i.e the frequency of table motion was slightly higher than the actual recorded value.

The comparison of the theoretically computed and experimental values of displacements with the model subjected to random base excitations show that both the curves follow the same pattern. The experimental results confirm the trend in the behaviour of the structure. The use of LVDT's to measure the displacements of the structure had two drawbacks. Firstly they offered a slight resistance to free movement of the structure and secondly as slight bending

occured in the structure, the LVDTs' plungers were rubbing against the transformers within the body of the transducers . This in effect resulted in lower than actual values being recorded. It can be seen from Fig. 5–13 that the computed values are slightly higher than the corresponding experimental values. One of the reasons for this difference could be the effect of damping in the structure. In the mathematical analysis damping was assumed to be constant, in reality, however, the damping in any structure varies with frequency and this effect was not investigated here.

5.5 EXPERIMENTAL STUDY OF MODEL 'B'

Having studied the behaviour of a model shear building, it was decided to test a truly three dimensional model. Model 'B' was designed as a 1/25 scale model of a pseudo prototype structure shown in Fig. 5–14 . The reason for not constructing a reduced scale model of a real steel structure was to avoid the complications involved in the fabrication of miniature I–sections. Small scale I–sections would have to be fabricated by milling mild steel bars, this was thought as being a very intricate and time consuming task. Moreover, high initial stresses would have been induced by the fabrication process and hence reproducing the initial stress state in the prototype would have involved complex heat treatment procedures.

The natural frequencies of the model were determined in a similar fashion as for model 'A'. The modes of vibration of the model were deduced by comparing the phase differences between the output signals. It was then subjected to random vibrations to try and induce non–linear beahviour. Comparisons of results obtained using experimental and analytical techniques were made later.

5.5.1 Description of model 'B' and instrumentation used

This model was designed as an adequate model of the prototype using

artificial mass simulation to achieve density similitude. The model shown in Figs. 5–15 and 5–22 was a one storey three dimensional structure which was constructed using mild steel. The members were made from 3 mm rolled bar stock, which was obtained easily from suppliers. All the connections were made using spot welds. The model was braced in the direction perpendicular to the direction of vibration to eliminate the effects of cross vibrations. The columns were welded to two 2mm mild steel plates at the upper and lower levels, thus forming a rigid open ended box type framework. A lumped mass of 5 kg was attached to the upper plate by bolts, it was however seperated from the plate by means of washers to effectively isolate it, in a structural sense, from the main body of the structure.

As the structure could vibrate in more than one direction, it was necessary to monitor the various possible motions. A line diagram and a photograph of the experimental equipment used is shown in Figs. 5–16 and 5–21 respectively. Accelerometers in the three orthogonal directions were attached to the lumped mass and to obtain direct readings of displacements LVDT's were also used. LVDT's were located parallel to each other and rigidly fixed to a common bracket which served as a reference line (Fig. 5–22). The LVDT in the middle was used to monitor actual displacements, while the outer two were primarily attached to see whether torsional behaviour was induced by the vibrations. Base accelerations were monitored from the accelerometer attached at this level. Accelerometers at the upper level were used to check whether strong movements were induced in the directions perpendicular to the direction of motion of the shaking table.

5.5.2 Determination of damping ratio

The damping ratio of the model was found in exactly the same manner as for model 'A'. The model was disturbed from its equilibrium position and from the trace of the decay of acceleration (Fig. 5–10), the damping ratio

was evaluated as 0.018.

5.5.3 Determination of the natural frequencies

Using the computer program developed for three dimensional frames, the first six natural frequencies and mode shapes for the prototype were determined. Examination of the eigenvectors revealed that the first mode shape was pure bending about the weak axis, the second mode was also pure bending, but about the other axis. In the third mode the structure reverted to bending about the weak axis, the fourth and fifth modes were composed of combined bending and torsion and the sixth mode was axial extension in the vertical direction. Scaling the natural frequency values of the prototype using similitude laws the corresponding values for the model were evaluated.

The model was attached to the shaking table and excited by feeding signals from the sine wave generator. As the input frequency values corresponded with any of the expected frequency values, the output from the appropriate accelerometer was fed into the oscilloscope and the input signal was fine tuned until a point of maximum amplitude was displayed on the oscilloscope. Table 5−3 shows the results obtained from the experimental study and corresponding theoretical values for the prototype and the model.

5.5.4 Response to random excitation

In this part of the study the model was subjected to random vibrations in the frequency range which covered the first six natural frequencies of the model. To achieve this a white noise signal (A signal where the Power Spectral Density of each of the frequency components is the same) was used as the input (Fig. 5−12). To try and induce non−linear behaviour of the model, the amplitude of the random input signal was increased to a maximum such that the output current produced by the amplifier was the maximum of 15 Amps.

The model was vibrated for a period of 10 secs. during which continuous recordings of output from the accelerometers and LVDT's were made. The base acceleration values were digitised and used as data input for the computer program in which the prototype was analysed. The displacement values obtained while monitoring the response of the model were scaled using similitude laws. A comparison of these two sets of values is made in Fig. 5–18

5.5.5 Discussion of results

In studying the response of model 'B' displacements and accelerations in the three orthogonal directions were monitored. In determining the natural frequencies, the procedure was only successful for the first three values. Occurence of resonance was clearly noticeable when the first three natural frequencies were excited. For the higher values, even at maximum amplification, the signals from the accelerometers were too weak, and failed to produce any visible effect on the oscilloscope screen. At these higher frequencies no motion, either of the table or the model was visible, only high frequency sound produced by the vibrator was audible. The first three mode shapes were clearly observable and the modes of vibration corresponded with those obtained by interpretation of the calculated eigenvectors.

The difference between the analytical and experimental results was probably because the actual elastic stiffness of the model was smaller than the calculated value. The welding process produced distortions in two of the columns. Even though the members were rigidly fixed to a jig during the welding process, one of the columns was slightly off plumb.

Bracing which was added to the model was effective in reducing any cross axis vibration to a very large extent. Fig. 5–17 shows the oscillograph trace from the three LVDT's which were used to monitor the displacements. The diagram clearly shows that the three traces are identical, indicating that the

torsional effect is negligible.

Since movement in the direction perpendicular to that of applied motion was negligible only displacements occuring in the primary direction were monitored. Fig. 5−18 shows a comparison of experimental values and theoretically computed displacements in this direction. As with model 'A' at higher amplitudes of table motion, the experimental values were lower than the corresponding theoretically computed values. The two curves follow a similar pattern indicating that the experimental results accurately predict the trend in the response of the structure. On average the variation between the values plotted amounts to about 10−12 %. However, losses were encountered in recording the experimental results. The frictional effects which were described for model 'A' were more prominent in this test as three LVDT's were used as opposed to one for the previous test.

The effect of variation of damping ratio is thought to be of significance but no definite figure could be attributed to this effect. As the model behaved linearly elastic, the effect of strain rate was not taken into account.

5.6 CONCLUSIONS

The conclusions which may be drawn from this experimental study are

1) The behaviour of model 'A' which itself was the prototype was predicted accurately by the experimental study. The predicted natural frequency and response to harmonic motion was closely related to the mathematically computed values.

2) The experimental prediction of response of this model to random behaviour also showed a close correspondence to the mathematically evaluated response. However, losses were involved in the recording of signals.

3) The model accurately represented the behaviour of a shear building. This was confirmed by the fact the experimental and theoretical values corresponded closely, thus reinforcing the assumptions made in the mathematical modelling of

the system.

4) The artificial mass simulation technique for adequate models satisfied the necessary mass similitude laws.

5) The prediction of natural frequencies of model 'B' was not totally successful. The first three frequencies were predicted rather accurately, but distortions produced during fabrication led to a reduction in the stiffness of the structure. The procedure of sinusoidally exciting the structure at higher frequencies proved unsuccessful as the amplitude of the signals produced from the accelerometers were too small to be effectively recorded.

6) The response of the model to random vibration predicted the trend of the response of the pseudo prototype structure subjected to the same base accelerations. The experimental values underestimate the displacements produced in the structure. Experimental losses in recording the signal had a major contribution in the discrepancies produced.

7) It was not possible to induce nonlinear behaviour in this model in spite of using strong base accelerations. The capability of the vibrator limited the magnitude of base accelerations which would be required to cause nonlinear behaviour.

8) The use of small scale models was found to be a suitable technique for predicting the response of simple prototype structures. It was however a time consuming process and involved a lot of intricate work in the actual construction of the models and the monitoring of experiments.

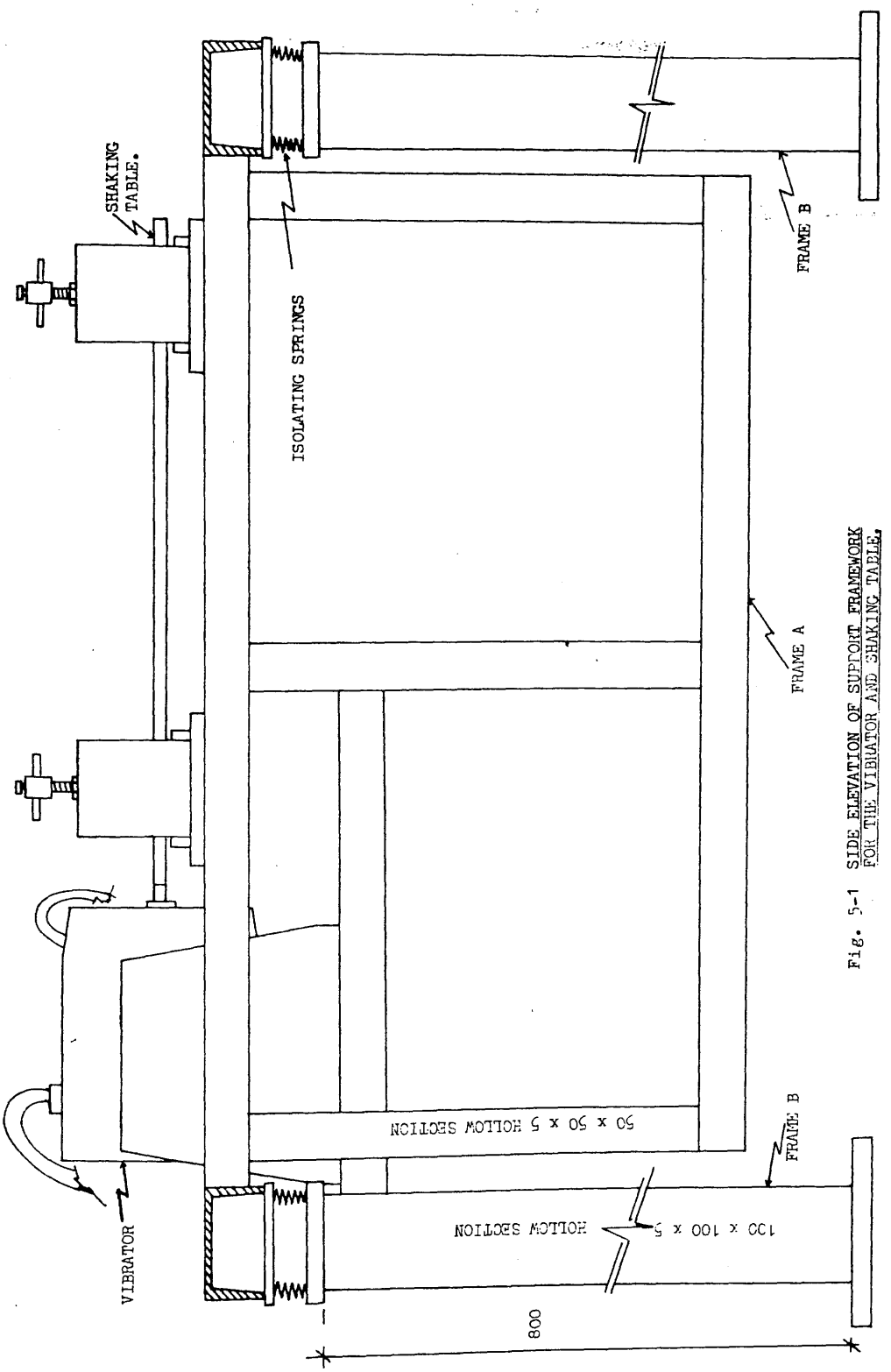

Fig. 5-1 SIDE ELEVATION OF SUPPORT FRAMEWORK FOR THE VIBIATOR AND SHAKING TABLE.

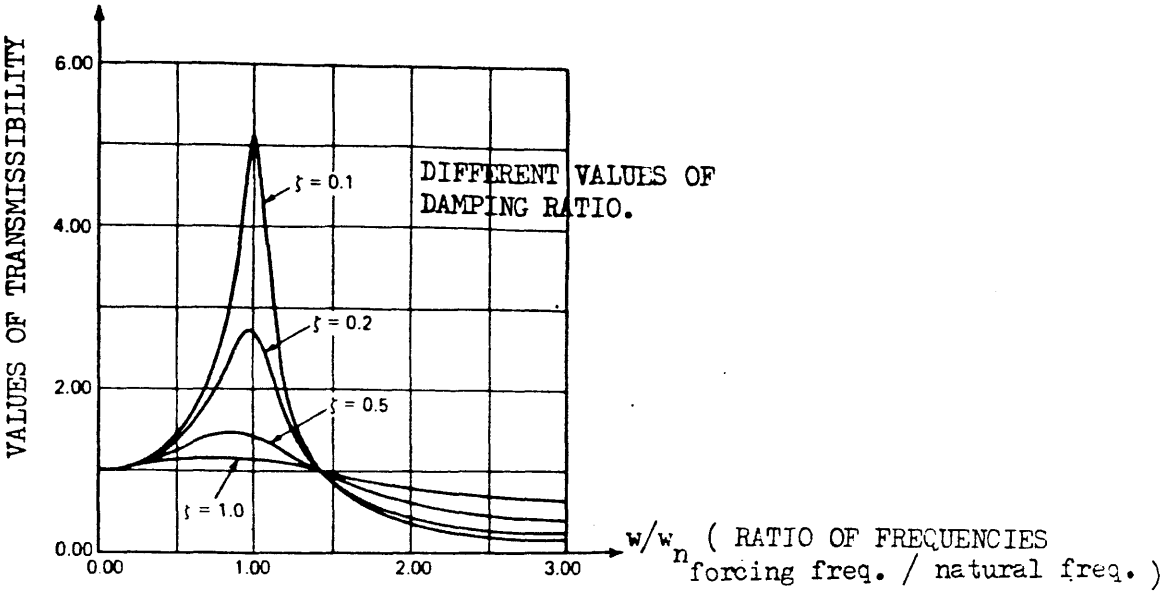

Fig. 5-2 TRANSMISSIBILITY CURVES

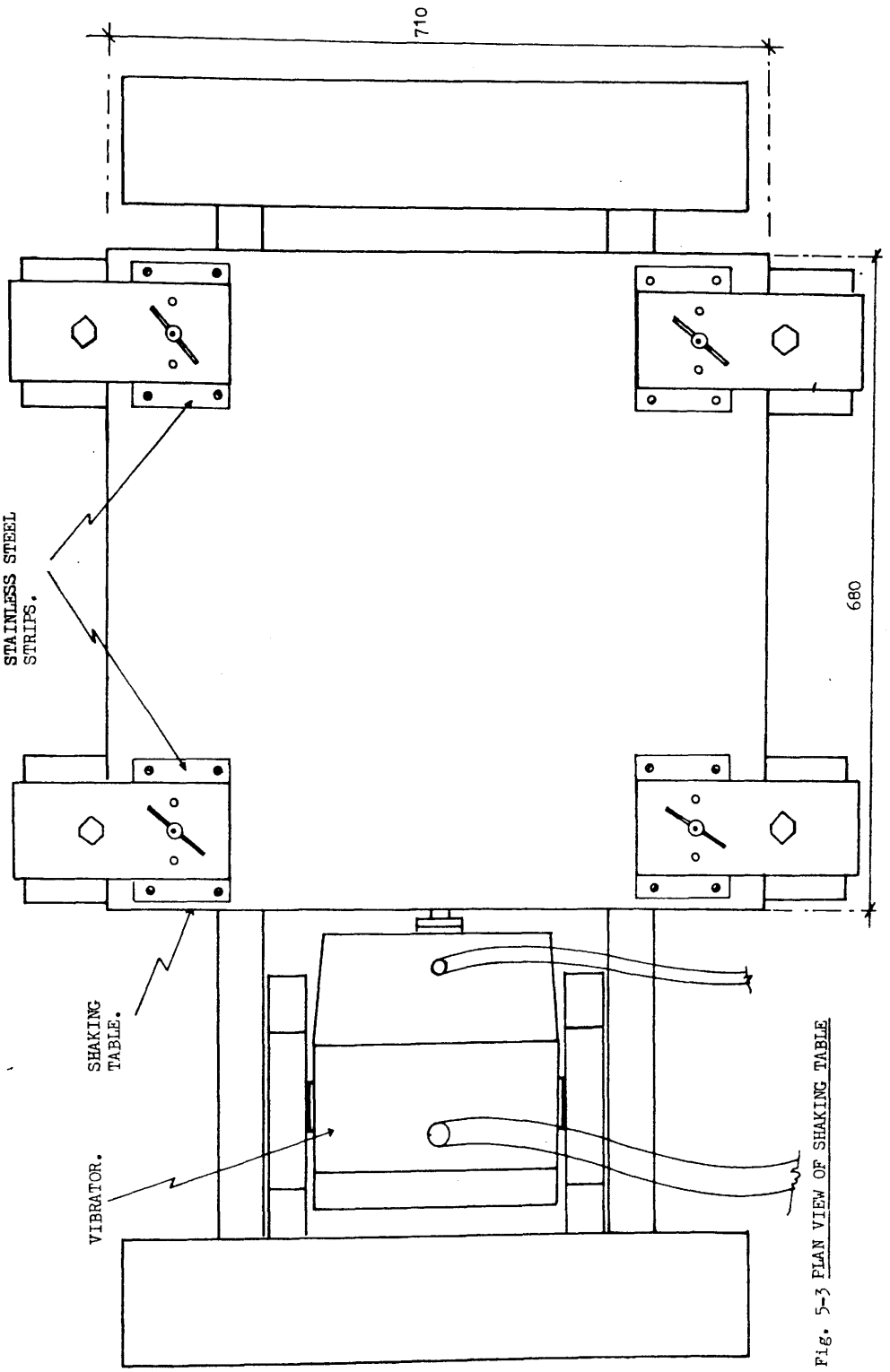

Fig. 5-3 PLAN VIEW OF SHAKING TABLE

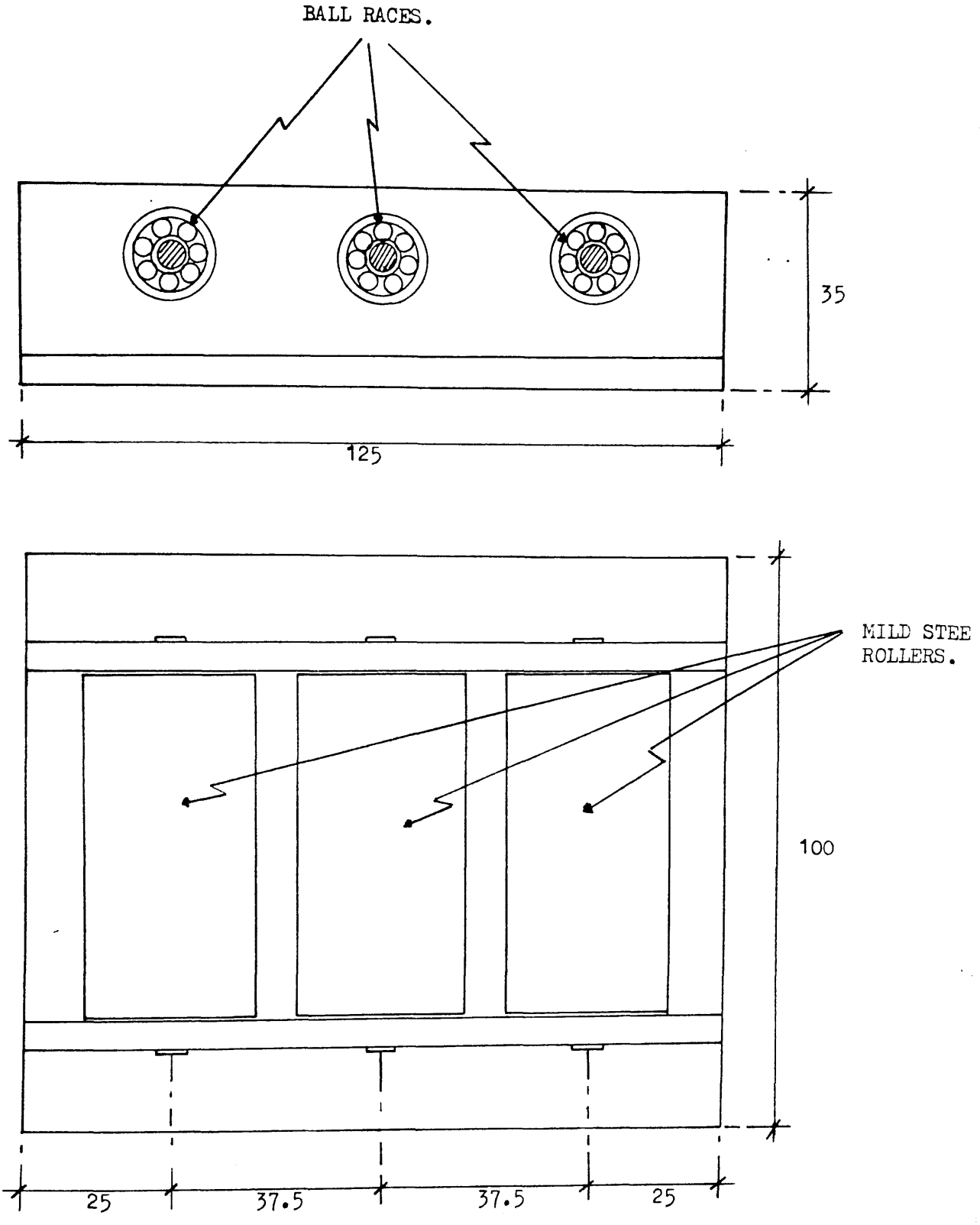

Fig. 5-4 SIDE ELEVATION AND PLAN VIEW OF ROLLER SUPPORT MECHANISM

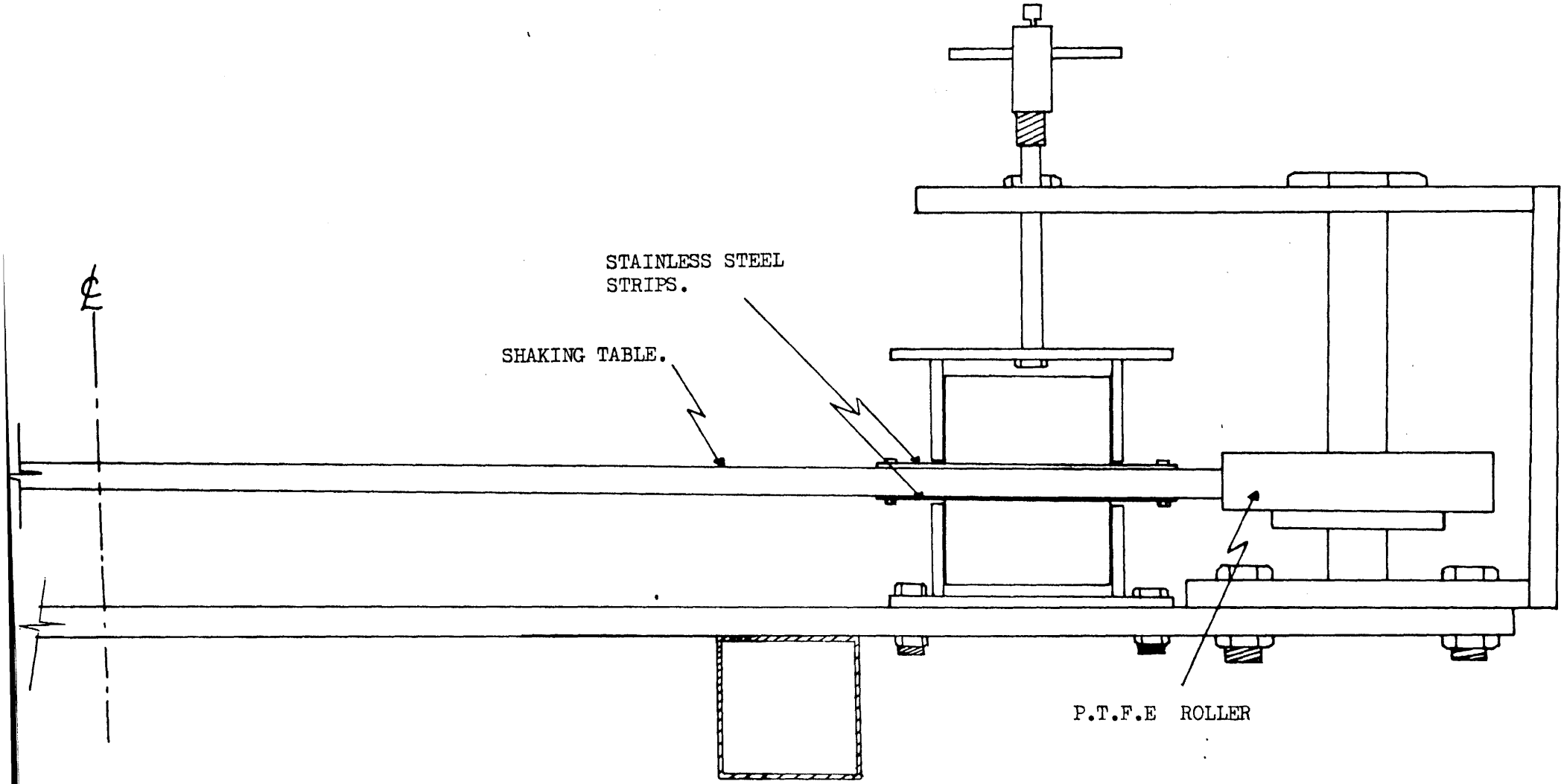

Fig. 5-5 FRONT ELEVATION OF A SINGLE TABLE SUPPORT MECHANISM.

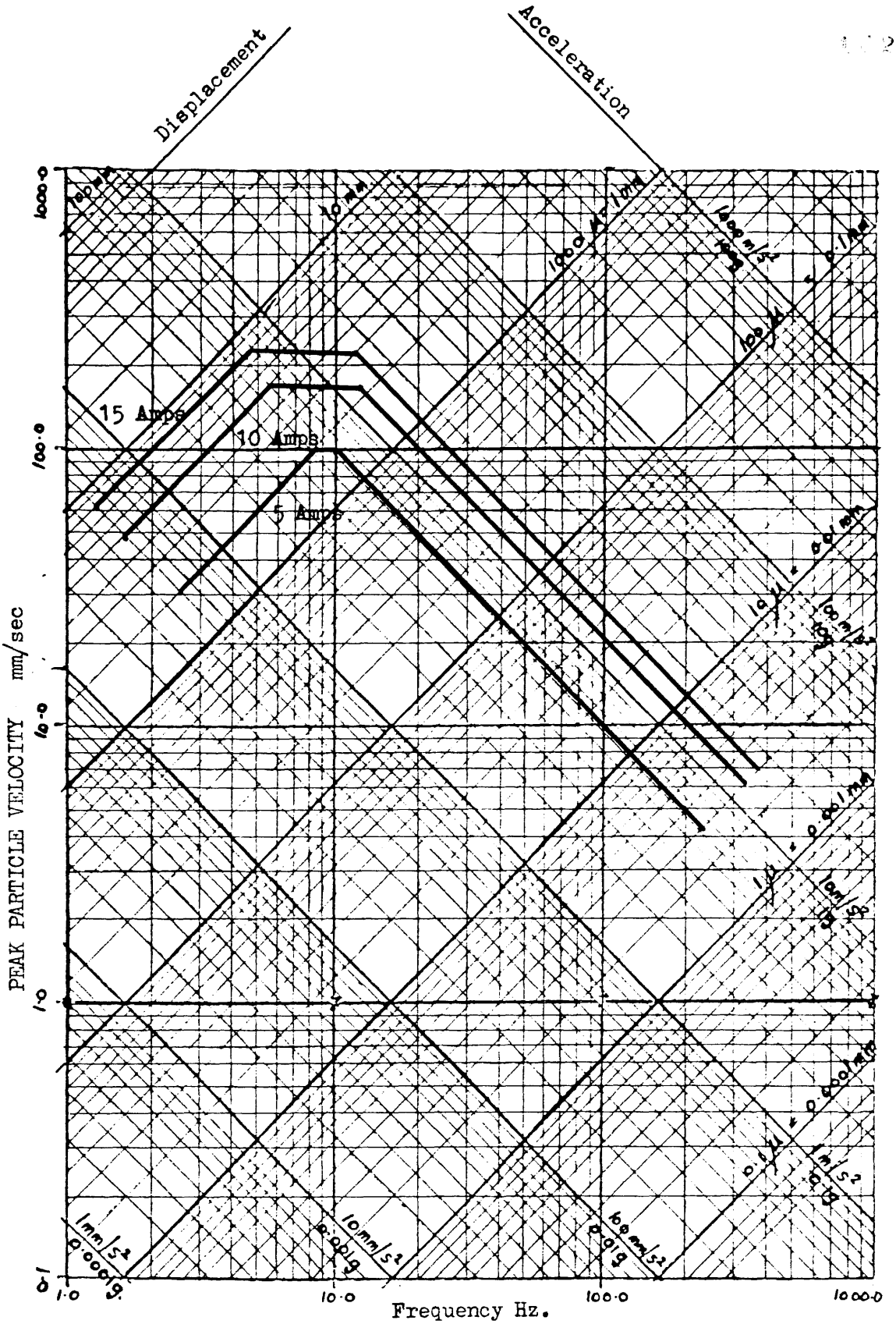

Fig. 5-6 RESPONSE CHARACTERISTICS OF BARE TABLE

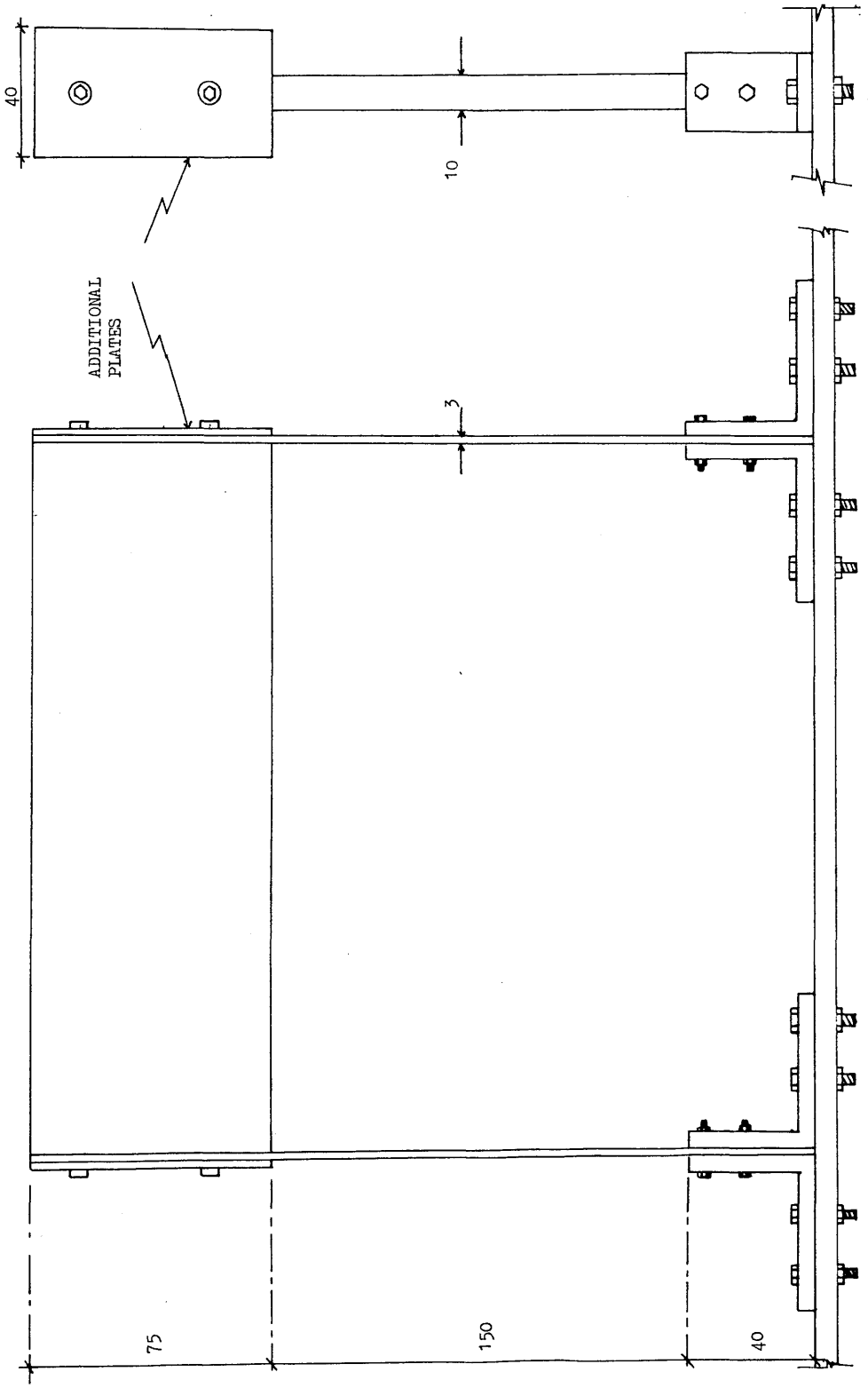

Fig. 5-7 FRONT AND SIDE ELEVATIONS OF MODEL 'A'

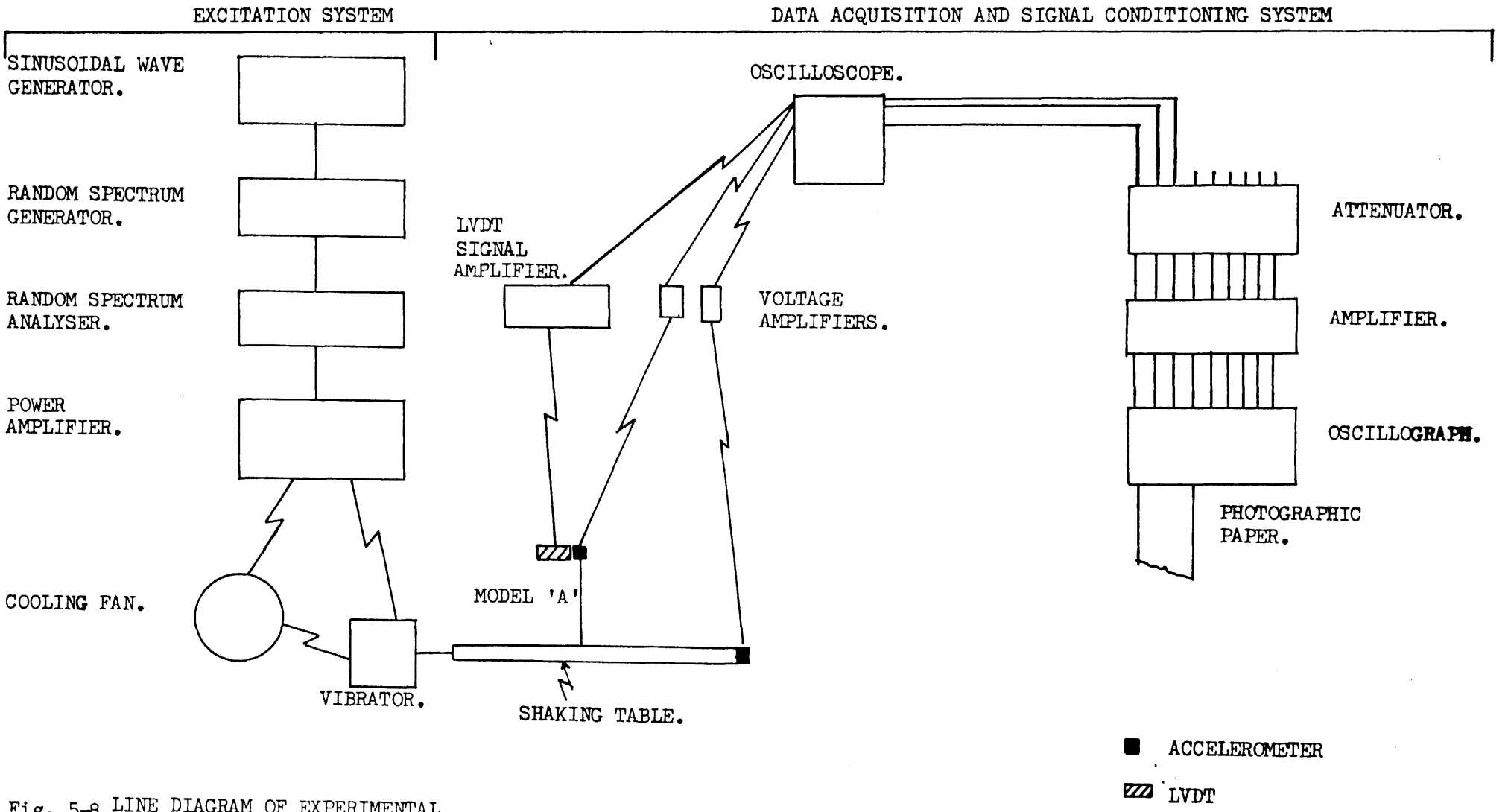

Fig. 5-8 LINE DIAGRAM OF EXPERIMENTAL SET UP FOR MODEL ' A '

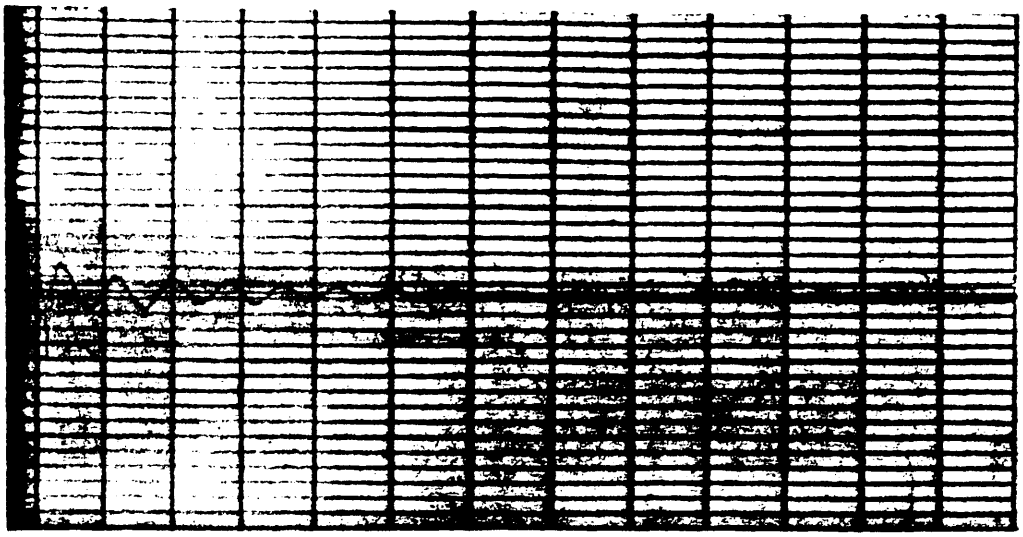

Fig. 5-9 ACCELERATION VS. TIME TRACE FOR MODEL 'A'. (FREE VIBRATION)

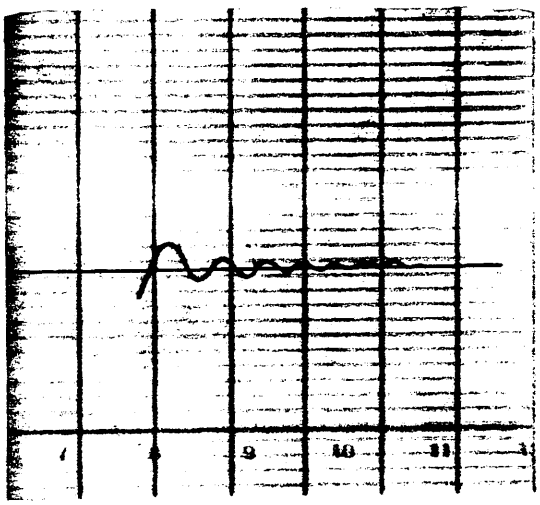

Fig. 5-10 ACCELERATION VS. TIME TRACE FOR MODEL 'B'. (FREE VIBRATION)

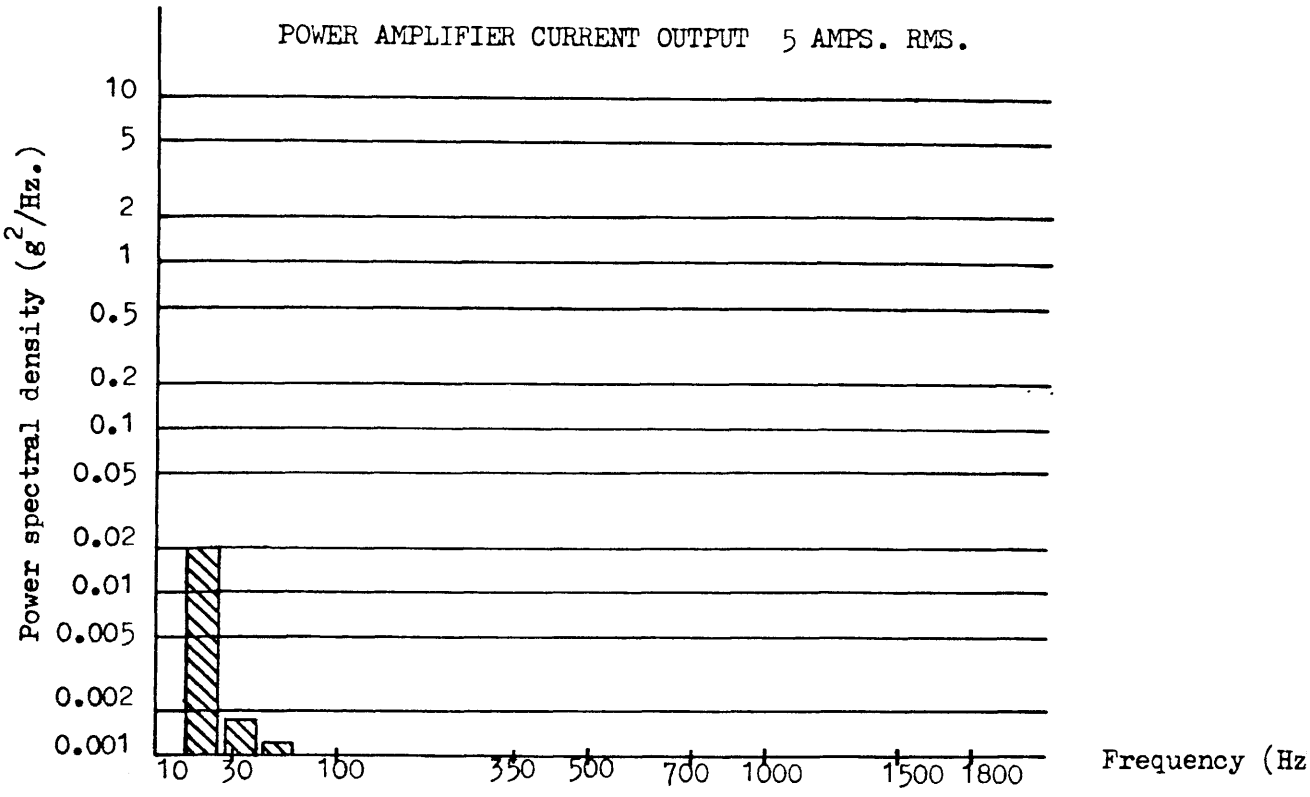

Fig. 5-11 HISTOGRAM OF FREQUENCY SPECTRUM INPUT FOR RANDOM VIBRATION OF MODEL 'A'.

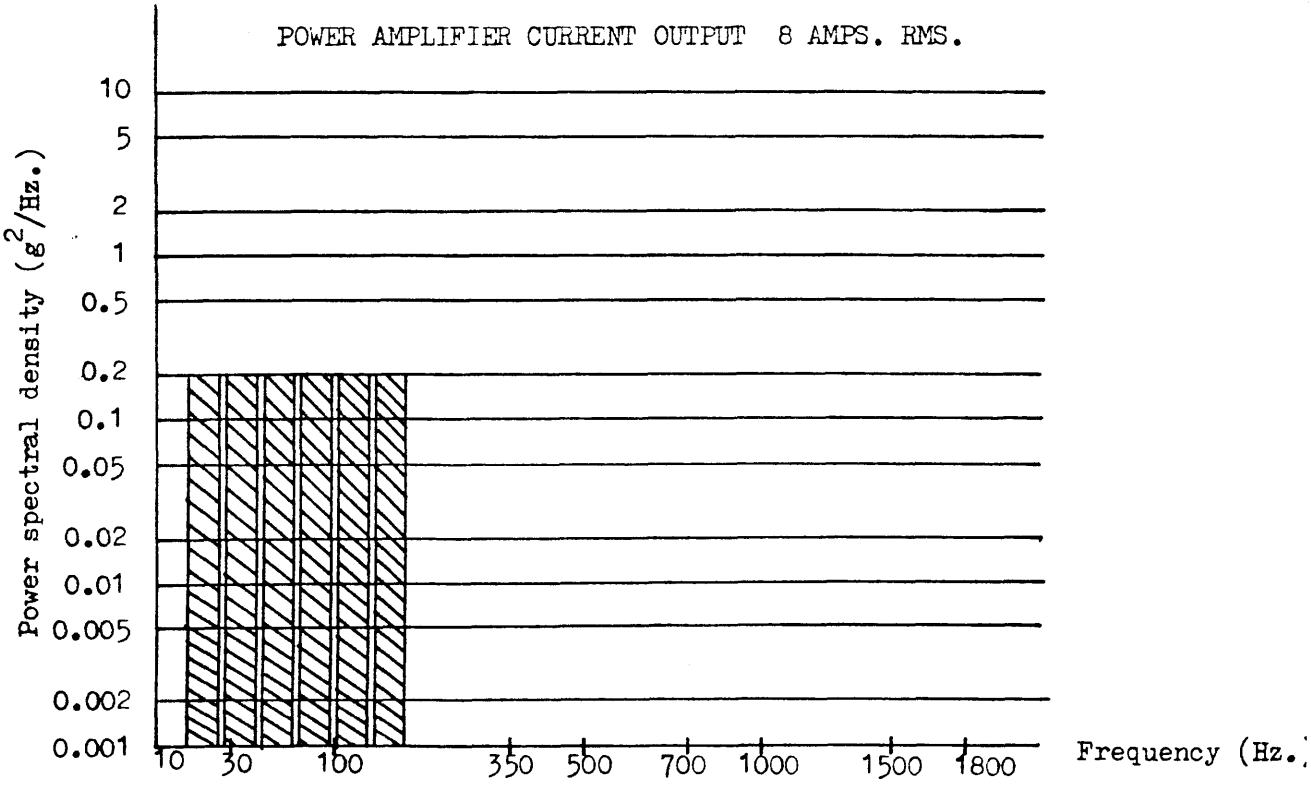

Fig. 5-12 HISTOGRAM OF "WHITE NOISE" INPUT FOR RANDOM EXCITATION STUDY OF MODEL 'B'.

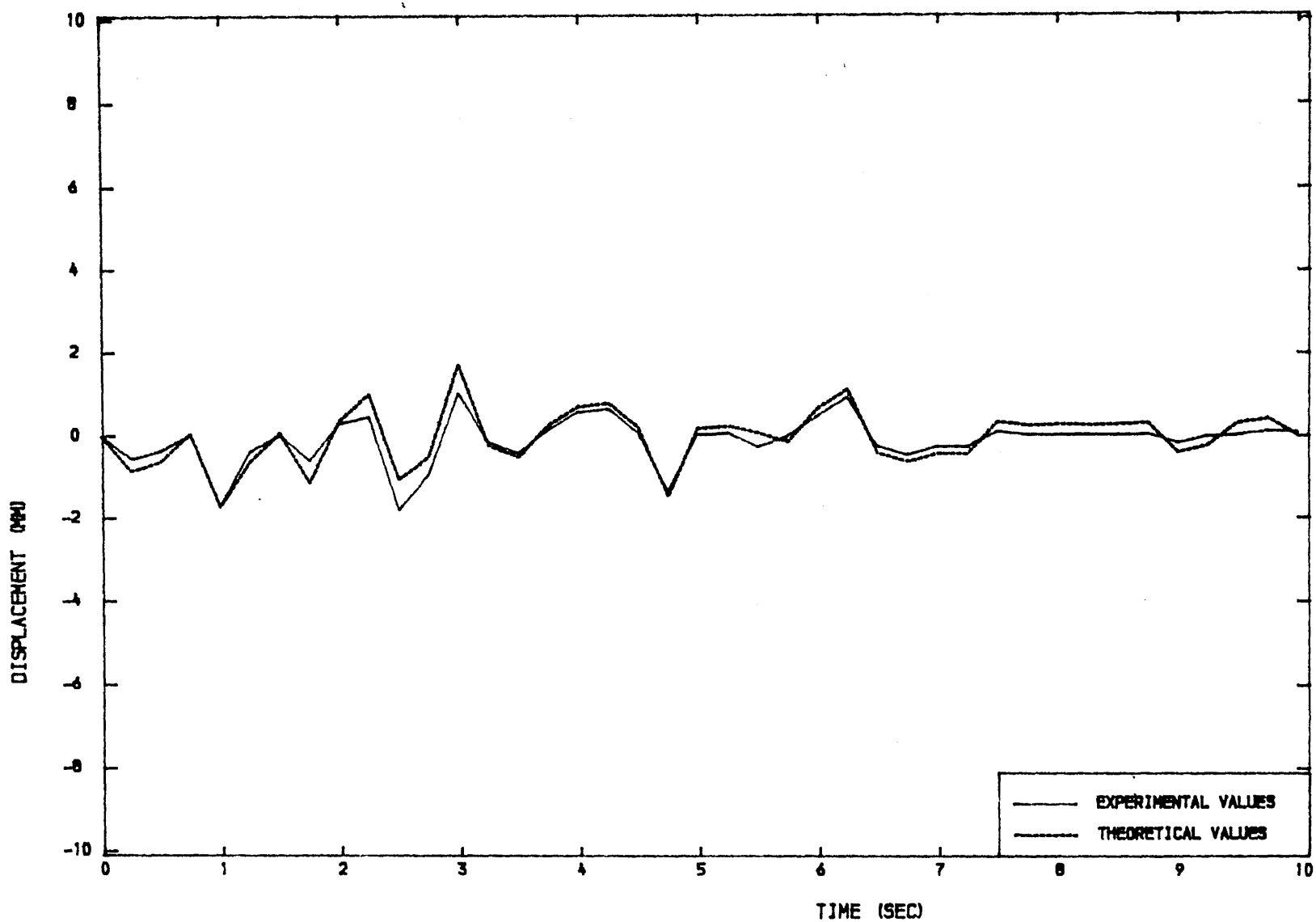

Fig. 5-13 *COMPARISON OF THEORETICALLY COMPUTED AND EXPERIMENTAL VALUES OF DISPLACEMENT AT MASS LEVEL FOR MODEL "A"*

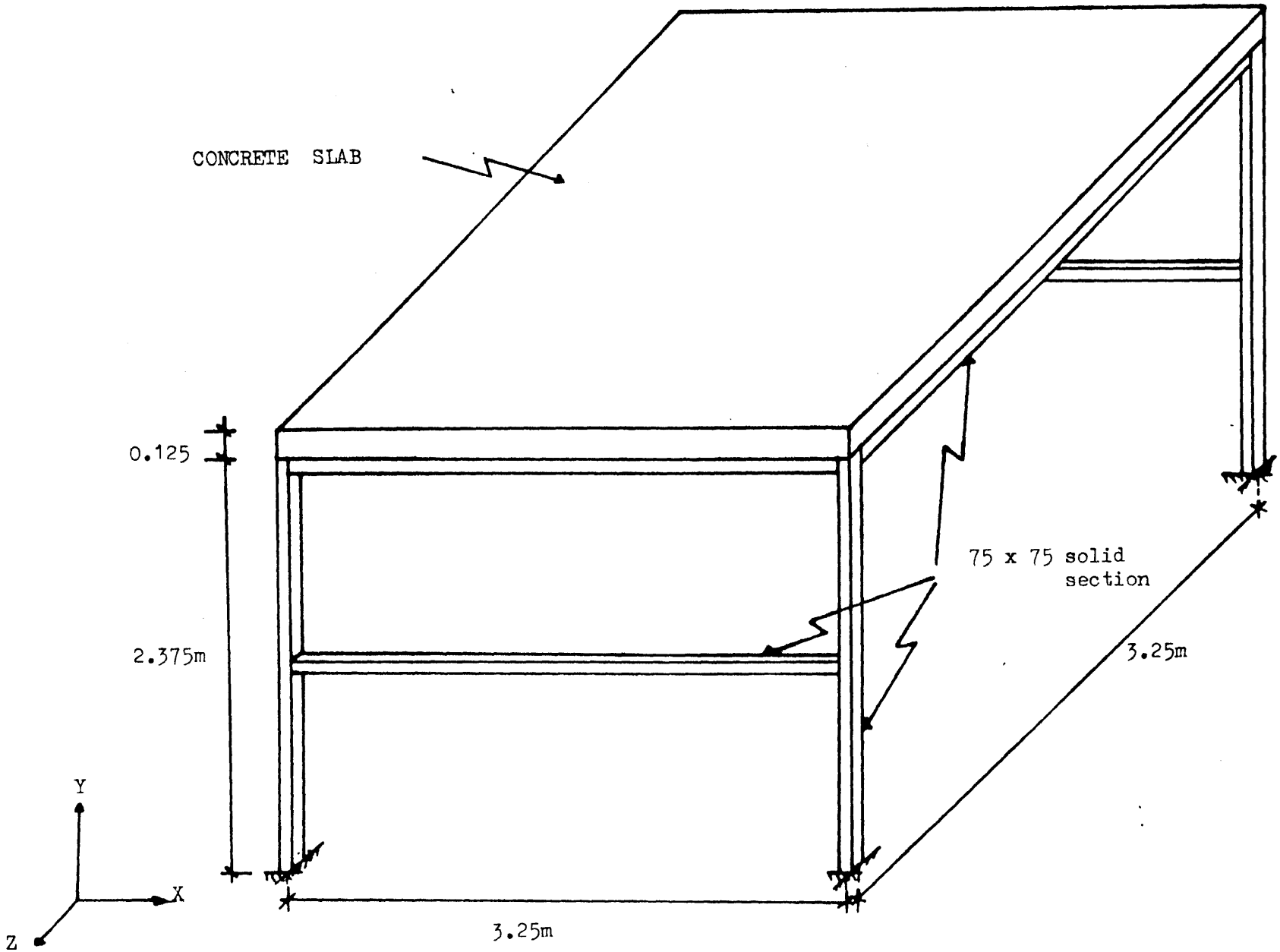

Fig. 5-14 DETAILS OF THE PROTOTYPE STRUCTURE.

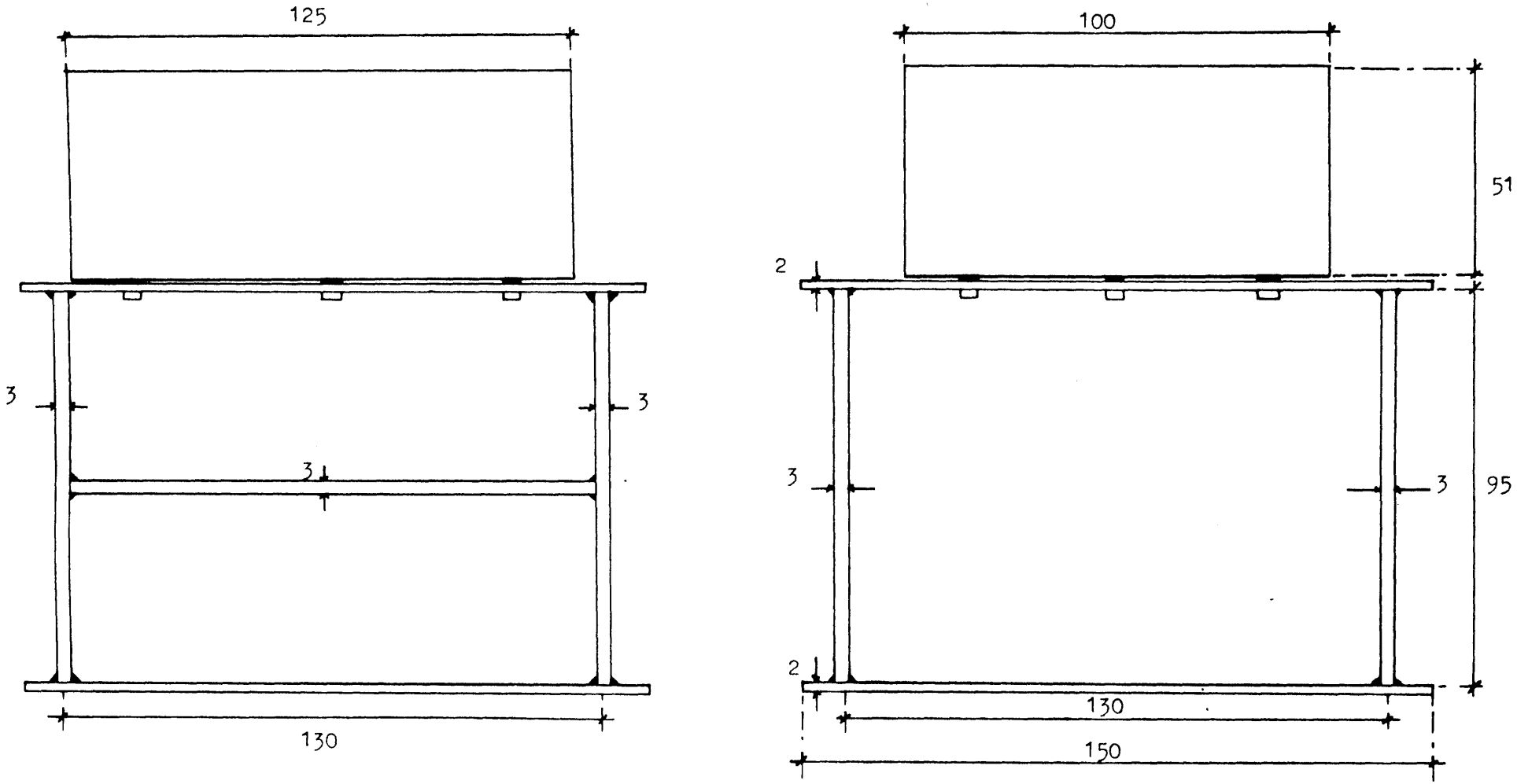

Fig. 5-15 FRONT AND SIDE ELEVATIONS OF MODEL ' B '

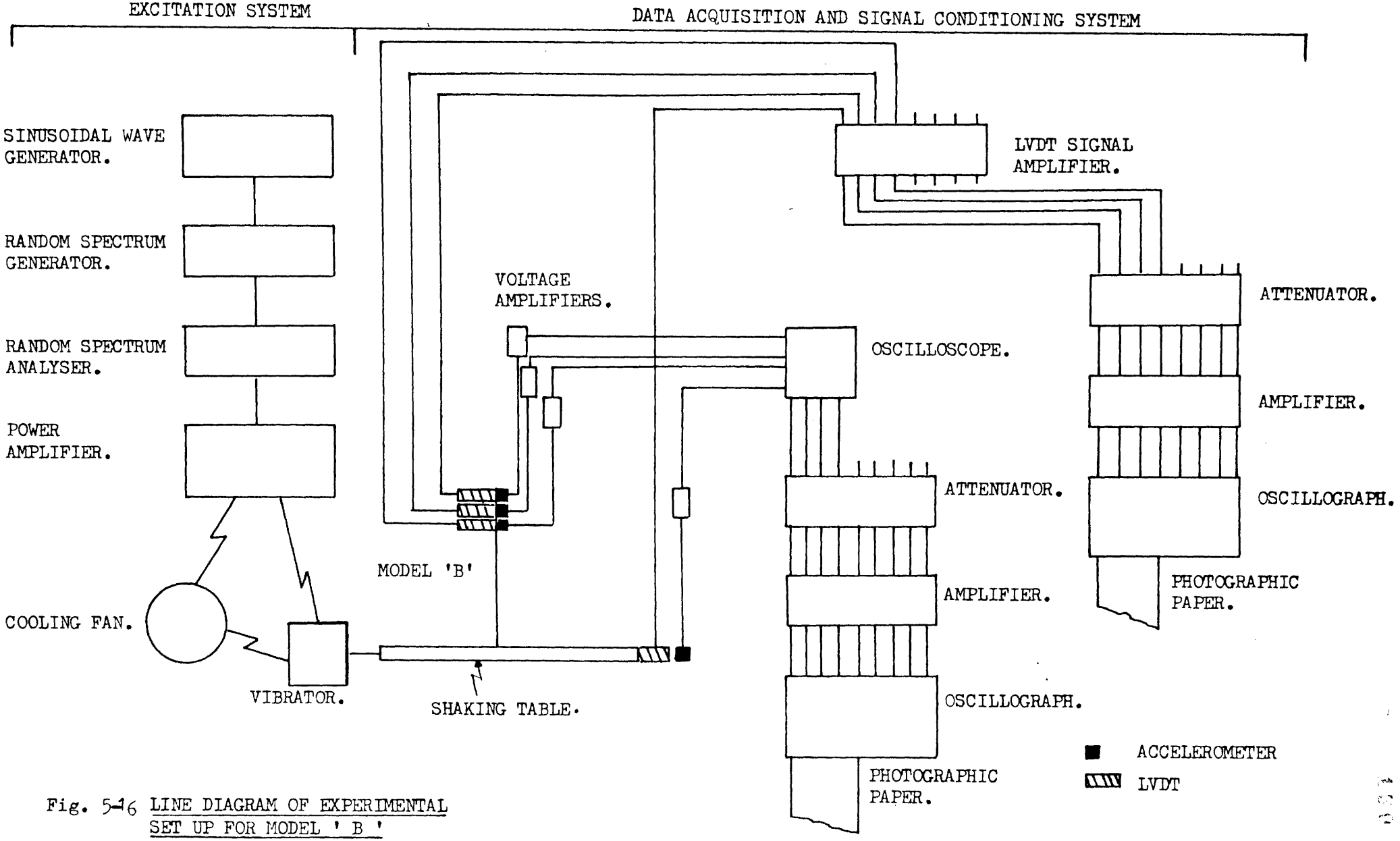

Fig. 5-16 LINE DIAGRAM OF EXPERIMENTAL SET UP FOR MODEL ' B '

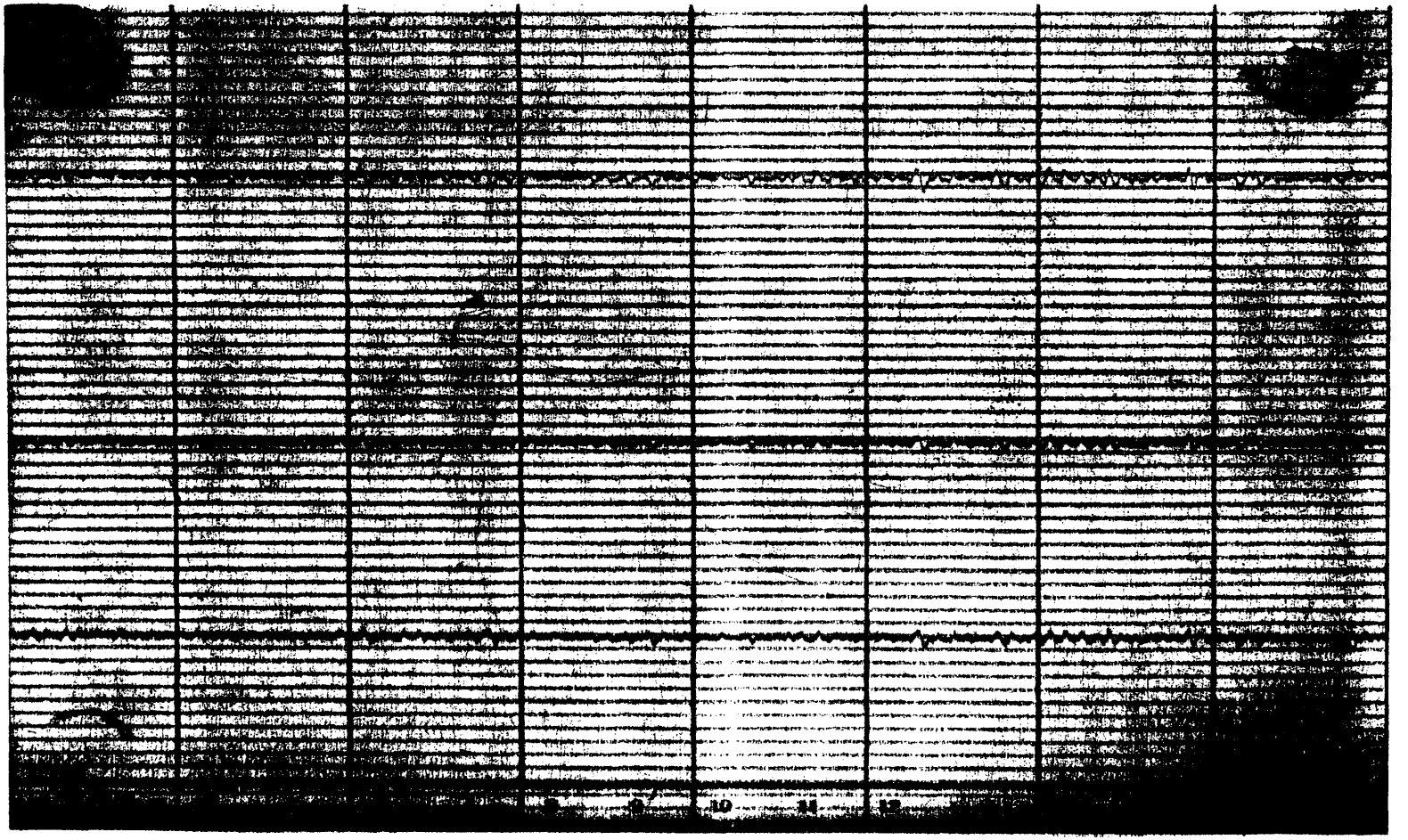

Fig. 5-17 OSCILLOGRAPH TRACE OF OUTPUT FROM THREE LVDT's (MODEL 'B')

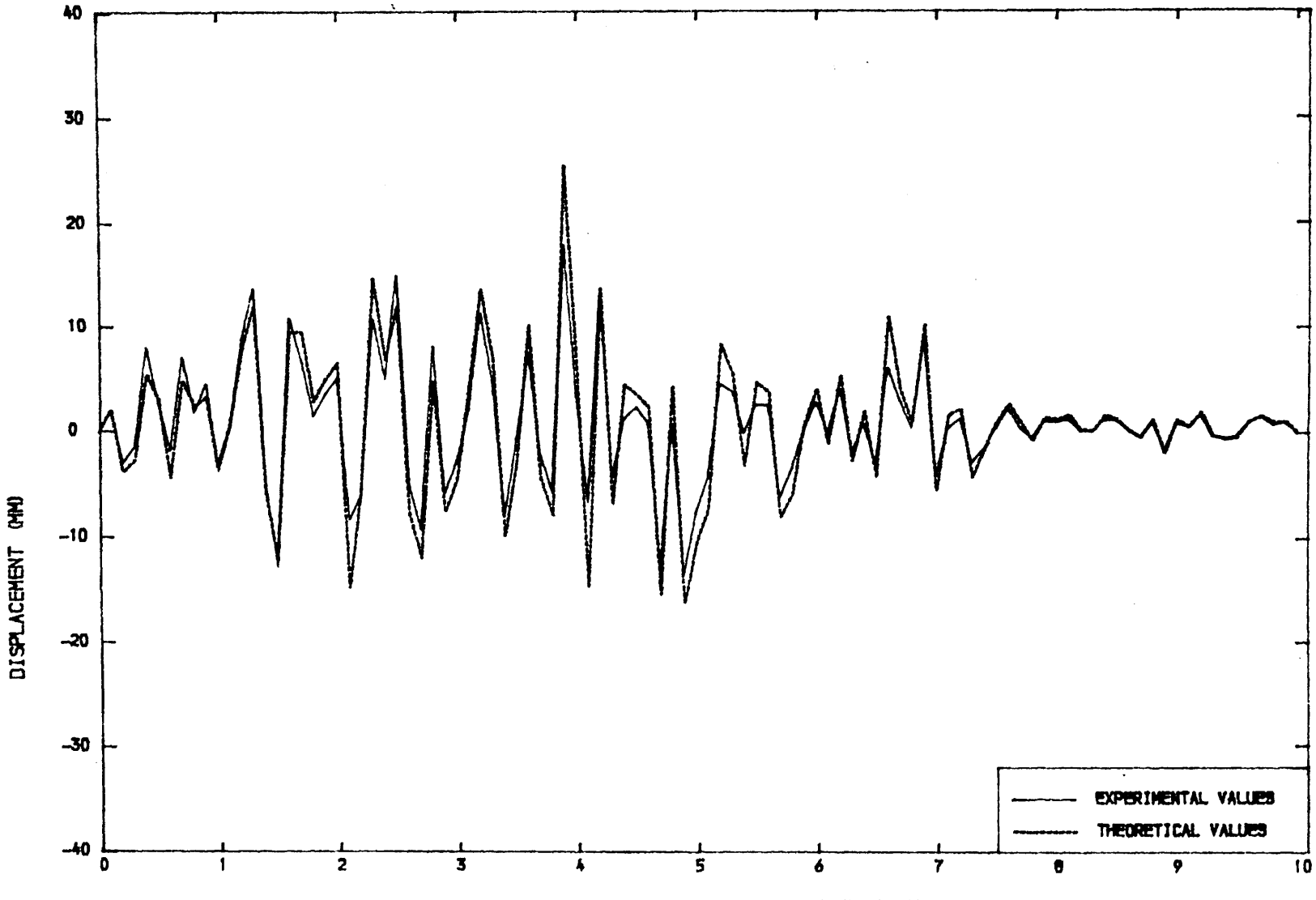

Fig. 5-18 COMPARISON OF THEORETICALLY COMPUTED AND SCALED EXPERIMENTAL VALUES OF MASS DISPLACEMENT IN THE 'Z' DIRECTION FOR THE PROTOTYPE STRUCTURE.

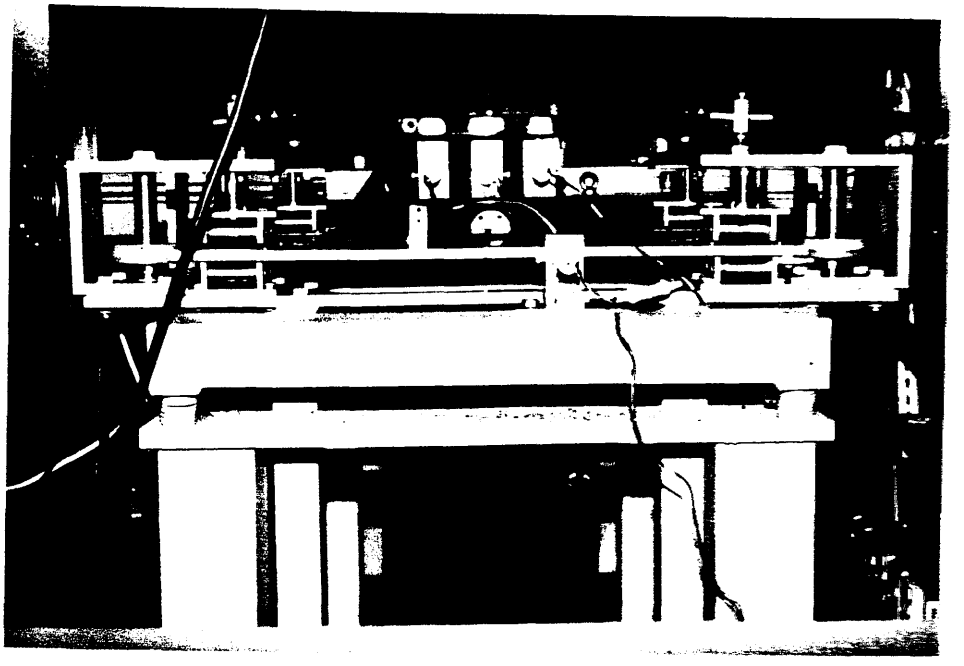

Fig. 5-19 ROLLER MECHANISMS USED FOR SUPPORTING AND GUIDING THE SHAKING TABLE.

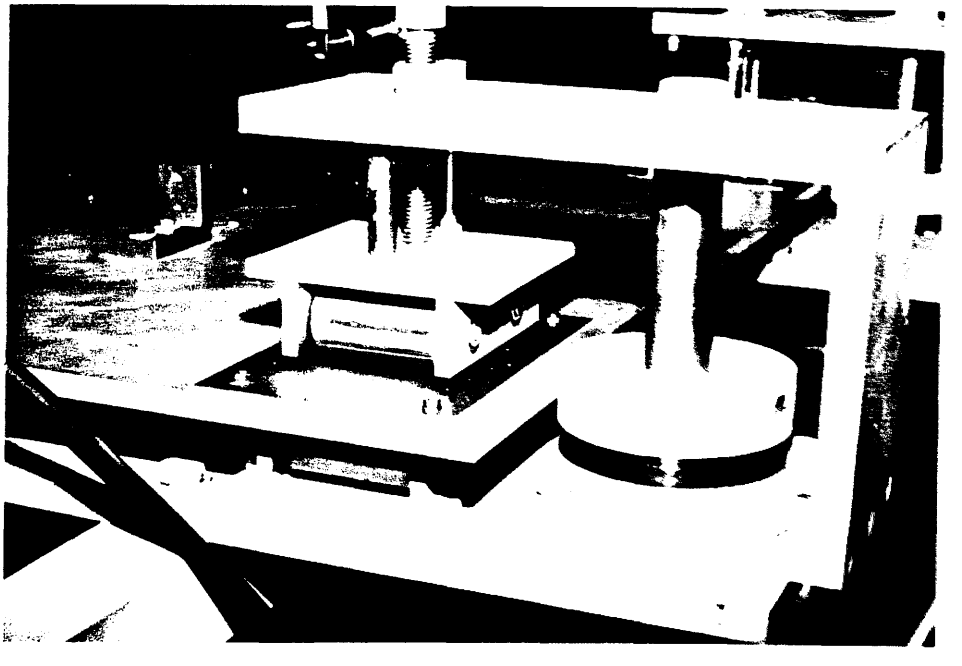

Fig. 5-20 CLOSE UP VIEW OF ONE ROLLER MECHANISM.

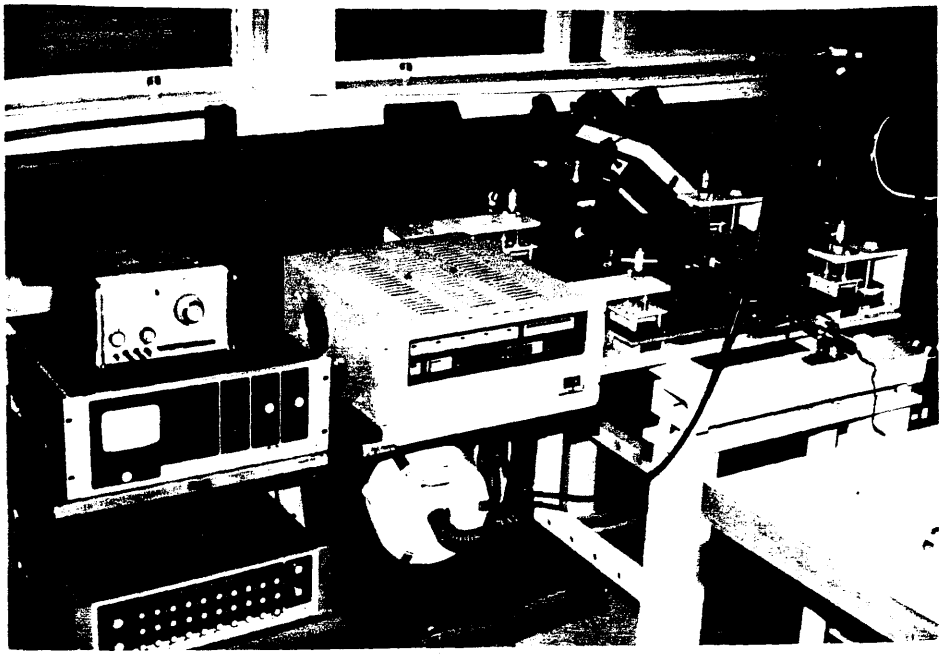

Fig. 5-21 OVERALL VIEW OF THE EXPERIMENTAL EQUIPMENT AND THE SHAKING TABLE.

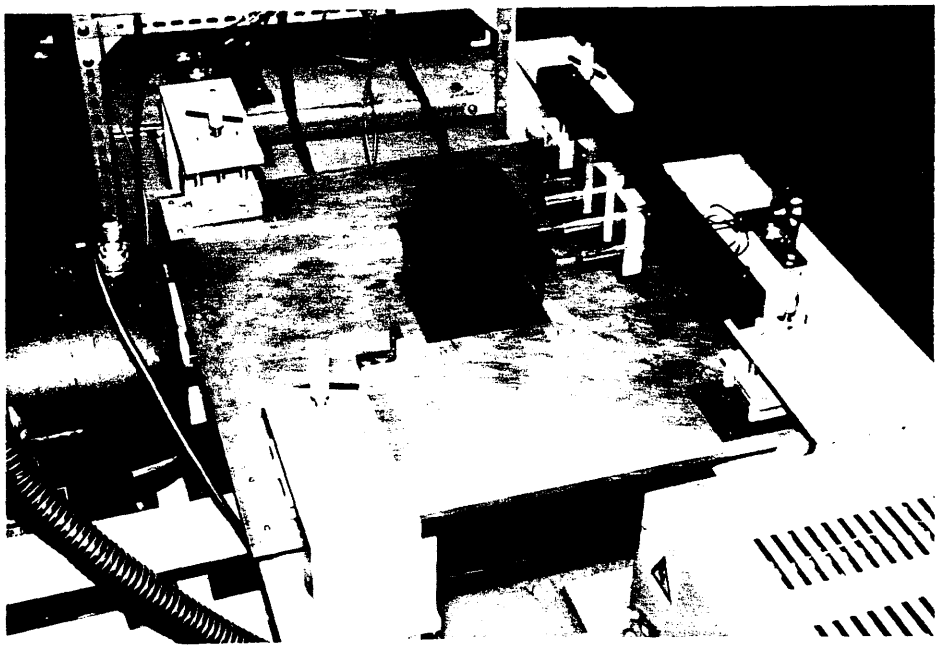

Fig. 5-22 MODEL 'B' WITH THE LVDT's ATTACHED TO IT.

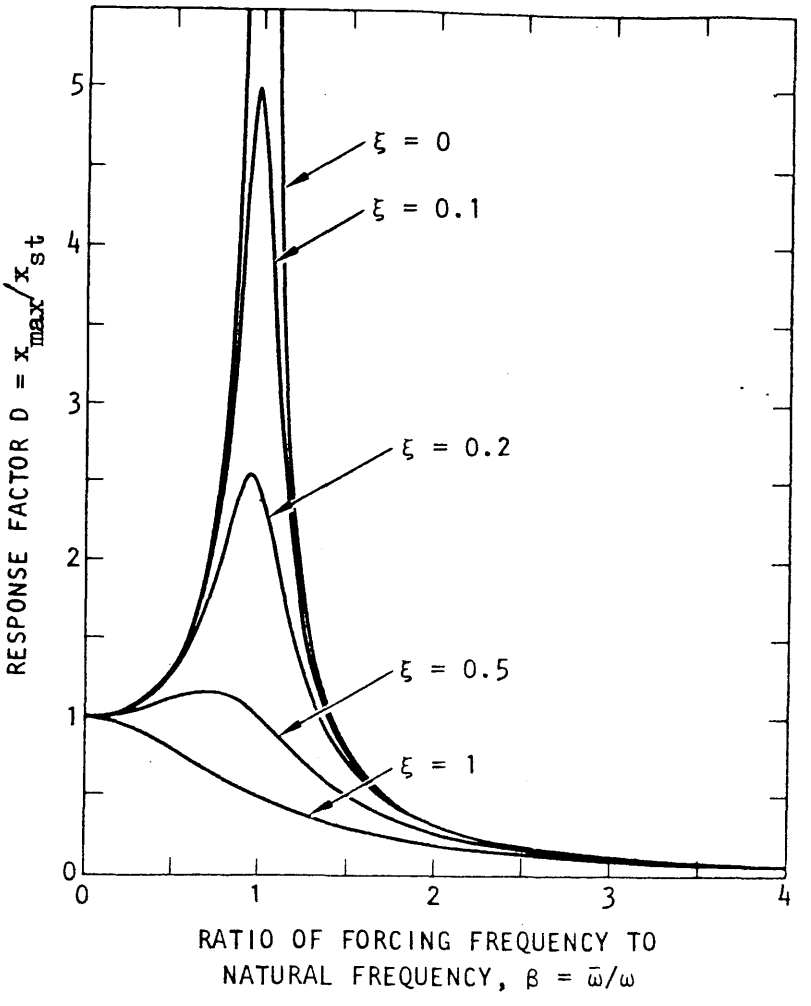

Fig. 5-23 Response factor for a one-story structure subjected to harmonic force.

The static displacement $x_{st} = f_o/k$

where f_o is the applied force at the mass level

$$f_o = m\ddot{x}_g$$

where m is the mass of the structure

and $\ddot{x}_g$ is the applied ground or base acceleration

k is the stiffness of the structure

x_{max} is the maximum dynamic displacement produced for the applied force.

TABLE 5-1 COMPARISON OF NATURAL FREQUENCY VALUES FOR MODEL 'A'

	THEORETICAL VALUE	EXPERIMENTAL VALUE	PERCENTAGE ERROR
FREQUENCY IN Hz.	18.15	17.50	3.58

TABLE 5-2 COMPARISON OF RESPONSE OF MODEL 'A' TO HARMONIC LOADING

	THEORETICAL VALUE	EXPERIMENTAL VALUE	PERCENTAGE ERROR
MASS DISPLACEMENT (mm)	1.98	1.84	7.0

TABLE 5-3 THEORETICAL AND EXPERIMENTAL VALUES OF NATURAL FREQUENCIES OF MODEL 'B'

FREQ. NO.	THEORETICAL VALUES (PROTOTYPE)	SCALED (*) THEORETICAL VALUES (MODEL 'B')	EXPERIMENTAL VALUES (MODEL 'B')	PERCENT ERROR	MODE
1	3.310	16.655	16.50	0.9	BENDING ABOUT X
2	4.265	21.326	20.75	2.7	BENDING ABOUT Z
3	7.780	38.898	37.50	3.6	BENDING ABOUT X
4	69.051	345.256	--	--	
5	76.107	380.534	--	--	
6	123.335	616.675	--	--	

(*) By similitude $\omega_r = l_r^{-\frac{1}{2}}$, for this model $l_r = 1/25$

CHAPTER 6 CONCLUSIONS AND RECOMMENDATIONS

As stated in Chapter 1 there were two major objectives to be achieved by this research work. The first was to carry out a mathematical study of the dynamic behaviour of both two and three dimensional frames. The second objective was to examine the feasibility of using small scale models to predict the behaviour of prototype structures and to examine how well the experimental and analytical results matched.

From the mathematical study the following conclusions can be drawn :—

1) The concept of using two dimensional mathematical models to represent the single or multistorey skeletal frames is a valid one provided that the behaviour of such frames is essentially two dimensional. Such models are particularly suitable for shear buildings where the structures are assumed to vibrate primarily in only one plane.

2) Using nonlinear models, a more realistic behaviour pattern of structures subjected to large ground accelerations is obtained. It would therefore be uneconomical to design structures to remain elastic in regions where strong earthquakes occur.

3) For structures whose behaviour is three dimensional, by using more sophisticated mathematical models, in which six degrees of freedom are allowed per node and consistent mass matrices are used to accurately account for the mass of the structure, a clear understanding of the behaviour of the complete structure was achieved.

4) The effect of torsional behaviour in the structures was highlighted by the results shown for the numerical example analysed. At higher frequencies torsional behaviour torsional behaviour has a major contributionin determining the dynamic behaviour of structures.

5) The Dynamic condensation used to reduce the size of a large eigenvalue problem was not found to entirely successful in the evaluation of the natural frequncies for large structural systems.

From the experimental study the following conclusions can be made :–

1) Modelling laws should be applied meticulously when designing a model. The choice of the type of model depends to a large extent upon the type of material used and the parameters which are to be studied.

2) The experimental study of the first model was successful in accurately predicting the behaviour of a two dimensional prototype which was the model itself. Close comparisons were achieved between the experimental and theoretically computed results. This proved that the mathematical model used to predict the behaviour of shear buildings was valid and effective when the structure's behaviour was predominantly two dimensional.

3) The experimental behaviour of the second model, which was a reduced scale model of a pseudo prototype structure, was close to the predicted mathematical behaviour. The behaviour trend was very similar but due to experimental losses and inaccuracies in the fabrication process the displacements in the structure were underestimated.

4) The capability of the equipment used was not enough to induce nonlinear behaviour in the model. This was one of the objectives of the study that was'nt achieved.

5) The use of small scale models is a suitable technique to predict the behaviour of prototypes provided that the model accurately reproduces the characteristics of the prototype which are to be examined.

For the mathematical model used for three dimensional frames, the following enhancements can be made

1) To reduce the size of the eigenvalue problem, by using geometric constraints, the number of degrees of freedom per storey can be set to three i.e two translation degrees of freedom and one rotational degree of freedom.

2) Nonlinear modelling can be introduced in a similar manner as for two dimensional structures.

3) Inclusion of effect of shear deformation in the structural stiffness matrix.

4) Better modelling of the floor slab and possible inclusion of shear walls and infill panels.

For the experimental study of small scale models the following suggestions can be made :–

1) Models using smaller members and hence lower stiffness can be used to study the nonlinear behaviour of prototypes.

2) If more poweful equipment is available, multistorey models should be tested.

3) The effect of varying damping, with frequency, on the behaviour of models.

4) Improvements in fabrication techniques to reduce the effect of distortions produced.

REFERENCES

1) BATHE K.J (1982) *"Finite Element Procedures"* - Prentice-Hall Inc. , Englewood Cliffs, New Jersey.

2) BATHE K.J and WILSON E.L (1973) *"Solution Methods for Eigenvalue Problems in Structural Mechanics"* - International Journal for Numerical Methods in Engineering Vol.6 pp 213-226.

3) BATHE K.J and WILSON E.L (1973) *"Eigensolution of Large Structural Systems with Small Bandwidths"* - Journal of the Engineering Mechanics Division of A.S.C.E Vol.87 pp 467-479.

4) BHATT P (1981) *"Problems in Structural Analysis by Matrix Methods"* - Construction Press, Harlow, Essex, England.

5) BREBBIA C.A and FERRANTE A.J (1986) *"Computational Methods for the Solution of Engineering Problems"* - Pentech Press, London.

6) BREEN J.E (1968) *"Fabrication and Tests of Structural Models"* - Proceedings of the American Society of Civil Engineers, Vol. 94 ST 6 ,pp 1339-1352.

7) BURNS J (1986) *"Dynamic Modelling and Monitoring of Bridge Decks"* - PhD. thesis, University of Glasgow.

8) CARPENTER J.E, ROLL F and ZELMAN M.I (1970) *"Techniques and materials for structural models"* - Symposium on models for concrete structures, ACI SP-24 Detroit.pp. 41-63.

9) CHOPRA A.K (1981) *"Dynamics of Structures - A Primer"* - EERI, California.

10) CHOWDHURY A.H and WHITE R.N (1977) *"Materials and modelling techniques for reinforced concrete frames"* Proc. of ACI Vol 74 pp. 546-551.

11) CLARKE J.L, GARAS F.K and ARMER G.S.T (1985) *"Design of Concrete Structures, The use of Model Analysis"* - Elsevier Applied Science Publishers, London.

12) CLOUGH R.W and PENZIEN J (1975) *"Dynamics of Structures"* - McGraw Hill, New York.

13) CLOUGH R.W and TANG D (1975) *"Seismic response of a steel building frame"* - Proc. of U.S Nat. conf. earthquake engg. Ann Arbor, Michigan pp. 268-277.

14) COATES R.C, COUTIE M.G and KONG F.K (1980) *"Structural Analysis"* - Nelson, Surrey England.

15) CRAIG R.R (1981) *"Structural Dynamics"* - John Wiley & Sons, New York.

16) FORTRAN REFERENCE MANUAL (1984) Mark 11 Vol.4 - Numerical Algorithms Group ltd., Oxford, England.

17) FERTIS D.G (1973) *"Dynamics and Vibration of Structures"* - John Wiley & Sons, New York.

18) HANSON N.W and CONNER H.W (1967) *"Seismic resistance of reinforced concrete beam-column joints"* - Proc. ASCE, Journal of the Structural Division. Vol. 93 pp 533-560.

19) HART G.C and NELSON R.B (1986) *"Dynamic Response of Structure"* - Proceedings of the Third Conference organised by the Engineering Mechanics Division of the A.S.C.E .

20) KRAWINKLER H and MONCARZ P.D (1981) *"Theory and Application of Experimental Model Analysis in Earthquake Engineering"* - Stanford University, California.

21) KRISHNA J and SEKARAN C (1972) *"Elements of Earthquake Engineering"* - Sarita Prakashan, Nanchandi India.

22) LITLE W.A and FOSTER D.C (1966) *"Fabrication Techniques for Small Scale Steel Models"* - Dept. of Civil Engineering, Masachusetts Institute of Technology, Cambridge, Masachusetts.

23) MILLS R.S (1981) *"Small scale modelling of the nonlinear response of steel framed buildings to earthquakes"* - Proceedings, Dynamic Modelling of Structures, Building Research Station, Garston, Watford, England.

24) MONCARZ P.D and KRAWINKLER H (1981) *"Modelling of steel and reinforced concrete structures for seismic response simulation"* -Proceedings, Dynamic Modelling of Structures, Building Research Station, Garston, Watford, England.

25) NAGARAJA R.N.R, LOHRMANN M and TALL L (1966) *"Effect of strain rate on the yield stress of structural steel"* Journal of Materials Vol. 1 .

26) NAKAMURA T.N, YOSHIDA N, IWAI S and TAKAI H (1980) *"Shaking table test of steel frames"* Proc. of 7th World conference in earthquake engg. Istanbul pp.165-172.

27) PAZ M (1985) *"Structural Dynamics"* - Van Nostrand Reinhold, New York.

28) PAZ M (1985) *"Dynamic Condensation"* - AIAA Journal Vol.22 pp. 724-727.

30) PILKEY W.D and CHANG P.Y (1978) *"Modern Formulas for Statics and Dynamics"* - McGraw Hill, New York.

31) PREECE B.W and DAVIES J.D (1964) *"Models for structural concrete"* - C.R Books Ltd. London.

32) RAO S.S (1982) *"The Finite Element Method in Engineering"* - Pergammon Press, Oxford, England.

33) ROLL F (1968) *"Materials for structural models"* - Proc. ASCE, Journal of the Structural Division. Vol. 94 pp. 1353-1382.

34) SABNIS G.M, HARRIS H.G, WHITE R.N and MIRZA M.S (1983) *"Structural Modelling and Experimental Techniques"* - Prentice -Hall Inc. Englewood Cliffs, New Jersey.

35) STRUCTURAL STEELWORK HANDBOOK (1978) B.S.C.A and CONSTRADO.

36) TRBOJEVIC V.M, KUNAR R.R and WHITE D.C (1981) *"The reduction of degrees of freedom in the dynamic analysis of complex three dimensional structures"* - Proceedings, Dynamic Modelling of Structures, Building Research Station, Garston, Watford, England.

37) WAKABAYASHI M (1986) *"Design of Earthquake Resistant Buildings"* - McGraw Hill, New York.

38) WARBURTON G.B (1980) *"The Dynamical Behaviour of Structures"* Pergammon Press, Oxford.

39) WEIGEL R.L (1970) *"Earthquake Engineering"* - Prentice-Hall Inc. Englewood Cliffs, New Jersey.

40) WILSON E.L, FARHOOMAND I and BATHE K.J (1973) *"Nonlinear Dynamic Analysis of Complex Structures"* - International Journal of Earthquake Engineering and Structural Dynamics Vol.1, pp 241-252.

APPENDIX 1

Jacobi's method

Jacobi's method provides a convenient scheme to compute all the eigenvalues and eigenvectors of a system such as

$$AX = \lambda X \qquad (A1.1)$$

when the system matrix A is a real symmetric matrix. To explain the method the n matrix equations corresponding to each eigenvalue is expressed in terms of the normalised eigenvectors

$$AX_1 = \lambda_1 X_1$$

$$AX_2 = \lambda_2 X_2$$

$$\vdots \qquad \vdots$$

$$AX_n = \lambda_n X_n \qquad (A1.2)$$

or in compact form

$$A(X_1\ X_2 \ldots X_n) = (\lambda_1\ X_1,\ \lambda_2\ X_2, \ldots,\ \lambda_n\ X_n) \qquad (A1.3)$$

Substituting

$$Q = (X_1\ X_2 \ldots X_n) \qquad (A1.4)$$

it can be seen that

$$(\lambda_1 X_1,\ \lambda_2 X_2, \ldots, \lambda_n X_n) = Q\lambda \qquad (A1.5)$$

where λ is the diagonal matrix of eigenvalues

$$\lambda = \begin{bmatrix} \lambda_1 & 0 & \ldots & 0 \\ 0 & \lambda_2 & \ldots & 0 \\ \vdots & \vdots & & \vdots \\ 0 & 0 & \ldots & \lambda_n \end{bmatrix} \qquad (A1.6)$$

Eqn. (*A1.3*) can then be written as

$$AQ = Q\lambda \qquad (A1.7)$$

Examining the matrix product

$$B = Q^T . Q \qquad (A1.8)$$

The coefficient of B located on the i^{th} row and j^{th} column will be given by

$$b_{ij} = X_i^T . X_j \qquad (A1.9)$$

corresponding to the scalar product of the i^{th} and j^{th} eigenvectors, associated with the two different eigenvalues λ_i and λ_j by the expressions

$$AX_i = \lambda_i X_i \qquad (A1.10a)$$

$$AX_j = \lambda_j X_j \qquad (A1.10b)$$

Postmultiplying the transpose of (*A1.10a*) by X_j, and premultiplying (*A1.10b*) by X_i^T gives

$$X_i^T \, A^T \, X_j = \lambda_i \, X_i^T \, X_j \qquad (A1.11a)$$

and $$X_i^T \, A \, X_j = \lambda_j \, X_i^T \, X_j \qquad (A1.11b)$$

Subtracting Eqn. (*A1.11b*) from (*A1.11a*), and considering that $A = A^T$ for a symmetric matrix A, the result is

$$(\lambda_j - \lambda_i) \, X_i^T X_j = 0 \qquad (A1.12)$$

which shows that

$$X_i^T X_j = 0 \qquad (A1.13)$$

for two different eigenvalues λ_i and λ_j. If $i = j$ then

$$X_i^T X_i \neq 0 \qquad (A1.14)$$

and in particular if the eigenvectors are normalised

$$X_i^T X_i = 1 \qquad (A1.15)$$

From this discussion it can be concluded that

$$b_{ij} = \begin{cases} 0, \text{ for } i \neq j \\ 1, \text{ for } i = j \end{cases} \qquad (A1.16)$$

so that

$$B = I \qquad (A1.17)$$

and

$$Q^T = Q^{-1} \qquad (A1.18)$$

A matrix having the property of eqn. (*A1.18*) is called an orthogonal matrix

Now premultiplying eqn.(*A1.7*) by Q^T the result is

$$Q^T . A . Q = Q^T . Q . \lambda = \lambda \qquad (A1.19)$$

which shows that if an orthogonal matrix Q, such that applying to A the orthogonal transformation $Q^T.(\ ).Q$, produces a diagonal matrix, then the diagonal coefficients of that matrix are the eigenvalues of system *(A1.1)*, and the columns of matrix Q are the corresponding eigenvectors. Therefore the problem reduces to try and diagonalise the matrix A.

Jacobi's method provides a scheme to eliminate, in turn, selected off–diagonal terms of matrix A by performing a sequence of elementry orthogonal transformations.

Considering the symmetric matrix of order 4

$$A = \begin{bmatrix} a_{11} & a_{12} & a_{13} & a_{14} \\ a_{12} & a_{22} & a_{23} & a_{24} \\ a_{13} & a_{23} & a_{33} & a_{34} \\ a_{14} & a_{24} & a_{34} & a_{44} \end{bmatrix} \qquad (A1.20)$$

and assuming that the term a_{24} is to be eliminated. Working with the orthogonal transformation matrix matrix

$$R_1 = \begin{bmatrix} 1 & 0 & 0 & 0 \\ 0 & C & 0 & -S \\ 0 & 0 & 1 & 0 \\ 0 & S & 0 & C \end{bmatrix} \qquad (A1.21)$$

where $C = cos\theta$ and $S = sin\theta$, with θ being a rotation angle to be determined, the result of a matrix operation of type *(A1.19)* is

$$R_1^T A R_1 = \begin{bmatrix} a_{11} & ca_{12} + sa_{14} & a_{13} & -sa_{12} + ca_{44} \\ ca_{12} + sa_{14} & c^2a_{22} + s^2a_{44} + 2sca_{24} & ca_{23} + sa_{34} & -cs(a_{22} - a_{44}) + a_{24}(c^2 - s^2) \\ a_{13} & ca_{32} + sa_{34} & a_{33} & -sa_{32} + ca_{34} \\ -sa_{12} + ca_{14} & -cs(a_{22} - a_{44}) + a_{24}(c^2 - s^2) & -sa_{23} + ca_{34} & s^2a_{22} + c^2a_{44} - 2sca_{24} \end{bmatrix}$$

(A1.22)

To eliminate the term in the second row and fourth column it must be

$$-cos\theta.sin\theta\ (a_{22} - a_{44}) + a_{24}(cos^2\theta - sin^2\theta) = 0 \qquad (A1.23)$$

which can be transformed into

$$a_{24}\ tan^2\theta + tan\theta(a_{22} - a_{44}) - a_{24} = 0$$

The roots of this second order equation are

$$tan\theta = \frac{-(a_{22} - a_{44}) \pm [(a_{22} - a_{44})^2 + 4a_{24}^2]^{\frac{1}{2}}}{2a_{24}} \quad (A1.24)$$

Considering only one of these roots, for instance

$$tan\theta = \frac{-(a_{22} - a_{44}) + [(a_{22} - a_{44})^2 + 4a_{24}^2]^{\frac{1}{2}}}{2a_{24}} \quad (A1.25)$$

It can be noticed that the other root will be 180^0 out of phase and would not affect the results. Working with root (*A1.25*) is equivalent to considering only the $-\pi/2 < \theta < \pi/2$ interval.

Having $tan\theta$ the following can be computed

$$cos\theta = (1 + tan^2\theta)^{-\frac{1}{2}}$$

and $$sin\theta = cos\theta tan\theta \quad (A1.26)$$

Jacobi's method consists of applying the above transformation to all the off–diagonal terms until all of them are, to a small error, equal to zero. Normally the initial starting value is taken to be the off diagonal term with the largest absolute value. Assuming that it occupies the location (i,j) the expression (*A1.26*) becomes

$$tan\theta = \frac{-(a_{ii} - a_{jj}) \pm [(a_{ii} - a_{jj})^2 + 4a_{ij}^2]^{\frac{1}{2}}}{2a_{ij}} \quad (A1.27)$$

from which $cos\theta$ and $sin\theta$ can be evaluated using eqns.(*A1.26*). Next the matrix R_1 is built taking a unit matrix and placing $cos\theta$ in location (i,i) and (j,j), $-sin\theta$ in location (i,j) and $sin\theta$ in location (j,i). The orthogonal transformation $R_1^T.A.R_1$,which is equivalent to modify the i^{th} and j^{th} rows and columns of A according the following scheme, is performed next.

Row i

$$a_{ii} = cos^2\theta.a_{ii} + sin^2\theta.a_{jj} + 2\, sin\theta.cos\theta.a_{ij}$$

$$a_{ij} = -\, cos\theta.sin\theta\, (a_{ii}-a_{jj}) + a_{ij}(cos^2\theta-sin^2\theta) = 0$$

$$a_{ik} = cos\theta.a_{ik} + sin\theta.a_{jk}$$

$$k = 1,n \text{ but } k \neq i,\ k \neq j \quad (A1.28)$$

Row j

$$a_{jj} = sin^2\theta.a_{ii} + cos^2\theta.a_{jj} + 2\, cos\theta.sin\theta.a_{ij}$$

$$a_{ji} = -\, cos\theta.sin\theta\, (a_{ii}-a_{jj}) + a_{ji}(cos^2\theta-sin^2\theta) = 0$$

$$a_{jk} = \sin\theta . a_{ik} + \cos\theta . a_{jk}$$

$$k = 1,n \text{ but } k \neq i,\ k \neq j \qquad (A1.29)$$

$$\text{Column } i \quad a_{ki} = \cos\theta . a_{ki} + \sin\theta . a_{kj}$$

$$k = 1,n \text{ but } k \neq i,\ k \neq j \qquad (A1.30)$$

$$\text{Column } j \quad a_{kj} = -\sin\theta . a_{ki} + \cos\theta . a_{kj}$$

$$k = 1,n \text{ but } k \neq i,\ k \neq j \qquad (A1.31)$$

It can be noticed that the orthogonal transformation preserves symmetry which allows the number of operations required by eqn.(*A1.28*) to be reduced to the same number as eqn. (*A1.31*). Again the largest absolute value non zero off–diagonal term is selected and the transformation outlined above is repeated. These transformations are repeatedly applied until no other zero off diagonal terms remain. It should be noticed however,that when applying the transformations (*A1.31*) to (*A1.28*) at a given stage, a non zero value for a term previously eliminated might be obtained, which indicates the iterative nature of this method. Nevertheless, it can be shown that this method is always convergent, and that is completely stable against rounding off errors.

Assuming that n iterations are needed to diagonalise A, after all transformations have been applied, the result obtained is

$$R_n^T \ldots R_3^T . R_2^T . R_1^T . A . R_1 . R_2 . R_3 \ldots R_n = Q^T . A . Q = \lambda \qquad (A1.32)$$

so that the eigenvector matrix Q is given by

$$Q = R_1 . R_2 . R_3 \ldots R_n \qquad (A1.33)$$

APPENDIX 2

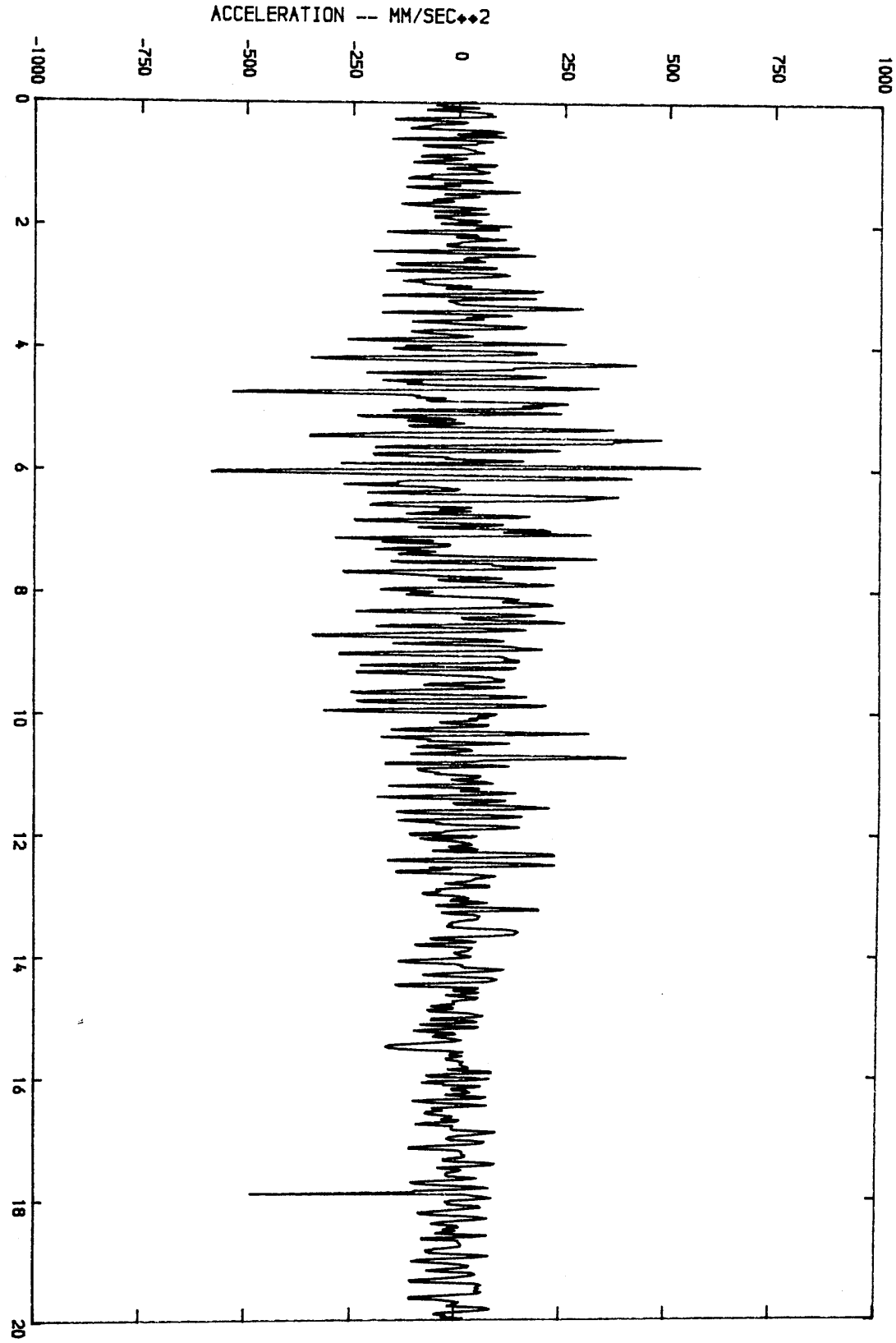

ACCELEROGRAM OF ADAK, ALASKA EARTHQUAKE OF 1 MAY 1971